Evaluation of the Antibacterial and Cytotoxic Activity of Gallium Doped Bioactive Glass Versus 45S5 Bioglass®

Miss Saima Begum

Doctor of Philosophy

ASTON UNIVERSITY

September 2015

Aston University

Evaluation of the Antibacterial and Cytotoxic Activity of Gallium Doped Bioactive Glass versus 45S5 Bioglass®

Saima Begum

Doctor of Philosophy

September 2015

Thesis Summary

In the healthcare setting, approximately 2 million bioinert devices are implanted into patients on an annual basis. However, interfacial instability of bioinert implants leads to reduced implant survivability and as a result revision surgery. Implant related infections are also a major concern which are associated with considerable repercussions for both the patient and healthcare system. Therefore, to overcome these failures materials that stimulate growth, repair and regeneration of tissues whilst simultaneously preventing infections need to be developed. A growing body of clinical data demonstrates that bioactive glasses offer great hope as they endorse these properties. Melt quench derived 3 mol% gallium doped bioactive glass was tested for antibacterial and cytotoxic activity. The results were compared with archetypal 45S5 Bioglass®, prepared and processed under identical conditions to allow a direct comparison. The antibacterial activity was studied using *Escherichia coli* (NCTC 10538) and *Staphylococcus aureus* (ATCC 6538). The cytotoxic activity was evaluated using osteosarcoma Saos-2 cells and bone marrow derived mesenchymal stem cells.

The group IIIa metal, gallium is known to possess antibacterial, antiresorptive and osteogenic properties and is therefore of interest for biological and tissue engineering applications. Results of the current work illustrated that 3 mol% gallium doped bioactive glass behaves in a similar manner to 45S5 Bioglass®. The antibacterial studies demonstrated that 3 mol% gallium doped bioactive and 45S5 Bioglass® do not possess a broad-spectrum antibacterial activity, as growth inhibition was only observed for *E. coli*; they were also rendered ineffective following pH neutralisation. Additionally studies with mammalian cells revealed that 3 mol% gallium doped

bioactive glass did not exhibit significant osteogenic activity, in comparison to 45S5 Bioglass®, after pH neutralisation.

Keywords: gallium, antibacterial, cytotoxic, bioactive glasses

Acknowledgements

I would like to thank my supervisor Dr Richard Martin for his support and advice, but especially for giving me the freedom to be independent, which has helped me to grow as a research scientist. I would also like to thank my secondary supervisors Dr Tony Worthington and Professor Eustace Johnson for their support and advice throughout my PhD.

I would like to thank my dearest friends Sameena Hareem, Tahreem Bhatti and Aisha Jama for their amazing support, and for sticking with me through this journey. Karan Rana, Erin Tse, Anjana Patel and Emily Summers, thank you for your constant support, advice and companionship through these last years. I would also like to thank Ibtesam Al-delfi and Farah Raja who have been a huge help.

Finally, I would like to thank my family, especially my parents for their unconditional love and unwavering support.

List of Contents

List of Abbreviations

ALP	Alkaline Phosphatase
ANOVA	Analysis of variance
Ag^{2+}	Silver
BAG	Bioactive Glass
BMMSCs	Bone Marrow derived Mesenchymal Cells
CaSR	Calcium-sensing Receptor
Ca^{2+}	Calcium
$CaCO_3$	Calcium carbonate
CD	Cluster differentiation
cDNA	Complementary deoxyribonucleic acid
CFU	Colony forming unit
CO_2	Carbon dioxide
Cu^{2+}	Copper
DMEM	Dulbecco's Modified Eagle's Media
DNA	Deoxyribonucleic acid
DMSO	Dimethyl sulfoxide
EDTA	Ethylenediaminetetraacetic
FBS	Foetal Bovine Serum
Fe^{3+}	Iron
Ga/Ga^{3+}	Gallium
Ga_2O_3	Gallium oxide
GaM	Gallium maltolate
H^+	Hydrogen ion

H_2O	Water
H_6NO_4P	Ammonium dihydrogen phosphate
HA	Hydroxyapatite
HCA	Carbonated Hydroxyapatite
HCl	Hydrochloric acid
ICP-MS	Inductively coupled plasma mass spectrometry
IGF11	Insulin Growth Factor 2
Ig	Immunoglobulin
IgG1	Immunoglobulin G 1
IgG2a	Immunoglobulin G 2a
Mg^{2+}	Magnesium
MIC	Minimum inhibitory concentration
mRNA	Messenger ribonucleic acid
MRSA	Methicillin resistant *staphylococcus aureus*
MSCs	Mesenchymal Stem Cells
MTT	3-(4,5-dimethylthiazol-2-yl)-2,5-diphenyltetrazolium
Na^+	Sodium
NA	Nutrient Agar
Na_2CO_3	Sodium carbonate
NB	Nutrient Broth
NAD(P)H	Nicotinamide adenine dinucleotide phosphate
OCN	Osteocalcin
OD	Optical density

OH^-	Hydroxide ion
P	Phosphorus
P_2O_5	Phosphorus pentoxide
PO_4^{3-}	Phosphate/ion
PBS	Phosphate Buffered Saline
P/S	Penicillin/Streptomycin
PE	phycoerythrin
PTH	Parathyroid hormone
Si^{4+}	Silica
SiO_2	Silicon dioxide
SBF	Stimulated Body Fluid
Sr^{2+}	Strontium
$Si(OH)_4$	Silanol
SEM	Scanning electron microscopy
SEM	Standard error of mean
SD	Standard deviation
TCP	Tricalcium Phosphate
TF	Transferrin
TfR	Transferrin Receptor
XRD	X-ray powder diffraction

List of Figures

CHAPTER 1

CHAPTER 2

List of Tables

CHAPTER ONE

Introduction to Thesis

1.1 Structure and function of bone

The adult human skeleton has a total of 213 bones and is composed of the axial and appendicular skeleton (Clarke, 2008). The four general categories of bones are long bones, short bones, flat bones and irregular bones (Clarke, 2008; Scanlon and Sanders, 2007). Long bones include bones of the arms, hands, legs and feet. Short bones include wrist and ankle bones, and the flat bones include ribs, shoulder blades, hip and cranial bones. Irregular bones include the vertebrae and facial bones (Scanlon and Sanders, 2007).

The skeletal system provides both biomechanical support and metabolic supply for the entire body. The great rigidity and hardness of the bones of the skeletal system provide structural support for the rest of the body, protect the soft tissues of the thoracic, cranial and pelvic cavities, and permit movement and locomotion by providing levers for the muscles. It also contains and protects the red bone marrow, the primary haemopoietic tissue. Furthermore, the skeletal system also provides maintenance of mineral homeostasis; Calcium (Ca^{2+}) may be removed from bone to maintain a normal blood Ca^{2+} level, which is essential for blood clotting and for muscle and nerve functioning. It also acts as a reservoir of growth factors and cytokines (Scanlon and Sanders, 2007; Clarke, 2008; Kini and Nandeesh, 2012).

The bones have two structural components – the cortical bone and the trabecular bone (Kini and Nandeesh, 2012). The adult human skeleton is composed of 80% cortical bone and 20% trabecular bone (Clarke, 2008). Cortical bone is dense and solid and the trabecular bone is composed of a honeycomb like network of trabecular plates or rods interspersed in the bone marrow compartment (Clarke, 2008; Kini and Nandeesh, 2012). Trabecular bone is found in the ends of long bones and in the middle of most other bones, and it is always surrounded by the more durable cortical bone (Thompson, 2013). Cortical bone has an outer periosteal surface and inner endosteal surface (Clarke, 2008; Kini and Nandeesh, 2012). The periosteum is a dense fibrous connective tissue which contains osteoprogenitor cells, blood vessels and nerve fibres. It protects, nourishes, aides in bone formation and plays an important role in appositional

growth and fracture repair (Clark, 2005; Kini and Nandeesh, 2012). Furthermore, it also allows the attachment of tendons, ensuring a strong connection between muscle and bone (Thompson, 2013; Clark, 2005). The endosteum is a thin membranous structure that covers the inner surface of cortical and trabecular bone and the blood vessel canals present in bone (Kini and Nandeesh, 2012).

Both cortical and trabecular bone are composed of smaller units called osteons (Clark, 2005; Clarke, 2008). Cortical osteons are called haversian systems, which are cylindrical in shape (Clarke, 2008). Through each osteon runs a haversian canal that contains small blood vessels and nerves (Clark, 2005). Layers of calcified bone matrix are arranged in concentric lamellae around a haversian canal (Clark, 2005; Thompson, 2013). Osteocytes occupy the lacunae, which are tiny gaps between the concentric lamellae and are interconnected by canaliculi (Clark, 2005; Thompson, 2013). The canaliculi and lacunae also contain interstitial fluid which bathes the osteocytes. This arrangement allows nutrients, gases and wastes and signalling molecules to diffuse to and from the osteocytes (Clark, 2005). Volkmann's canals or perforating canals, connect the haversian canals (Thompson, 2013). These canals transport blood and nutrients from the bones exterior to the central canals and the medullary or marrow cavity. Interstitial lamellae are incomplete osteons (because they remain during the remodelling process) which lie between the osteons (Clark, 2005) (Figure 1.1).

Figure 1.1 The structure of bone (Nouri *et al*., 2010).

Woven bone and lamellar bone are the 2 sub-tissue types in the skeletal system based on matrix organisation (Kini and Nandeesh, 2012). Lamellar bone formation is characterised by collagen fibres being laid down layer by layer in an orderly fashion. For each layer, collagen fibres are laid parallel to each other, forming a bone matrix sheet, which is called a lamella (Clarke, 2008 & Kini and Nandeesh, 2012). Woven bone is produced when the collagen fibrils are laid down rapidly in a haphazard manner (Clark, 1958). Woven bone is weaker than lamellar bone and is produced during embryonic skeletal development, early fracture healing or the osteosarcoma formation. However, woven bone is short lived and is eventually replaced by lamellar bone (Kini and Nandeesh, 2012).

1.2 Bone formation and remodelling

Bone is composed of bone forming cells, namely osteoblasts and remodelling cells, osteoclasts. Furthermore, it also consists of an organic matrix with inorganic mineral salts deposited within the matrix (Kini and Nandeesh, 2012). The organic matrix mainly consists of type I collagen fibres and non-collagenous structural proteins, which include proteoglycans, sialoproteins and osteocalcin (OCN) (Hadjidakis and Androulakis, 2006; Kini and Nandeesh, 2012). However, the role of non-collagenous proteins has not been fully explained (Hadjidakis and Androulakis, 2006). The mineral content of bone hydroxyapatite [$Ca_{10}(PO_4)_6(OH)_2$], which is a crystalline complex of Ca^{2+} and phosphate (PO_4^{3-}) (Clarke, 2008; Kini and Nandeesh, 2012). For biological tissues, the major form is carbonated hydroxyapatite, where PO_4^{3-} or hydroxide can be substituted by carbonate. Traces of other minerals, such as magnesium, fluoride, potassium, sodium and chloride are also present in varying proportions (Lasch and Kneipp, 2008).

Each bone constantly undergoes remodelling during life to help it to adapt to changing mechanical forces, as well as to remove old, microdamaged bone and replace it with new, mechanically stronger bone (Raggat and Partridge, 2010). Bone remodelling occurs throughout life and can be divided into the following four phases (Figure 1.2):

Activation phase: The first stage of bone remodelling involves detection of an initiating signal (Raggat and Partridge,2010), which could be direct mechanical strain on the bone that results in structural damage or hormone (e.g. oestrogen or Parathyroid hormone (PTH)) action on bone cells (Raggat and Partridge, 2010; Kini and Nandeesh, 2012). The signals are detected by osteocytes and translated into biological signals which recruit and activate osteoclast precursor cells from the circulation, resulting in the interaction of osteoclast and osteoblast precursor cells (Raisz, 1999; Raggat and Partridge, 2010; Clarke, 2008). This action leads to the differentiation, migration and fusion of mononuclear monocyte-macrophage osteoclast precursors to the bone surface where they fuse together to form multinucleated osteoclasts (Raisz, 1999; Kini and Nandeesh, 2012). The osteoclasts bind to bone matrix via integrin

receptors present on their cell membranes, upon binding they become polarised with the bone resorbing surface developing a ruffled border (Raisz, 1999; Clarke, 2008).

Resorption phase: The resorption phase lasts approximately for 2 – 4 weeks during each remodelling cycle (Clarke, 2008; Kini and Nandeesh, 2012). The ruffled border of resorbing osteoclasts secrete hydrogen (H^+) ions via H^+ - ATPase proton pumps and chloride channels in their cell membranes into the resorbing compartment to lower the pH to as low as 4.6. The low pH created by the release of H^+ ions aids osteoclasts to dissolve the mineral component of bone (Clarke, 2008). These cells also release lysosomal enzymes, particularly cathepsin K, to digest organic matrix (i.e. type I collagen) resulting in the formation of irregular scalloped cavities on the trabecular bone surface, called Howship lacunae, or cylindrical haversian canals in cortical bone (Raisz, 1999; Clarke, 2008). The mineral salts of the bone matrix are released into the interstitial fluid, where they diffuse into the blood and are carried away, as are the peptides and amino acids of collagen fibres (Clarke, 2008).

Reversal phase: Following the resorption phase is the reversal phase, wherein bone resorption transitions to bone formation (Clarke, 2008). At the completion of bone resorption, resorption cavities contain a variety of mononuclear cells such as monocytes and osteocytes which are released from bone matrix, and pre-osteoblasts recruited to begin new bone formation (Clarke, 2008; Kini and Nandeesh, 2012). The events occurring during this stage are not well understood, but it has been proposed that they may involve further degradation of remnant collagen and release of growth factors to initiate the final phase (Raisz. 1999; Raggat and Partridge, 2010). Pre-osteoblast recruitment involves the release of several growth factors such as insulin growth factor (IGF) embedded within the bone matrix.

Formation phase: Bone formation takes approximately 4 – 6 months to complete and involves osteoblasts, which originate from mesenchymal stem cells (osteoprogenitor cells) of the bone marrow stroma that can give rise to bone, cartilage, fat or fibrous connective tissue (Raggat and Partridge, 2010; Kini and Nandeesh, 2012). Osteoblasts synthesise new collagenous matrix, which fills the perforated area and regulate mineralisation of matrix by releasing small, membrane-bound vesicles that concentrate Ca^{2+} and PO_4^{3-} (Clarke, 2008; Kini and Nandeesh, 2012). Once the osteoblast has completed its cycle of matrix synthesis, it can become a flattened bone lining cell found on the surface, be buried within the matrix as an osteocyte, or undergo apoptosis (Raisz, 1999). Once the formation phase has been completed approximately 50 to 70% of osteoblasts undergo apoptosis (Clarke, 2008).

Figure 1.2 Bone remodelling is initiated when osteoclast resorb bone mineral and matrix, which is followed by mononuclear cells preparing the resorbed surface for osteoblasts. Osteoblasts synthesise new matrix and differentiate into osteocytes, which completes the remodelling cycle (Kapinas and Delany, 2011).

1.2.1 Osteoblasts

Osteoprogenitor cells are derived from pluripotent stem cells, found in the bone marrow. Osteoprogenitor cells give rise to osteoblasts that are responsible for the synthesis of bone matrix and its subsequent mineralisation (Hadjidakis and Androulakis, 2006; Kini and Nandeesh, 2012). Osteoblasts are mononucleated, and depending on their cellular activity can either be flat or plump (Kini and Nandeesh, 2012). Osteoblasts synthesise and lay down collagen I, which constitutes 90-95% of the organic matrix of bone. Collagen is deposited in concentric layers to produce mature (lamellar) bone. However, osteoblasts deposit collagen rapidly in a basket-like weave resulting in woven, immature bone, commonly seen in conditions such as fracture callus. Osteoblasts also produce and deposit non-collagenous proteins, of which osteocalcin and alkaline phosphatase (ALP) are the most abundant proteins present in bone (Clarke, 2008; Kini and Nandeesh, 2012). The roles of each protein have yet to be determined, and many seem to serve multiple functions, including regulation of bone mineralisation and of bone cell activity. It is thought that ALP and OCN are $Ca^{2+}$and PO_4^{3-} binding proteins which help ordered deposition of mineral by regulating the amount and size of hydroxyapatite crystals formed (Clarke, 2008).

Following mineralisation of bone matrix, mature osteoblasts undergo apoptosis, revert back to bone lining cells or become embedded within the matrix and differentiate into osteocytes, which account for 90-95% of all bone cells (Raggatt and Partridge, 2010). These embedded cells form a network throughout mineralised bone, and maintain connection with each other and with osteoblasts on the bone surface via dendritic like processes that lie within the canaliculi (Raggatt and Partridge, 2010). They normally do not express ALP but do express OCN and several other matrix proteins that support intracellular adhesion and regulate exchange of mineral in the bone fluid within lacunae and the canalicular network. Osteocytes detect stress signals from bending and stretching of bone and convert these signals into biological activity. Osteocytes have the ability to live within human bone that is not turned over for decades (Clarke, 2008).

1.3 Bone repair

Bone remodelling does not only occur during bone formation but also in bone repair, where a bone is injured due to fracture. Despite the bone's natural healing capacity, it is susceptible to fracture (Geris *et al*., 2009). When there is a change in external stimulus, the bone either remodels itself to withstand the pressure or it fractures when the energy from the impact exceeds the energy the bone can absorb (Turner, 2002).

Following bone trauma, the cortical bone and the periosteum are damaged, rupturing numerous blood vessels resulting in bleeding and the formation of a clot (hematoma) enclosing the trauma site (Geris *et al*., 2009; Thompson, 2013). As a consequence of the vascular damage, the injured bone becomes hypoxic, affecting the osteocytes which go onto necrose with the damaged tissue. The necrotic process recruits the inflammatory cells, such as macrophages and neutrophils to the site to remove debris. This is followed by the invasion of fibroblasts which produce a fibrous network, soft callus (Geris *et al*., 2009). The soft callus is remodelled into cartilage forming a temporary repair called procallus, mechanically stabilising the fracture site (Geris *et al*., 2009; Steele and Bramblett, 2007). Blood vessels invade the procallus, bringing along osteoblasts that produce a hard callous tissue of mineralised woven bone matrix (Geris *et al*., 2009). The remodelling phase begins with osteoclastic resorption of poorly placed bone matrix and the formation of lamellar bone by osteoblasts (Geris *et al*., 2009).

The success of many medical interventions has increased the lifespan of humans from an average of 45 years to 78 years (Hench *et al*., 2010). It has been estimated that by 2050 nearly one in five people will be over the age of 60 (Hench *et al*., 2010). An increased lifespan poses a problem as the quality of life often deteriorates due to the gradual degradation of tissue, including bone (Hench *et al*., 2000). Normal bone function is a consequence of a balance between bone resorption and bone formation, however this system declines with age. It has been observed that with increasing age, bone becomes porous, the harversian canals and canaliculi become plugged and the number of empty osteocyte lacunae increases. Furthermore,

osteoblast number and activity decreases which in effect results in decreased bone formation and delayed mineralisation. In addition the number of osteocytes decline with age (Kloss and Gassner, 2006). The increase in bone loss is supposedly in part due to the decreased activity of osteoblasts and a prolongation of the lifespan of osteoclasts. An increase in bone resorption is prevalent in ageing women as a result of menopause, although resorption is thought to increase mildly in ageing men too (Clarke, 2008; Lane, 2006).

Consequently, the probability of fracture of long bones, hips and collapse of vertebrate increases significantly (Hench *et al*., 2000). The consequences in treating patients with bone fractures has become a major health care concern, in the UK it costs £2 billion each year (Mitchell *et al*., 2010). This cost is expected to rise in the future in light of the ageing population. It has been estimated that each year in the UK approximately 300,000 fractures occur amongst the ageing population due to osteoporosis (decreased bone turnover due to impaired formation of osteoclasts and loss of function). High rates of morbidity and mortality are associated particularly with hip fractures, with fewer than half of the patients retuning home following surgery (Rose and Oreffo, 2002). Furthermore, it has been reported that 1,150 people die every month in the UK following a hip fracture (Mitchell *et al*., 2010).

1.4 Current treatment for bone tissue repair

Most fractures are treated by immobilising the bone with bioinert implants such as corrosion resistant metals (i.e. stainless steel alloys) and insoluble, non-toxic polymers (i.e. ultrahigh molecular weight polyethylene) (Hench *et al*., 2010; Bock *et al*., 2003). The first generation of bone replacement materials were selected to be as chemically inert in the body as possible (so not to induce an inflammatory response). These bioinert materials have enhanced the quality of life of millions during the last 40 years (Hench *et al*., 2000). However, all so-called bioinert materials elicit a host immune response to act against the foreign body resulting in the formation of a non-adherent fibrous capsule between the material and living bone, which isolates the implant from the host (Long, 2008; Anderson, 2001; Nuss and Rechenberg, 2008).

The foreign body reaction starts within seconds or minutes after tissue contact with a conditioning film of proteins (e.g. fibrinogen, fibronectin, immunoglobulin G) on the surface of the implant. This protein film initialises the recruitment and migration of monocytes and fibroblasts through the endothelium (Sevastianov, 1988; Nuss and Rechenberg, 2008). After adhesion the monocytes transform into macrophages which recruit other monocytes and coalesce to form foreign body giant cells (Nuss and Rechenberg, 2008; Anderson *et al*., 2008). Macrophages and foreign body giant cells ingest and dissolve implanted material intracellularly or by the release of degradative agents like lysosomal enzymes, and reactive oxygen intermediates. However, bioinert implants cannot be ingested by macrophages and foreign body giant cells resulting in implant isolation. Foreign body giant cells form a layer, in a fibrous quite avascular capsule around the implant, limiting interaction between host and the implant (Nuss and Rechenberg, 2008). The thickness of the fibrous capsule depends on the conditions of the implant (Cao and Hench, 1995).

Nearly 2 million orthopaedic devices are implanted annually worldwide (Hench *et al*., 2000). In spite of this, survivability analysis demonstrates an increasing population of implants, such as total hip prostheses, failing before the patient dies (Hench *et al*., 2000). The reason for failure is related to the progressive deterioration of the bone in contact with the implant. As a result bioinert implants are a compromise because they do not form a real chemical bond with living tissue (Hench *et al*., 2010; Tilocca, 2010). Therefore, over time tissue breakdown and implant detachment becomes inevitable resulting in the need for revision surgery (Hench *et al*., 2010). Loosening and detachment is estimated to occur in many as 50% of cemented total-hip replacements. Loosening of an implant could be attributed to several biomechanical factors such as excessive activity by the patient, debonding at the tissue-implant interface, material fatigue, inflammation, infection and osteolysis (Long, 2008).

However, approximately 10% of bone defects due to fractures, surgery or tumours cannot be treated using the conventional method, because the damaged sites are too large and also due to

eventual implant failure (Bock *et al*., 2003). Therefore, the most prevalent clinical approach is bone graft, which is the second most common transplantation tissue with the exception of blood (Giannoudis *et al*., 2005). More than 2.2 million bone grafting procedures are taking place annually worldwide in order to repair bone defects in orthopaedics and dentistry (Martin, 2012).

Autograft and allograft are the preferred choices, with autograft being the golden standard of bone grafting (Giannoudis *et al*., 2005; Moore *et al*., 2001). Autograft involves harvesting cancellous bone from the iliac crest (upper hip) due to ease of access and recovery of good quality cancellous bone (Martin, 2012; Giannoudis *et al*., 2005; Moore *et al*., 2001). Autograft is the most effective bone graft material, because it is natural tissue that contains the progenitor cells and growth factors necessary for bone remodelling (Martin, 2012). However, few mature osteoblasts survive the transplantation process, but adequate numbers of precursor cells do survive resulting in bone repair (Moore *et al*., 2001). Unfortunately, autograft has several drawbacks, such as increased operative time, donor site morbidity related to blood loss, wound complications, and most importantly chronic pain (Moore *et al*., 2001; El-Ghannam *et al*., 1995).

Allograft bone is obtained from cadaver sources and is regarded as a surgeon's second choice, as it offers the same characteristics as autograft with the exclusion of osteogenic cells (Moore *et al*., 2001; Giannoudis *et al*., 2005; Nandi *et al*., 2010). Allograft use permits the avoidance of morbidity associated with autograft harvesting and is of particular importance when inadequate volume of autograft is available for large defects (Moore *et al*., 2001). Allograft bone is implanted up to 300,000 times worldwide, which is 100 times more than heart transplantations and 25 times more than kidney transplantations (Zimmermann and Moghaddam, 2011). Despite its increasing availability the complications associated with allograft include fracture and infection. Fracture rates of up to 19% associated with allograft use have been reported. Furthermore bacterial infection is more common, especially with

increased sized grafts and may be seen in more than 10% of massive allografts (Moore *et al*., 2001). In addition, viral transmission is also a potential risk and to prevent this from occurring allograft tissue is processed, which lowers the risk but significantly reduces the initial mechanical and biological properties present in the bone tissue (Moore *et al*., 2001; Giannoudis *et al*., 2005). These limitations surrounding the biological grafts have directed attention towards the use of synthetic bone graft materials, such as Ca^{2+} and PO_4^{3-} ceramics. They have an excellent record of biocompatibility; also no systemic toxicity has been reported with minimal foreign body reactions (Moore *et al*., 2005; Giannoudis *et al*., 2005). Shortly after implantation a layer of carbonated hydroxyapatite (HCA) forms that is responsible for the bond observed between the graft and bone tissue, inducing bone remodelling (Moore *et al*., 2005). The Ca^{2+} and PO_4^{3-} ions required for this action are derived from the implant and the surrounding bone (Moore *et al*., 2005).

Dense and porous hydroxyapatite (HA), which forms the mineral component of bone, and tricalcium phosphate (TCP) ceramics are the materials most widely used (El-Ghannam *et al*., 1995; Martin, 2010). Synthetic HA has been successfully used to coat bioinert implants, and as a porous granular form with bone graft to fill bone defects, as it supports the growth of bone on its surface (Moore *et al*., 2005). One of the main drawbacks of synthetic HA is that it is poorly resorbed *in vivo*, and due to this the rate of bone formation is slow (El-Ghannam *et al*., 1995; Moore *et al*., 2005). Additionally the particulates that are at a distance from the defect will become encapsulated by fibrous tissue (El-Ghannam *et al*., 1995). TCP is more bioresorbable than synthetic HA, it is removed from the implant site as bone grows into the scaffold whereas HA is more permanent (Giannoudis *et al*., 2005). Furthermore, the porosity of TCP allows resorption via dissolution and fragmentation over a 6-18 month period, and infiltration by bone forming cells and nutrients for bone recovery (Giannoudis *et al*., 2005). The solubility of TCP is higher than the rate of tissue regeneration, there is always less bone volume produced than the volume of TCP reabsorbed (Giannoudis *et al*., 2005). This is a major

setback hence why TCP is used as an adjunctive with other less resorbable materials (such as HA) or as an expander for autograft (Giannoudis *et al*., 2005; Martin, 2012).

1.5 Bioactive glasses

A bioactive material is a material that elicits a specific biological response at the material surface, which results in the formation of a bond between the tissues and the materials (Gerhardt and Boccaccini, 2010). Two classes of bioactive materials have been recognised, Class A and Class B.

Class A bioactive materials have the following characteristics (Cao & Hench. 1995; Hench *et* al., 2000; Hench. 2006; Hench *et al*., 2010):

1. The material forms a bond to both bone and soft connective tissues.
2. The material is osteoproductive, which means colonisation and proliferation of bone distant from the implantation site.
3. The material is osteoconductive, the ability to support the growth of bone over its surface (Moore *et al*., 2001).
4. The material resorbs as new bone replaces it.

The characteristics of Class B bioactive materials include (Cao & Hench. 1995; Hench *et al*., 2000):

1. The material bonds to bone but not soft tissues.
2. The material is not osteoproductive.
3. The material is osteoconductive.
4. The material resorbs very slowly and may not be in contact with newly formed bone.

Bioactive glasses (BAGs) are one of the most promising synthetic materials for bone repair, replacement, and regeneration because they have the potential to be more bioactive than calcium phosphate based materials (Martin, 2012). They are an example of class A bioactive

materials whereas calcium phosphates (i.e. synthetic HA) are an example of class B bioactive materials. Oonishi *et al*. (1997) reported that Bioglass® allowed full bone restoration in 2 weeks, whereas synthetic HA following implantation needed 12 weeks to produce comparable results.

The first BAG was invented in 1969 by Larry Hench following a conversation with a US Army colonel who queried if a material could be developed that was able to survive the conditions of the human body. Larry Hench then set out to develop a material which would not form a fibrous encapsulation but instead a living bond with the host tissue. He went on to develop several compositions all based around the Na_2O-CaO-SiO_2-P_2O_5 glass system. However, the composition selected was that of 46.1 mol % SiO_2, 24 mol% Na_2O, 26.9 mol% CaO and 2.6 mol% P_2O_5 which was later termed 45S5 Bioglass® (Jones, 2013). This composition was successful due to the strong bond formed *in vivo* between 45S5 Bioglass® and rat bone, it was noted that 45S5 Bioglass® could not be removed without breaking the bone (Hench. 2006; Jones, 2013). Following the discovery of 45S5 Bioglass® the field of bioactive ceramics was established, with many new materials formed including various compositions of bioactive glasses, calcium phosphate ceramics such as synthetic hydroxyapatite and other composites (Hench *et al*., 2010; Jones, 2013). However, bioactive glasses remain popular because they allow control of a range of chemical properties and the rate of bonding to different tissues (Hench, 2006).

Since its discovery, 45S5 Bioglass® has shown great success in many clinical applications particularly in the dental and orthopaedic fields (Abou Neel *et al*., 2009). In 1984 it was used as middle ear prostheses (MEP®) to restore the ossicular chain and treat conductive hearing loss. The second commercial device was the Endosseous Ridge Maintenance Implant (ERMI®) in 1988, used to preserve the alveolar ridge from the bone resorption that follows tooth extraction (Jones, 2013; Hench. 2002). However, neither of these products is in widespread clinical use, due to their fixed size and shape. The lack of successfulness of monolithic shapes led to particulate use (Jones, 2013). In 1993 the first 45S5 Bioglass® particulate product was

produced, PerioGlas® was used to repair defects in the jaw that resulted from periodontal disease (Hench, 2006). Following the success of PerioGlas® in dental bone regeneration, the product NovaBone® was manufactured for orthopaedic bone grafting in 1999, though it was not available for clinical use until 2000 for non-load bearing sites. More recently, 45S5 Bioglass® particulates (NovaMin®) have been used in toothpastes for treating tooth hypersensitivity, which affects 35% of the population of US and similarly in Europe (Hench, 2006). 45S5 Bioglass® is not the only bioactive glass in clinical use, BioGran® is another synthetic bone graft used in jaw bone defect regeneration, which has a similar composition but a narrower particle size range (Jones, 2013). There are now several types of BAGs, the traditional silicates, which include the 45S5 Bioglass®, phosphate-based glasses and borate-based glasses. Various compositions are constantly being designed and investigated for potential clinical use within many fields.

1.5.1 Structure of bioactive glasses

A glass is a network of atoms (mostly silicon) bonded together via covalent bonds with oxygen atoms. The base components of most BAGs are SiO_2, Na_2O, CaO and P_2O_5. Silicate based glasses are composed of silica tetrahedral (SiO_4) that are connected to each other by oxygen atoms (- Si – O – Si -). The role of silicon (SiO_4) is that of a network former which maintains the glass structure (Hench *et al*., 1971; Jones, 2013). Sodium (Na^+) and Ca^{2+} ions are added to the glass system because they make it easier to melt the glass, and secondly they dissolve from the glass and modify the local pH (Hench *et al*., 1971). But most importantly they disrupt the network by forming non-bridging oxygen bonds, whereby some of the oxygen atoms are no longer bonded to two silicon atoms, forming bonds such as Si – O^{-} $^{+}$ Na, and are therefore network modifiers (Jones and Clare, 2012) (Figure 1.3).

Figure 1.3 (**A**) two-dimensional presentation of the structure of crystalline SiO_2. (**B**) Two-dimensional presentation of glass SiO_2. (**C**) Two-dimensional presentation of a glass network composed of network modifiers and network formers.

The silica content determines the solubility of the glass (Figure 1.4). If the silica content is high (> 60 mol%), a highly connected network with a large proportion of bridging oxygen bonds is formed, resulting in low dissolution and low bioactivity. This is true of traditional soda-lime-silica glass systems, which consist of more than 65 mol% SiO_2 and therefore fail to undergo reactions with body fluids (Jones and Clare, 2012). Connectivity is lowered when the silica content is less than 60 mol%, and by the addition of network modifiers such as Ca^{2+} and Na^{+}.

It was presumed that P_2O_5 was also required for a glass to be bioactive. However, later on it became known that phosphate played a role in nucleation of the calcium phosphate phase that occurred on glass surface (Jones, 2013). It is believed that phosphate is not an important constituent since the surface can adsorb PO_4^{3-} ions from solution (Jones and Clare, 2012).

Figure 1.4 Bioactivity map of BAGs in the SiO_2 – Na_2O – CaO system (2.6 mol% of P_2O_5) showing regions of bioactive response (Jones and Clare *et al*., 2012; Hench). Bioactive glass compositions in region A bond to bone, whilst those in region B are effectively bio-inert and become encapsulated in scar tissue. This is due to the silica content being too dense and resistant to reaction with body fluid. Glass systems in region C degrade too rapidly, as the silica content is too low and the soda content too high, resulting in a highly disrupted network. Region D contains BAGs with such low silica that a glass network cannot form. Bioactive glasses within regions A and E strongly form bonds with collagenous (soft) tissue and with the inorganic part of the bone. 45S5 Bioglass falls within regions A and E. (Jones and Clare, 2012).

1.5.2 The bioactivity of bioactive glasses

The ability of BAG to bond to bone and stimulate new bone growth is attributed to the formation of a HCA layer, which interacts with collagen fibrils of damaged bone to form a bond. The process for HCA layer formation is relatively well understood, however the biological interactions occurring at the HCA – host bone interface are poorly understood (Jones, 2013). Nevertheless, Hench and his co-workers have revealed that 11 reaction stages are involved in bone regeneration, which occur at the BAG surface (Hench *et al*., 2003; Hench *et al*., 2010).

The first five reaction stages involve the rapid release (within 2-24 hours) of soluble ionic species from the BAG into the interfacial solution, and the formation of a high surface area hydrated silica and polycrystalline HCA layer on the BAG surface (Martin, 2012; Jones, 2013).

1. Rapid ion exchange of cations, Na^+ or Ca^{2+} ions from the BAG surface with (hydrogen) H^+ ions from solution, creating silanol bonds (Si – OH) on the glass surface:

   $Si - O - Na^+ + H_2O \longrightarrow Si - OH^- + Na^+_{(aq)} + OH^-$

   pH of the solution increases and a silica rich (cation-depleted) region forms near the glass surface. If P is present in the composition it is also lost from the glass.

2. OH^- ions attack the silica network of the glass, by breaking the Si – O – Si bonds. Soluble silica is released in the form on $Si(OH)_4$ into the solution, leaving more silanol groups at the glass – solution interface:

3. Condensation of the silanol groups near the glass surface resulting in the repolymerisation of the silica rich layer.

4. Migration of Ca^{2+} and PO_4^{3-} groups to the surface through the silica-rich layer and from the solution, forming a film rich in amorphous $CaO – P_2O_5$ on the silica rich layer.

5. Incorporation of hydroxyls and carbonate from the surrounding solution and crystallisation of the $CaO – P_2O_5$ film to form HCA layer.

Once the HCA layer has formed, the next stages are less clear, as the exact mechanism is difficult to elucidate.

6. Macrophages are recruited as a response to the damage caused by implantation. However, they do not react to the glass, and therefore do not remain at the site of defect for very long. They do not evolve into foreign body giant cells in an effort to digest the material

7. Progenitor cells of the osteoblast lineage attach rapidly on to the HCA surface during the first 24-48 hours.

8. The osteoprogenitor cells on the HCA surface begin to proliferate.

9. The cells differentiate into the osteoblast phenotype; this occurs rapidly on the surface of BAGs, whereas it takes several weeks for similar cellular events to occur on the surface of bioinert materials. In contrast, osteoprogenitor cells colonise the surface of bioactive materials within 24-48 hours.

10. The new osteoblasts that colonise the surface begin to produce extracellular matrix, and induce nucleation of the HCA bone mineral.

11. HCA mineralisation continues until the osteoblasts are completely embedded in mineralised extracellular matrix. The result is new bone formation.

1.5.3 Control of osteoblast cell cycle

The formation of the biologically active surface HCA layer, lays down the foundation for chemical events which lead to bone regeneration (Gerhardt and Boccaccini, 2010; Hench *et al*., 2010; Hoppe *et al*., 2011). The key mechanism is the controlled release of ionic dissolution products from the degrading BAG, especially critical concentrations of soluble $Si^{4+}$and Ca^{2+} ions (Gerhardt and Boccaccini, 2010; Hench *et al*., 2010). For the formation of new bone, osteoprogenitor cells need to undergo mitosis. However, there are very few osteoprogenitor cells in the bones of older people that are capable of dividing and forming new bone. Therefore, cells that are present must receive the correct chemical stimuli from their local environment instructing them to enter the cell cycle (Hench *et al*., 2003; Hench *et al*., 2010).

Studies have shown that 45S5 Bioglass® promotes human osteoblast proliferation by limiting the amount of time the cell spends in G_1 (where it grows and carries out normal metabolism) and the S phase (DNA synthesis) of the cell cycle and then prompting its quick entry into the G_2/M phase, when the cell is ready to undergo mitosis (Gerhardt and Boccaccini., 2010). Xynos *et* al. (2000) showed that within 48 hours in the presence of critical concentrations of soluble Si^{4+} (17-20 ppm) and Ca^{2+} (88-100 ppm) ions, there is a 100% increase-fold in osteoblasts in the S phase (Gerhardt and Boccaccini, 2010; Hench *et al*., 2003; Xynos *et al*., 2000). Furthermore, the percentage of osteoblasts in the G2/M phase on 45S5 Bioglass® was significantly higher in comparison to osteoblasts on the control (polystyrene) substrate on days 2 and 12 (Hench *et al*., 2003; Xynos *et al*., 2000).

Other studies also conducted by Xynos *et al*. (2000) have shown that the osteoblast cell cycle is under genetic control. Within a few hours, exposure of human primary osteoblasts to the dissolution products of 45S5 Bioglass® results in the activation of several families of genes, including those encoding transcription factors and potent growth factors such as, the insulin-growth factor (IGF) ll with IGF-binding proteins and proteinases that cleave IGF-ll from their binding proteins (Hench *et al*., 2003; Hench 2006). IGF-ll is the most abundant growth factor in bone, which is produced locally by bone cells and is considered to have autocrine and/or paracrine effect (Hench *et al*., 2003; Xynos *et al* 2000). Xynos *et al* (2000) cDNA microarray analysis showed a 320% increase in the expression of IGF ll in osteoblasts that were exposed to bioactive glass. The results show that 45S5 Bioglass® may increase the availability of IGF-ll in osteoblasts by stimulating the transcription of IGF-ll and its binding protein and also by regulating its dissociation from the binding protein (Hench *et al*., 2003; Hench 2006). Consequently the unbound IGF-ll is likely to be responsible for increased cell proliferation seen in culture (Hench *et al*., 2003; Hench 2006).

Not only does the cell cycle induce cell proliferation but to some extent it also determines cell commitment and differentiation (Hench, 2006). Osteoblast differentiation has been investigated by measuring ALP activity and OCN synthesis (Xynos *et al*., 2000). ALP is a cell membrane associated enzyme, which regulates phosphate metabolism and locally down-regulates inhibitors of apatite crystal growth (Kini and Nandeesh, 2012,). It is a marker that appears early during osteoblast differentiation but both its expression and activity diminish with the onset of mineralisation (Kini and Nandeesh, 2012). OCN is a non-collagenous matrix protein with a high affinity for Ca^{2+}, which is also known to inhibit apatite crystal growth both *in vitro* and *in vivo* (Clarke, 2008). OCN is thought to be a marker which appears late during osteoblast differentiation and characterises osteocytes (terminally differentiated osteoblasts), which are post-mitotic and incapable of cell division (Hench 2006; Kini and Nandeesh, 2012). Xynos *et al*. (2000) have shown osteoblast ALP activity to be markedly increased on day 6 of culture when grown on bioactive glass, but declined by day 12 to levels significantly less than

in control cultures. Likewise, OCN synthesis was significantly higher in osteoblast cultures grown on the bioactive substrate in comparison to those grown on control substrate following 6 days in culture. These findings indicate that BAG has the ability to stimulate the development of a mature osteoblast phenotype (Xynos *et al*., 2000).

The studies reported above investigated the osteogenic properties of 45S5 Bioglass® and have shown promising results. Nonetheless numerous research groups have fabricated and investigated other BAG compositions which have also influenced osteoblast proliferation and differentiation. The 58S (60 mol% SiO_2, 36 mol% CaO and 4 mol% P_2O_5) BAG dissolution products stimulated the proliferation of osteoblast cells and upregulated the expression of many genes including ALP, OCN and the extracellular matrix protein collagen I (Christodoulou *et al*., 2004). In addition 60S BAG (59.9 mol% SiO_2, 38.4 mol% CaO and 1.74 mol% P_2O_5) showed a 50% increase in osteoblast proliferation and increased collagen I production (Valerio *et al*., 2003). 47S (47 mol% SiO_2, 26 mol% CaO, 21 mol% Na_2O and 6 mol% P_2O_5) highlighted the biocompatibility of this glass as it enhanced osteoblast proliferation in culture (Mohamed *et al*., 2008). Mesenchymal stem cells are capable of skeletal repair and regeneration due to their ability to differentiate into osteoblasts. This ability is important for successful osteointergration of implanted materials. Bosetti and Cannas. (2004) reported that a significant effect of 45S5 Bioglass® and 77S (80 mol% SiO_2, 16 mol% CaO, 4 mol% P_2O_5) BAG was observed on early differentiation of mesenchymal stem cells into osteoblast cells. Additionally, Radin *et al*. (2005) and Reilly *et al*. (2007) reported similar findings, 45S5 Bioglass® cultured with mesenchymal stem cells elevated ALP activity. Furthermore, in order to enhance the bioactivity of BAGs towards desired biological responses glass systems have been doped with metal ions such as strontium (Sr^{2+}), magnesium (Mg^{2+}), and copper (Cu^{2+}) (Gentleman *et al*., 2010; Tousi *et al*., 2013).

1.5.4 Antibacterial properties

Lack of tissue integration is not the only factor that compromises the integrity of current bone implants, as infection also plays a major role in implant failure. It has been reported that approximately 50% of the 2 million nosocomial infections that occur annually are implant related (Mortazavi *et al*., 2010). Although the infection rate following implantation of orthopaedic devices has decreased in the past 50 years the number of older patients requiring replacement surgery is steadily increasing, and thus the number of patients with implant related infections are rising (Zimmerli and Ochsner, 2003). Implant related infections are associated with high complications, particularly in the elderly who are susceptible to infection due to immunosenescence, poor nutrition, and multiple commodities and impaired wound healing. Furthermore, these infections have considerable repercussions for the healthcare system with long hospital stay and increased morbidity and mortality (Mortzavi *et al*., 2010; McGarry *et al*., 2004). The mortality rate due to surgical intervention for implant infections has been estimated to be 0.4%-1.2% for 65 year old patients and 2%-7% for 80 year old patients (Lentino, 2003).

Implant devices can become colonised by bacteria at the time of surgery or via a haematogenous route from a distant source (Long, 2008; Schierholz and Beuth, 2001). The current bioinert implants are susceptible to microbial adhesion, which may colonise the implant surface and thus lead to inflammation at the implantation site. Infections at the site of implantation occur at a frequency of up to 4.3% and in the case of revision surgery up to 17% (Moseke *et al*., 2011). Implant related infections are related to the highly adaptive ability of bacteria to colonise the surfaces of inert implants or of adjacent, damaged tissue cells (Gristina, 1987). Many implants are composed of one or more metals or polymers and are inanimate in a biological environment and thus do not resist infection (Gristina, 1987). Despite their inertness, most implant surfaces are physiocochemically active and modulate events such as cellular adhesion and integration, and inflammatory and immunomodulating responses (Gristina, 1987; Schierholz and Beuth. 2001). Furthermore, implant surfaces adsorb host extracellular matrix

proteins such as fibronectin, fibrinogen, elastin and collagen and thus provide receptor sites for bacterial adhesion (Gristina, 1987; Hudson *et al*., 1999). Several microbial species possess adhesins which mediate cell anchorage and fixation to host extracellular proteins (Compoccia *et al*., 2006). For instance *Staphylococcus aureus* has discrete binding sites for extracellular matrix proteins, collagen and fibronectin (Gristina, 1987; Schierholz and Beuth. 2001). The family of adhesins not only facilitate adhesion to orthopaedic implants but also to bone matrix (Hudson *et al*., 1999).

The most recovered isolates from infected implant surfaces are Gram-positive *S. aureus* and *Staphylococcus epidermidis* (Gristina, 1987; Arciola *et al*., 2005; Cordero *et al*., 1996). Additional microorganisms isolated include *Escherichia coli*, *Pseudomonas aeruginosa*, *Proteus mirabilis*, and beta haemolytic *Streptococcus* (Gristina, 1987; Arciola *et al*., 2005). However, a very large proportion of implant related infections occur due to *S. aureus* and *S. epidermidis* as infections caused by other pathogenic microbial species represent only a minority of implant related infections, approximately about 22% (Campoccia *et al*., 2006). The success of *S. aureus* in part is due to the alarming level of antibiotic resistance it exhibits, as four out five strains do not respond to penicillin drugs, whereas methicillin/oxacillin resistance is observed in four out of ten strains (Campoccia *et al*., 2006). Moreover, *S. aureus* possesses the ability to form biofilms on implant surfaces. Within the biofilm, bacteria can persist in a low metabolic, stationary growth phase, in which they resist the action of host immune system and antibiotics (Baldoni *et al*., 2010).

Antibiotic resistance and systemic toxicity with associated renal and liver complications render antibiotics ineffective in preventing implant-related infections (Ahmed *et al*., 2006; Mulligan *et* al., 2002). Therefore, good medical management dictates removal of colonised or infected devices (Long, 2008). Both the spread of antibiotic resistance and the increased use of implants, warrant the need for new and innovative therapeutic strategies. Bioactive glasses could be the ideal implants because not only do they promote regeneration of living tissue but they have

also been shown to exhibit antibacterial activity when used as therapeutic materials (Munukka *et al*., 2007; Mortazavi *et* al., 2009). Furthermore, they could provide a sustained delivery of antibacterial ions to the local microenvironment.

There are numerous experiments *in vitro* which show silicate-based BAGs to display a broad and certain antibacterial effect against various pathogenic bacteria. 45S5 Bioglass® was the first silicate-based BAG to be composed and it was shown to reduce microbial infections when it was used to repair periodontal defects, which are prone to infection following surgery with bioinert materials. Based on these findings Stoor *et al*. (1998) set out to prove that BAGs were antibacterial, and in 1998, through experiment *in vitro* they demonstrated that the bioactive glass S53P4 (53 mol% SiO_2, 20 mol% CaO, 23 mol% Na_2O, 4 mol% P_2O_5) had a broad antibacterial effect on oral bacteria in the planktonic phase (Stoor *et al*., 1998). Thereafter, many authors including Allan *et al*. (2000) found BAGs to exhibit a similar antibacterial effect against certain oral bacteria.

Since then *in vitro* studies have been conducted to determine whether BAGs exerted a similar antibacterial effect on skin pathogenic bacteria. Initial antibacterial studies revealed that the antibacterial activity of BAGs was attributed to the high pH levels caused by the release of alkali ions from BAG particles (Hu *et al*., 2009). When BAGs are immersed into an aqueous environment they undergo a series of surface reactions resulting in the release of soluble Na^+ and Ca^{2+} ions, which increase the aqueous pH value (Munukka *et al*., 2007; Hu *et al*., 2009). However, the mechanisms of antibacterial activity remained unknown and are still not clearly understood, but several theories have been proposed.

Elevated pH can alter the pH gradient of the bacterial cytoplasmic membrane, which is required for the movement of organic nutrients and components into the cell (Xie *et al*., 2008). As a result the permeability of the cytoplasmic membrane is compromised and the bacteria eventually succumb to death due to increased toxicity. Another theory is that hydroxyl (OH^-)

ions can react with fatty acids in the membrane to form free lipid radicals which weaken the bacterial membrane structure causing it to collapse (Xie *et al*., 2008). Ion concentrations and changes in osmotic pressure may also play a role in the antibacterial action of BAGs. The release of ions from BAGs cause a rise in the salt concentration creating an osmotic pressure that would be inhibitory to most bacteria.

Allan *et al*. (2000) emphasised the important role the pH plays in inhibiting oral bacterial growth. They found that the antibacterial activity between Bioglass® supernates and media adjusted with sodium hydroxide to the same pH, demonstrated similar antibacterial activity against certain oral bacteria (Allan *et al*., 2000). Furthermore, Hu *et al*. (2009) and Mortazavi *et al*. (2009) conducted antibacterial studies on skin pathogens, the results of which highlighted the importance of pH. In the study conducted by Hu *et al*. (2009) the pH value for the media without 45S5 Bioglass® particles was 7.0 and the bactericidal percentage was below 10%. By contrast the bactericidal percentages for *S. aureus*, *S. epidermidis* and *E. coli* increased up to 98% when tested against the 50 mg/ml concentration, the pH value for which was 9.8 (Hu *et al*., 2008). Likewise, Mortazavi *et al*. (2009) also demonstrated the importance of high pH levels, the initial pH value of the broth was measured at 7.3 but following the addition of 58S (60 mol% SiO_2, 36 mol% CaO, 4 mol% P_2O_5) nanoparticles the pH value was 8.3, which resulted in sparse *E. coli* growth and moderate growth for *S. aureus* (Mortazavi *et al*., 2009). These results confirm that a high pH value is a critical factor in BAG antibacterial activity. However, Munukka *et al*. (2008) showed that the BAG with a high CaO content (42.3 mol%) had a greater antibacterial effect on aerobic bacteria than BAG with lower amounts of CaO (31.27 mol%). They postulated that the high concentration of Ca^{2+} ions may have inhibited bacterial growth by providing a hyperosmotic environment and caused perturbations in the membrane potential.

On the contrary, Bellantone *et al*. (2002) have demonstrated that BAGs do not possess either bacteriostatic or bactericidal activity. They found no significant difference between the mean

cell viabilities for control cultures and for those containing 45S5 Bioglass®, when tested against *S. aureus*, *E. coli* and *P. aeruginosa*. Results obtained from the Bellantone *et al*. (2002) study, are in agreement with Stoor *et al*. (1996), who reported that BAGs are not antibacterial and may only be subject to bacterial adhesion. A large number of *in vitro* studies show that BAGs possess antibacterial properties but one particular *in vivo* study conducted by Xie *et al*. (2008) contradicts such findings. They investigated the efficacy of 45S5 Bioglass® in reducing the rate of infection with *S. aureus* in open fractures in male rabbits. The culture results showed no significant difference between the rates of infection in the control group and in the Bioglass® group. These results indicate that particulate 45S5 Bioglass® may have no antibacterial activity *in vivo*. This may be due to the big buffer system in body fluid which exchanges alkali ions released from the 45S5 Bioglass® with nearby blood and other body fluid, and as a result the ionic concentration and pH at the site of implantation cannot increase to the levels required for bacterial growth inhibition (Xie *et al*., 2008).

Although, BAGs have been found to exert an antibacterial effect on a range of pathogenic bacteria *in vitro*, the addition of antibacterial metal ions within the glass system have also demonstrated antibacterial efficacy. Most research in this field has been done by developing Silver (Ag^{+}) ion doped BAGs which have shown promising results (Ahmed *et al*., 2006; Valappil *et al*., 2007; Pratten *et al*., 2004; Bellantone *et al*., 2002). Copper ion doped phosphate-based glasses have also shown to inhibit bacterial growth (Mulligan *et al*., 2002; Abou Neel *et al*., 2005). Bioactive glasses could potentially be used to deliver antibacterial ions to prevent possible bacterial colonisation of implants following surgery and thus preventing poor tissue integration.

1.6 Biological properties of Gallium

Gallium (Ga^{3+}) was discovered in 1875 by the French chemist P.E.F. Lecoq de Boisbaudran (Bonchi *et al*., 2014). Ga^{3+} is a group IIIa metal, and is present at a concentration of 5 – 15 mg/kg in the earth's crust and is obtained as a by-product from the extraction of aluminium and

zinc ores (Chitamber, 2010). More than 95% of Ga^{3+} consumed is utilised in the electronics industry for optoelectronic devices and integrated in circuits (Collery *et al*., 2002; Chitamber, 2010). Although, Ga^{3+} has no known physiological properties in the human body, it does however possess biological properties. In the 1970s the role of Ga^{3+} in living organisms was demonstrated by using radioactive ^{67}Ga in medical imaging to detect and locate tumour sites (Lessa *et al*., 2012; Bonchi *et al*., 2014). Over the past few decades, ^{67}Ga scanning has been used to detect residual disease or disease that has relapsed following conventional therapy in patients with Hodgkin's and non-Hodgkin's lymphoma (Chitamber, 2010). This phenomenon propelled investigations into the therapeutic applications of Ga^{3+}.

1.6.1 Antineoplastic properties

The ability of Ga^{3+} to localise in tumour cells led researchers to investigate the antineoplastic activity of Ga^{3+} compounds. Based on its clinical efficacy, gallium nitrate proved to be highly effective in the treatment of non – Hodgkin's lymphoma and bladder cancer. Studies revealed that 30% of patients with relapsed lymphomas responded to treatment with Ga^{3+} nitrate. Although, the initial studies were conducted to investigate the antineoplastic activity of Ga^{3+}, the studies also revealed that patients being treated with Ga^{3+} nitrate showed significant decrease in blood calcium levels (Chitamber, 2010). Furthermore, Ga^{3+} nitrate was shown to inhibit increased bone turnover and to decrease osteolysis (active resorption of bone matrix by osteoclasts) in patients with bone metastases from a variety of different cancers and metabolic bone diseases (Chitamber; 2010; Warrell, *et al*., 1984; Warrell, 1997). After extensive clinical studies the Food and Drug Administration (FDA) approved Ga^{3+} nitrate to be used (Ganite™) as a treatment for cancer-associated hypercalcaemia.

1.6.1.1 Mechanisms of action

Since the chemical properties of Ga^{3+} are similar to those of Fe^{3+} many biological systems cannot distinguish between these two metals (Bonchi *et al*., 2014). This similarity allows Ga^{3+} to interact with cellular processes and important proteins, especially those involved in iron

metabolism in mammalian and bacterial cells. *In vivo* studies using ^{67}Ga have revealed that almost all Ga^{3+} in plasma is bound to the iron-transport protein transferrin (Tf) (Lessa *et al*., 2012; Bonchi *et al*., 2014). The complexes formed with Tf are almost as stable as those formed with Fe^{3+}. Gallium not only binds to Tf but also to lactoferrin, which can remove it from Tf, and it can also bind to ferritin. Gallium accumulates in tissues expressing high levels of Tf receptor (TfR), lactoferrin and ferritin receptors (Lessa *et al*., 2012).

Gallium locates in proliferating tissue, including most tumours that express large amounts of TfR and it is due to this feature that tumour cells are rendered susceptible to Ga^{3+} cytotoxicity. Gallium enters the cells via endocytosis and once inside it perturbs cellular Fe^{3+} metabolism by interfering with the uptake of Fe^{3+} via the TfR and also with the endosomal release of Fe^{3+} from Tf to the cytoplasm (Collery *et* al., 2002; Chitamber, 2010). This action deprives the cell of Fe^{3+} which affects the function of the iron-dependent enzyme ribonucleotide reductase, which catalyses the reduction of ribonucleotides into deoxyribonucleotides during DNA synthesis (Collery *et al*., 2002; Lessa *et al*., 2012). Chitamber (2010) determined that the inhibitory effect was exerted through an interaction with the R2 sub-unit of the enzyme that contains a binuclear iron centre essential for enzyme activity. This interaction limits iron availability for R2 activity thus blocking ribonucleotide reductase activity and DNA synthesis. Therefore, Ga^{3+} has a dual action, as it blocks the availability of Fe^{3+} to ribonucleotide reductase and directly inhibits the enzyme.

The iron-mimicking properties of Ga^{3+} may not solely be responsible for its antineoplastic activity as additional mechanisms could also be involved. *In vitro* studies have shown that the presence of Ga^{3+} induces structural changes in DNA. When low concentrations of Ga^{3+} ions are present, Ga^{3+} binds to DNA phosphate forming a stable complex, whereas, at higher concentrations bonds appear between Ga^{3+} and nucleic bases, resulting in DNA destabilisation (Collery *et al*., 2002). However, the association of these interactions with Ga^{3+} antineoplastic activity remain to be determined. Gallium does not only affect DNA synthesis and/or structure

but has also been reported to affect mitochondrial function. Ga^{3+} induces an efflux of Ca^{2+} from mitochondria, which is a necessary step in apoptosis. It has been suggested that the mechanism of action of Ga^{3+} may be targeted towards the mitochondrial membrane pore (Collery *et al*., 2002).

1.6.2 Effects on bone

Animal and clinical investigations into the biological activities of Ga^{3+} revealed the tendency of Ga^{3+} to concentrate in bone. Following administration bone can accumulate large amounts of Ga^{3+}, particularly in those regions where active, bone cell metabolism and thus bone matrix turnover are occurring (i.e. the endosteal and periosteal surfaces of bone) and it is also concentrated in regions of fracture healing (Bockman *et al*., 1990; Bernstein, 1998; Bernstein, 2013). However, the mechanisms of Ga^{3+} accumulation are largely unknown. Accumulation of Ga^{3+} decreases the solubility of hydroxyapatite and renders bone more resistant to resorption (Bockman *et al*., 1990). Furthermore, significant increases in bone calcium and phosphate content are observed in Ga^{3+} treated bone which also makes bone less likely to be resorbed (Chitamber, 2010). Repo *et al*. (1988) found that rat bone treated with Ga^{3+} nitrate was less soluble in acetate buffer and less readily resorbed by monocytes.

Additionally, Ga^{3+} prevents excessive bone resorption by blocking osteoclast activity without being toxic to the osteoclasts, whereas the antiresorptive activity of current therapeutic agents (e.g. bisphosphonates) involves toxicity to osteoclasts. Gallium produced a concentration-dependent inhibition of osteoclast resorption activity when cultured onto the surface of dentin slices (Verron *et al*., 2010). Mills *et al*. (1988) reported that ^{67}Ga citrate almost exclusively localised in the nuclei of osteoclasts however the significance of this localisation remains unclear, but indicates the potential of Ga^{3+} to affect gene expression and protein synthesis in these cells. Verron *et al*. (2010) demonstrated that Ga^{3+} can affect not only osteoclastic resorption but also the formation and differentiation of osteoclasts, as a marked reduction was observed in the expression level of transcripts coding for specific osteoclastic markers. In

addition, to acting directly on osteoclasts and preventing bone resorption, Ga^{3+} can also stimulate bone formation through the action on osteoblasts (Bernstein, 1998). *In vitro* studies have investigated the effects of Ga^{3+} on rat osteogenic sarcoma osteoblast like cells and normal rat osteoblasts. These studies found that Ga^{3+} markedly increased type I collagen (a marker for bone matrix formation) expression whilst vitamin D_3-stimulated OCN mRNA levels were reduced (Guidon *et* al., 1993; Jenis *et al*., 1993; Bockman *et al*., 1993). Contradictory to these earlier findings, Verron *et al*., (2010) found that Ga^{3+} did not affect the activity or viability of primary mouse and MC3T3-E1 osteoblasts (non-transformed cell line established from newborn mouse calvaria).

1.6.3 Antibacterial properties

The first investigation on the antibacterial action of Ga^{3+} was reported in 1931, when Ga^{3+} tartrate was shown to eradicate experimental syphilis in rabbits. However, despite the efficacy and lack of toxicity of Ga^{3+} at high doses, the antibacterial properties of Ga^{3+} were overlooked due to the advent of antibiotics (Bonchi *et al*., 2014; Lessa *et al*., 2012). The ability of Ga^{3+} to interfere with the uptake and utilisation of Fe^{3+} by tumour cells launched investigations in the 1970s to explore whether Ga^{3+} was able to reproduce similar effects in microorganisms.

Due to its ability to interfere with Fe^{3+} metabolism in microorganisms, Ga^{3+} has been extensively investigated as a potential antibacterial agent (Lessa *et al*., 2012). Gallium compounds have been assayed against several Gram-positive and Gram-negative species. Gallium nitrate was found to inhibit growth of *Mycobacterium tuberculosis* and *M. avium* complex extracellularly and within macrophages, which could be reversed by excess Fe^{3+} (Lessa *et al*., 2012). In another study, Ga nitrate inhibited *P. aeruginosa* growth and biofilm formation, and killed planktonic and biofilm bacteria *in vitro* by interfering with Fe^{3+} uptake mechanisms (Chitamber, 2010). Gallium maltolate (GaM) when administered subcutaneously were effective in reducing *S. aureus* colonisation in burn wounds in the thermally injured mouse model (DeLeon *et al*., 2009). Gallium maltolate has also exhibited antibacterial activity

against *S. aureus* and methicillin-resistant *S. aureus* (MRSA) in different growth phases, including in stationary phase and biofilms, however high concentrations were required (Baldoni *et al*., 2010; Arnold *et al*., 2012).

Gallium doped phosphate based glasses (PBGs) have recently been shown to have antibacterial activity (Valappil *et al*., 2008). Incorporating Ga^{3+} into a PBG system allows controlled delivery of Ga^{3+} ions which have been found to reduce biofilm growth of *P. aeruginosa* within 48 hours (Valappil *et al*., 2008). In another study Valappil *et al*. (2008) reported that Ga^{3+} doped PBG demonstrated a bactericidal activity against *E. coli*, *S. aureus* and MRSA. However the degree of the activity varied between the bacterial species, with Gram- negative bacteria found to be the most susceptible to Ga^{3+} action.

1.6.3.1 Mechanisms of action

Iron is an essential nutrient as it acts as a cofactor of crucial enzymes involved in DNA synthesis, metabolism and oxidative stress response (Bonchi *et al*., 2014). The primary defence mechanism in mammalian hosts against infection is limitation of iron (Kelson *et al*., 2013; Ballouche *et al*., 2009). Iron is largely sequestered in either iron-transport proteins such transferrin and lactoferrin, stored intracellularly by ferritin, or bound in heme molecules such that small amounts are in the free form (Kelson *et al* 2013). Since the concentration of free circulating Fe^{3+} is too low for bacteria to grow, they have developed iron-acquisition and uptake mechanisms to sequester Fe^{3+} from the host environment (Kelson *et al*., 2013; Ballouche *et al*., 2009). Bacteria can utilise siderophores, haem acquisitions systems and transferrin/lactoferrin receptors (Kelson *et al*., 2013). Siderophores are small molecules secreted by bacteria that can bind and internalise Fe^{3+}. Haem uptake systems involve receptors that recognise haem, internalising heme via ABC-dependent transporter receptors and removing the Fe^{3+} by haem oxygenases. Some bacteria secrete haemophores, which are proteins that take up heme in the surroundings or extract heme from haemoproteins. Other bacteria can sequester Fe^{3+} directly from transferrin and lactoferrin via receptors that recognise these iron transport proteins

(Kelson *et al*., 2013; Ballouche *et al*., 2009). Despite the various uptake systems employed by pathogenic bacteria, the inability to distinguish Ga^{3+} from Fe^{3+} allows simple Ga^{3+} salts such as Ga^{3+} nitrate and GaM to reduce bacterial growth (Kelson *et al*., 2013; Minandri *et al*., 2014; Arnold *et al*., 2012).

Gallium is virtually irreducible under physiological conditions, whereas Fe^{3+} is readily reduced to Fe^{2+}. Therefore, by competing with Fe^{3+}, Ga^{3+} interferes with bacterial DNA and protein synthesis and blocks the redox reactions that depend on iron electron acquisition (Baldoni *et al*., 2010; Bernstein. 1998). The activity of different iron-containing enzymes such as catalase, superoxide dismutase and ribonucleotide reductase have been shown to be reduced in bacteria that have been exposed to Ga^{3+} (Bonchi *et al*., 2014; Olakanmi *et al*., 2010; Olakanmi *et al*., 2013). The ability of Ga^{3+} to act on several iron dependent enzymes suggests that mutation in a single intracellular target might not produce high level resistance to overcome Ga^{3+} toxicity (Valappil *et al*., 2008; Bonchi *et al*., 2014).

1.7 Aims of study

The aims of this thesis were to:

- Determine the antibacterial efficacy of 3 mol% gallium doped BAG at the concentration of 2.5 mg/ml, 5 mg/ml, 10 mg/ml, 25 mg/ml, 50 mg/ml and 100 mg/ml against clinically relevant microorganisms grown in planktonic cultures. The antibacterial efficacy of 45S5 Bioglass® will also be determined and compared to 3 mol% gallium doped BAG.
- Evaluate the antibacterial efficacy of the particles (direct contact) and dissolution products (indirect contact) of 3 mol% gallium doped BAG and 45S5 Bioglass® against microorganisms in planktonic phase of growth.
- Investigate whether pH influences the antibacterial efficacy of 3 mol% gallium doped BAG and 45S5 Bioglass® following neutralisation, against microorganisms grown in planktonic cultures.
- Assess the cytotoxic effect of 3 mol% gallium doped BAG at the concentration of 2.5 mg, 5 mg, 10 mg, 25 mg, 50 mg and 100 mg against osteosarcoma cell line (Saos-2) and bone marrow derived mesenchymal cells (BMMSCs). Cytotoxicity of 45S5 Bioglass® will also be determined and compared to 3 mol% gallium doped BAG.
- Evaluate the effect of the particles (direct contact) and dissolution products (indirect contact) of both 3 mol% gallium doped BAG and 45S5 Bioglass® on the growth and viability of Saos-2 cells and BMMSCs.
- Investigate the effect of 3 mol% gallium doped BAG and 45S5 Bioglass® on Saos-2 and BMMSCs following pH neutralisation.
- Assess and compare the influence of static incubation conditions and shaker incubation conditions on the antibacterial and cytotoxic activity of 3 mol% gallium doped BAG and 45S5 Bioglass®.

CHAPTER TWO

Antibacterial Activity of Gallium doped Bioactive Glass and 45S5 Bioglass® against Clinically Relevant Microorganisms in Planktonic Phase of Growth

2.1 INTRODUCTION

Since the discovery of 45S5 Bioglass®, BAGs have shown great success in many clinical applications particularly in the dental and orthopaedic fields (Hench, 2006; Jones, 2013). When BAGs were used as therapeutic materials to treat clinical conditions, such as infected frontal sinuses, periodontal defects, and atrophic rhinitis they were found to reduce microbial infections (Xie *et al*., 2008). Based on these results Stoor *et al*. (1998) explored the antibacterial properties of BAGs and in 1998 through experiments *in vitro*, they demonstrated that the bioactive glass S53P4 (53 mol% SiO_2, 23 mol% Na_2O, 20 mol% CaO, and 4 mol% P_2O_5) exhibited antibacterial efficacy on oral bacteria (Xie *et al*., 2008). Since then, *in vitro* studies have been conducted to determine whether BAGs exert similar antibacterial effects on skin pathogenic bacteria. Some authors have shown silicate-based BAGs and 45S5 Bioglass® to be ineffective whereas others have shown it to possess antibacterial activity.

The mechanics involved in tissue integration have extensively been studied and are well known (Tilocca, 2010; Hoppe *et al*., 2011; Hench *et a*/., 2010). However, the mechanisms of antibacterial activity are still not clearly understood. Initial studies on the antibacterial efficacy of BAGs revealed that the activity was attributed to the high aqueous pH values caused by the release of cations such as, $Ca^{2+}$and Na^{+} from BAG particles, when immersed into an aqueous environment (Hench *et al*., 1971; Mortazavi *et al*., 2009). It has also been reported that bacterial adhesion on BAG surfaces is a necessary step towards bacterial inactivation (Hu *et al*., 2009). On the contrary, Allan *et al*. (2000) reported that direct contact between Bioglass® and oral bacteria is not required to produce an antibacterial effect as the dissolution products significantly reduced viability in the absence of Bioglass®. Studies such as those conducted by Stoor *et al.* (1996) and Bellantone *et al*. (2002) demonstrated that BAGs do not possess bacteriostatic or bactericidal activity. The contradictory findings cast doubt on whether BAGs are indeed antibacterial in nature. Differences in the methodology used to measure antibacterial

activity, in the glass particle sizes, and in the bacterial strains may account for these contradictions.

However, other approaches (i.e. incorporation of antibacterial ions) have been shown to enhance the antibacterial activity of silicate-based BAGs, whilst maintaining their bioactivity as well as their osteoinductive and osteoconductive properties. Moreover, BAGs are regarded as potential delivery systems of ions such as Ag^{2+} and Cu^{2+} with known antibacterial properties (Ahmed *et al*., 2006; Valappil *et al*., 2007; Pratten *et al*., 2004; Bellantone *et al*., 2002; Mulligan *et al*., 2002; Abou Neel *et al* 2005). Several *in vitro* experiments have illustrated the successful delivery of antibacterial ions and their inhibitory effect on microorganisms. Another ion which is generating great interest is Ga^{3+}, which has been reported to target bacterial iron metabolism by exploiting the chemical similarities between Fe^{3+} ions and Ga^{3+} ions (Chitamber, 2010; Valappil *et al*., 2008).

In vitro experiments with Ga^{3+} citrate and other Ga^{3+} based compounds provide the evidence that Ga^{3+} ions are antimicrobial in nature (Bonchi *et al*., 2014). The antimicrobial activity of Ga^{3+} ions following their incorporation within phosphate based glass (PBG) systems have also been investigated *in vitro* (Valappil *et al*., 2008). Gallium doped PBG systems have produced promising results *in vitro*, however upon degradation the phosphate component of the glass produces an excessively acidic pH environment and hence cytotoxicity (O'Donnell *et al*., 2009; Abou Neel *et al*., 2009). Furthermore, an acidic pH environment is not desirable for HCA formation (O'Donnell *et al*., 2009; Abou Neel *et al*., 2009) However, the slow degradation rate of silicate based glass systems permits HCA formation. Although, characterisation studies have been performed on Ga^{3+} containing silicate based glasses, antibacterial and cytotoxicity studies have yet to be conducted.

2.2 AIMS

The aims of this part of the study were to:

- Investigate and compare the antibacterial activity of 3 mol% Ga doped silicate based BAG and 45S5 Bioglass®.
- Determine whether the dissolution products released from the BAGs also exhibited antibacterial activity.
- Determine the influence of pH following neutralisation of 3 mol% Ga doped BAG and 45S5 Bioglass®.

A variety of techniques, such as direct and indirect contact, static and shaker incubation conditions were used. *S. aureus* and *E. coli* were chosen to represent Gram-positive and Gram-negative bacteria, respectively.

2.3 METHODS AND MATERIALS

2.3.1 Media preparation

Nutrient agar (Oxoid Ltd, Basingstoke, UK) and nutrient broth (Oxoid Ltd, Basingstoke, UK) were prepared according to the manufacturer's instructions and autoclaved at 121ºC. After sterilisation, 20 ml of nutrient agar (NA) was poured into petri dishes and allowed to set at room temperature, and 10 ml of nutrient broth (NB) was dispensed into universals, which were refrigerated at 4ºC.

2.3.2 Microorganisms

E. coli (NCTC 10538) and *S. aureus* (ATCC 6538) were stored at – 70ºC on MicroBank beads (Pro-Lab Diagnostics, Neston, Cheshire, UK) until required. When required, the isolates were revived by culture onto appropriate media and incubated according to the requirements of the organism. To reduce contamination and maintain viability, cultures were sub-cultured onto fresh plates on a weekly basis.

2.3.3 Standard curves

Overnight cell suspensions of *S. aureus* and *E. coli* were prepared in NB and incubated at 37ºC. At each time point (0, 1, 2, 3, 4, 5, 6, 7, 8, and 24 hours), 1 ml was removed from the cell suspension and the optical density (OD) was read in a spectrophotometer set to 600 nm following appropriate broth blanking. A range of serial dilutions from 10^{-1} to 10^{-8} were made and were plated onto NA plates and incubated overnight at 37ºC. The colony forming units (CFU)/ml were determined for each test microorganism and then plotted against OD.

2.3.4 Preparation of starter cultures

Starter cultures for each test microorganism were prepared following inoculation of NB with a single colony from nutrient agar NA plates. After a 24 hour incubation period at 37ºC, the concentration of microorganism in each starter culture was determined by OD (600 nm) and

compared to the standard curve described in section 2.3.3. The cultures were then diluted in NB as required to generate a final working concentration of 10^6 CFU/ml.

2.3.5 Glass preparations

45S5 Bioglass® was selected for this study as it is the most widely used BAG within the orthopaedic and dental fields. In addition a BAG was prepared with a similar composition but containing 3 mol% Ga_2O_3. 45S5 Bioglass® was prepared using $CaCO_3$ (Alfa Aesar, Lancashire, UK) SiO_2 (Alfa Aesar, Lancashire, UK), Na_2CO_3 (Sigma-Aldrich, Dorset, UK), H_6NO_4P (Fluka, Dorset UK). 3 mol% Ga doped BAG was prepared using $CaCO_3$ (Alfa Aesar, Lancashire, UK) SiO_2 (Alfa Aesar, Lancashire, UK), Na_2CO_3 (Sigma-Aldrich, Dorset, UK), H_6NO_4P (Fluka, Dorset UK) and Ga_2O_3 (Alfa Aesar, Lancashire, UK) as starting materials. The precursors were weighed, thoroughly mixed and placed into a 59 ml volume (90% platinum and 10% rhodium) crucible. The crucible was placed into a furnace at room temperature and then heated at 10ºC/min to1450ºC and held at this temperature for 90 minutes. Glass was then poured into a graphite mould that had been preheated to 370ºC. The graphite mould was placed back into the furnace and left overnight to slowly cool to room temperature. The glass rod was ground into particles (<63 microns) using a pestle and mortar and the particles were selected using a 63 micron sieve. The overall composition of 45S5 Bioglass® and 3 mol% Ga doped BAG are in table 2.1.

	SiO_2 (mol%)	Na_2O (mol%)	CaO (mol%)	P_2O_5 (mol%)	Ga_2O_3 (mol%)
45S5 Bioglass®	46.1	24.4	26.9	2.6	0
3 mol% Ga doped BAG	43.8	23.5	25.5	2.47	3

Tale 2.1 Glass compositions.

2.3.6 pH analysis

2.3.6.1 pH analysis at concentrations 25-100 mg/ml

To determine the aqueous pH value of 3 mol% Ga doped BAG and 45S5 Bioglass® at concentrations of 25 mg, 50 mg and 100 mg, triplicate stock solutions (mg/ml) were prepared in 5 ml NB. Nutrient broth (5 ml) without particles served as the control. The particle suspensions and controls were incubated overnight at 37°C, and pH was measured using the Mettler Toledo pH probe (Fisher Scientific, Loughborough, UK) following 0, 6, 24, 48, 72 and 96 hours of incubation.

2.3.6.2 pH analysis at concentrations 2.5-10 mg/ml

To determine the aqueous pH value of 3 mol% Ga doped BAG and 45S5 Bioglass® at concentrations of 2.5 mg, 5 mg and 10 mg, triplicate stock solutions (mg/ml) were prepared in 5 ml NB. Nutrient broth (5 ml) without glass particles served as the control. The stock solutions and controls were incubated overnight at 37°C in static and shaker (with a shaking speed of 100 rpm) incubators. The pH of the stock solutions and controls was measured using the Mettler Toledo pH probe, following 24, 48, 72 and 96 hours of incubation.

2.3.7 Determination of the antibacterial activity of 3 mol% Ga doped BAG and 45S5 Bioglass®

2.3.7.1 Direct contact

Prior to their use, the particles were UV sterilised (wavelength of 365 nm) at a distance of 18.5 cm for 15 minutes in a UV Chromato-Vue viewing cabinet (UVP, Germany). UV sterilised particles of 3 mol% Ga doped BAG and 45S5 Bioglass® at 2.5 mg, 5 mg, 10 mg, 25 mg, 50 mg and 100 mg were added to triplicate 1 ml NB solutions. Nutrient broth without the particles served as the control. Samples were inoculated with the test microorganisms to give a final microbial concentration of 10^6 CFU/ml within the test carrier, then incubated overnight at 37ºC. Antibacterial properties of 3 mol% Ga doped BAG and 45S5 Bioglass® particles were evaluated under two different incubation conditions: - static and shaker (100 rpm). At each

time point (24, 48, 72 and 96 hours) the samples were removed, and following a serial dilute (10^{-1} to 10^{-8}) 100 µl aliquots were spread onto NA plates, which were then incubated overnight at 37ºC. Following incubation, the total viable count was determined, and log growth reductions calculated.

Log growth reduction = log cfu (control) – log cfu (sample) (Wiegand *et al*., 2015).

2.3.7.2 Indirect contact

Triplicate stock solutions (mg/ml) were prepared for UV sterilised 3 mol% Ga doped BAG and 45S5 Bioglass® particles at 2.5 mg, 5 mg, 10 mg and 100 mg in 5 ml NB. Nutrient broth (5 ml) without particles served as the control. The stock solutions were incubated for 72 hours at 37ºC in both static and shaker (with a shaking speed of 100 rpm) incubators. Following the 72 hour incubation period the stock solutions were filtered using a 0.45 micron syringe filter (Sartorius Stedim Biotech, Goettingen, Germany). One ml was removed from the filtered stock solution and inoculated with the test microorganisms at a final concentration of 10^6 CFU/ml. The inoculated samples were incubated at 37ºCover a 96 hour period. The pH of the stock solution was measured using the Mettler Toledo pH probe. Following 24 and 96 hours of incubation serial dilutions ranging from 10^{-1} to 10^{-8} were performed, and 100 µl aliquots were spread onto NA plates, which were incubated overnight at 37ºC Following incubation, the total viable count was determined, and log growth reductions calculated.

2.3.8 Determination of the antibacterial activity of 3 mol% Ga doped BAG and 45S5 Bioglass® following pH neutralisation

2.3.8.1Direct contact

UV sterilised particles of 3 mol% Ga doped BAG and 45S5 Bioglass® at 2.5 mg, 5 mg and 10 mg were added to triplicate 1 ml NB solutions. Nutrient broth without the 3 mol% Ga doped BAG and 45S5 Bioglass® particles served as the control. The samples were incubated overnight

at 37ºC in both static and shaker (100 rpm) incubators. After an overnight incubation period the samples were removed and pH readings obtained using pH probe. Once the pH was measured the samples were neutralised to pH 7.5. To achieve this 0.1M of hydrochloric (HCl) (Fisher Scientific, Loughborough, UK) acid was used with pH indicator strips (Life Technologies, Paisley, UK). The neutralised samples were inoculated with the test microorganisms at 10^6 CFU/ml, incubated overnight at 37ºC in both static and shaker (100 rpm) incubators. At each time point the samples were removed and the pH was measured, and if required the pH was further neutralised to 7.5 to ensure the pH remained in the range. Subsequently, serial dilutions ranging from 10^{-1} to 10^{-8} were performed, followed by 100 µl aliquots being spread onto NA plates that were incubated overnight at 37ºC. Following incubation total viable count was determined, and log growth reductions calculated.

2.3.8.2 Indirect contact

Triplicate stock solutions (mg/ml) were prepared for UV sterilised 3 mol% Ga doped BAG and 45S5 Bioglass® particles at 2.5 mg, 5 mg and 10 mg in 5 ml NB. Nutrient broth without 3 mol% Ga doped BAG and 45S5 Bioglass® particles served as the control. The stock solutions were incubated for 72 hours at 37ºC in both static and shaker (with a shaking speed of 100 rpm) incubators. Following the 72 hour incubation period the stock solutions were filtered using a 0.45 micron syringe filter. One ml was removed and neutralised to achieve a pH of 7.5 using 0.1M of HCl and inoculated with the test microorganisms at 10^6 CFU/ml. The remainder of the stock solution was used to measure the pH using a pH probe. The samples were incubated at 37ºC and after 24 and 96 hours of incubation, the samples were removed and pH measured using pH strips, serial dilutions from 10^{-1} to 10^{-8} were performed and 100 µl aliquots spread onto NA plates, which were incubated overnight at 37ºC. Following incubation, the total viable count was determined, and log growth reductions calculated.

2.3.9 Investigation of bacterial cell adhesion on 3 mol% Ga doped BAG and 45S5 Bioglass® particles by Scanning Electron Microscopy

Ten mg of 3 mol% Ga doped BAG and 45S5 Bioglass® particles were added to 1 ml NB and inoculated with the test microorganisms at 10^6 CFU/ml. Glass cover slips (12 mm) (Fisher Scientific, Loughborough, UK) inoculated with the test microorganisms served as the control. Following a 24 and 96 hour incubation period at 37°C, NB was removed and serial dilutions ranging from 10^{-1} to 10^{-8} were performed and 100 µl aliquots spread onto NA plates, which were incubated overnight at 37ºC. Total viable count was determined and log growth reductions calculated following overnight incubation. The particles were then fixed with 2.5% glutaraldehyde v/v in 0.1% w/v sodium cacodylate buffer (pH 7.4) for 10 minutes, followed by dehydration in graded ethanol series to 100% ethanol. Following the completion of the dehydration step, 100% ethanol was replaced by hexamethyldisilazane (HMDS) (Sigma Aldrich, Dorset, UK), which was left overnight in a fume cupboard to evaporate. The samples were mounted onto SEM stubs and gold-coated prior to observation with a Carl Zeiss EVO MA10 scanning electron microscope (SEM).

2.3.10 Statistical analysis

Two-way analysis of variance (ANOVA) was carried out to determine statistical significances (GraphPad Prism 6.0). If a significant difference was detected a Tukey test and a Sidak's test (for the neutralised experiments) were carried out to determine which values were significantly different. Differences were considered statistically significant at a level of $P < 0.05$.

2.4 RESULTS

2.4.1 pH analysis of 3 mol% Ga doped BAG and 45S5 Bioglass® particles at concentrations 25 mg – 100 mg/ml

The pH values of 45S5 Bioglass® and 3 mol% Ga doped BAG suspensions (Table 2.2) increased with the increase of BAG concentration over a 96 hour period. The pH value of NB prior to the addition of BAG particles was 8.01. Within 6 hours of soaking the pH values of 45S5 Bioglass® particles increased from 8.01 to 10.4, 10.6 and 10.8, for 25 mg/ml, 50 mg/ml and 100 mg/ml, respectively. A similar increase was also observed for the particles of 3 mol% Ga doped BAG, the pH values were 10, at 25 mg/ml, 10.6 at 50 mg/ml and 10.7 at 100 mg/ml, respectively. A further increase in the pH values occurred for 45S5 Bioglass® and 3 mol% Ga doped BAG suspensions at 24 hours for all the concentrations tested. However, 25 mg/ml of 3 mol% Ga doped BAG did not reach a pH of 11 until 72 hours of soaking.

	25 mg/ml	50 mg/ml	100 mg/ml
Time (hours)	**pH**	**pH**	**pH**
0	8.01	8.01	8.01
6	10.4	10.6	10.8
24	11.0	11.1	11.2
48	11.0	11.2	11.4
72	11.1	11.4	11.5
96	11.1	11.0	11.5

	25 mg/ml	50 mg/ml	100 mg/ml
Time (hours)	**pH**	**pH**	**pH**
0	8.01	8.01	8.01
6	10.4	10.6	10.7
24	10.9	11.2	11.4
48	10.9	11.3	11.3
72	11.0	11.3	11.3
96	11.1	11.2	11.3

Table 2.2 The pH values of 45S5 Bioglass® (top) and 3 mol% Ga doped BAG (bottom) particles at variable concentrations, immersed in NB over a 96 hour period.

2.4.2 The antibacterial effect of 3 mol% Ga doped BAG and 45S5 Bioglass® at concentrations 25 mg – 100 mg/ml

2.4.2.1 Direct contact

As shown in figure 2.1, 3 mol% Ga doped BAG and 45S5 Bioglass® particles exhibited a significant ($p = < 0.0001$) antibacterial effect against *E. coli*. Complete growth inhibition was observed at 24 hours, for *E. coli* cultured with 50 and 100 mg/ml of 3 mol% Ga doped BAG ($p = < 0.0001$) and 45S5 Bioglass® ($p = < 0.0001$) particles. At 24 hours, 25 mg/ml of 3 mol% Ga doped BAG particles exhibited a significant antibacterial effect against *E. coli*, with a log reduction of 6.45, whereas a log reduction of 5.57 was observed for the particles of 45S5 Bioglass®. The lower concentrations (25 mg/ml and 50 mg/ml) of both BAGs did not exhibit an antibacterial effect against *S. aureus* over a 96 hour incubation period (Figure 2.2). However the higher concentration tested, 100 mg/ml for both BAGs demonstrated a significant ($p = <0.0001$) growth inhibitory effect at 96 hours.

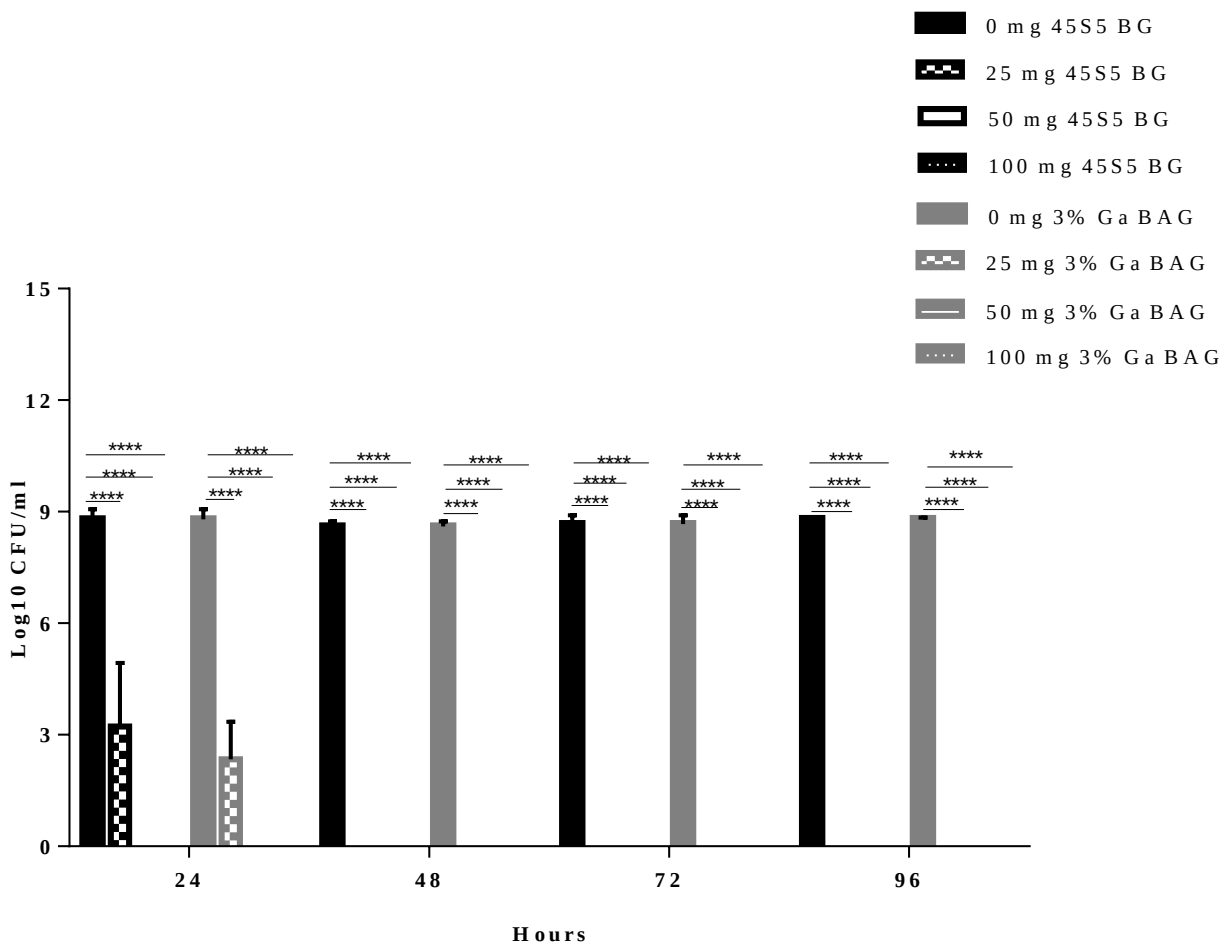

Figure 2.1 The antibacterial effect of 45S5 Bioglass® and 3 mol% Ga doped BAG particles against *E. coli*, at 25, 50 and 100 mg/ml over a 96 hour period. Data shown are expressed as mean (n=3) CFU/ml.

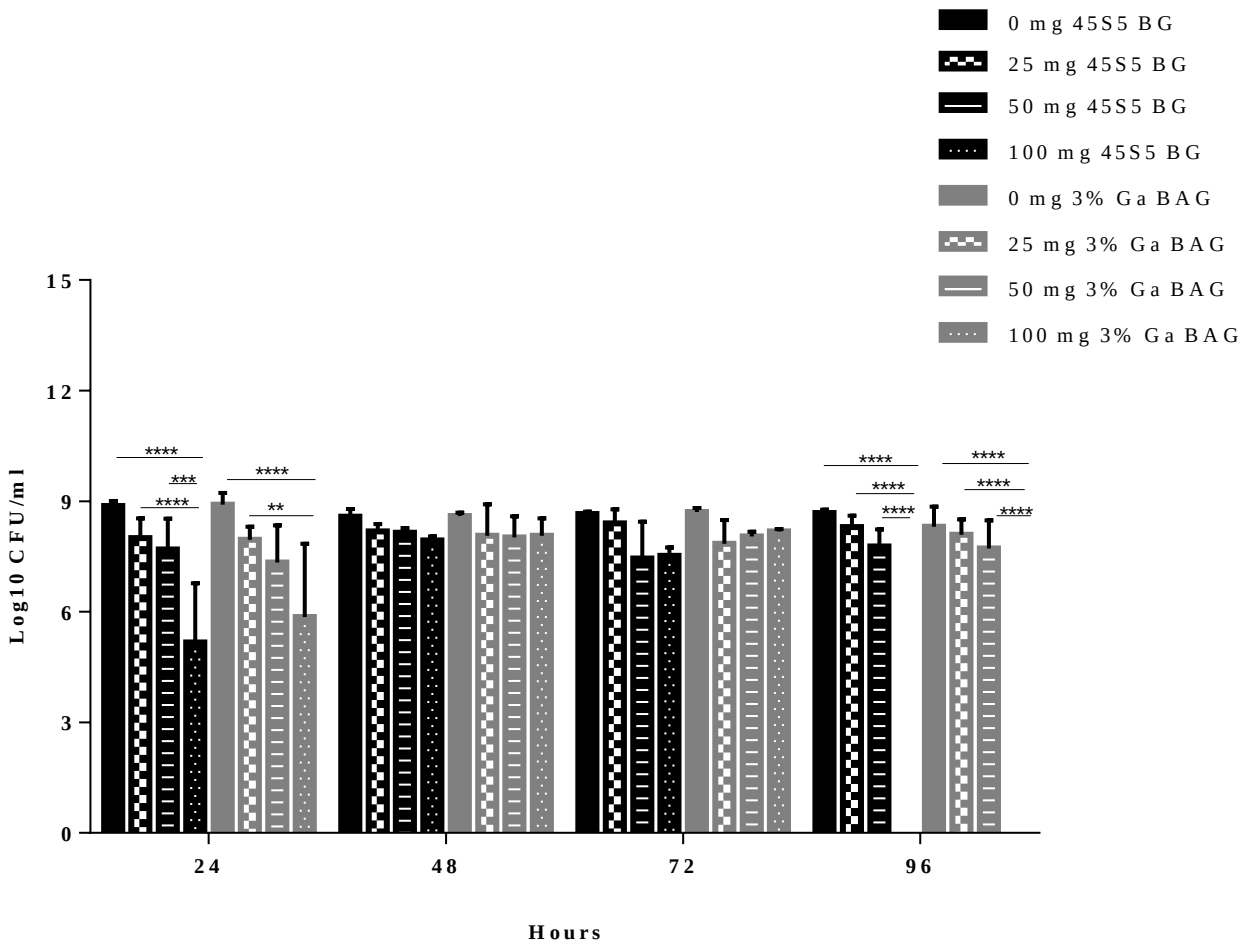

Figure 2.2 The antibacterial effect of 45S5 Bioglass® and 3 mol% Ga doped BAG particles against *S. aureus*, at 25, 50 and 100 mg/ml over a 96 hour period. Data shown are expressed as mean (n=3) CFU/ml.

2.4.2.2 Indirect contact

Figures 2.3 shows the antibacterial effect of the dissolution products of 3 mol% Ga doped BAG and 45S5 Bioglass® when tested against *E. coli*, at 100 mg/ml. At 24 hours, the dissolution products of 3 mol% Ga doped BAG and 45S5 Bioglass® completely inhibited ($p = < 0.0001$) the growth of *E. coli*, with a log reduction of 8.38. Figure 2.4 shows the antibacterial effect of the dissolution products for both BAGs when tested against *S. aureus*. 45S5 Bioglass® exerted a greater antibacterial action ($p = < 0.0001$) as *S. aureus* growth was completely inhibited within 24 hours, whilst the dissolution products of 3 mol% Ga doped BAG ($p = < 0.0001$) reduced *S. aureus* growth with a log reduction of 6.47.

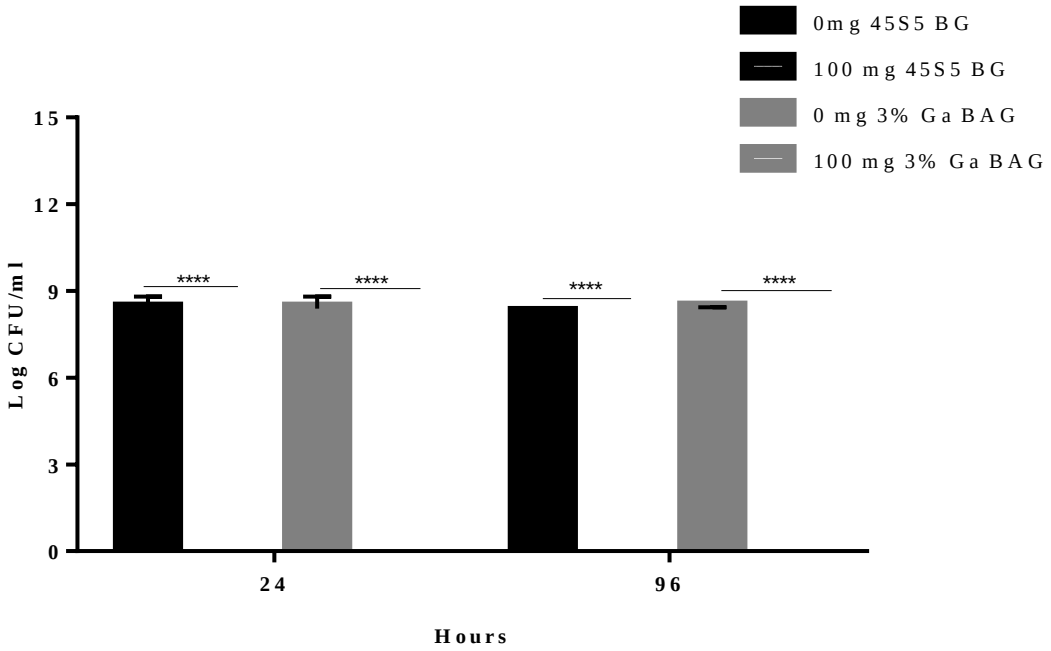

Figure 2.3 The antibacterial effect of 45S5 Bioglass® and 3 mol% Ga doped BAG dissolution products against *E. coli* at 100 mg/ml over a 96 hour period. NB was conditioned with 100 mg/ml of 45S5 Bioglass® and 3 mol% Ga doped BAG particles and kept in a static incubator. Data shown are expressed as mean (n=3) CFU/ml.

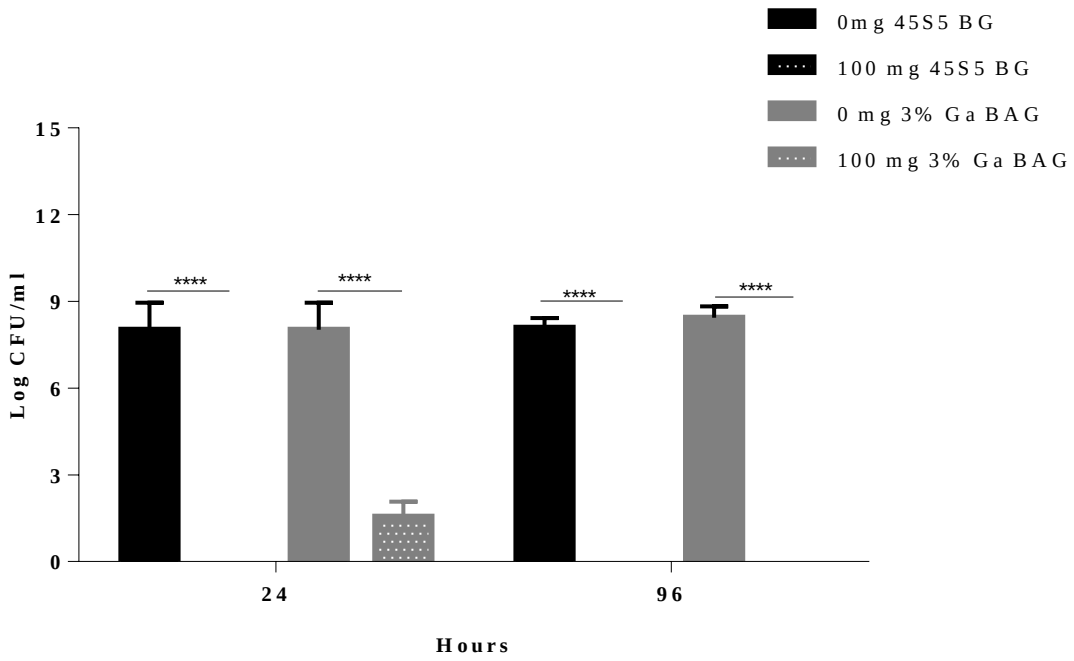

Figure 2.4 The antibacterial effect of 45S5 Bioglass® and 3 mol% Ga doped BAG dissolution products against *S.* aureus, over a 96 hour period. NB was conditioned with 100 mg/ml of 45S5 Bioglass® and 3 mol% Ga doped BAG particles and kept in a static incubator. Data shown are expressed as mean (n=3) CFU/ml

2.4.3 pH analysis of 3 mol% Ga doped BAG and 45S5 Bioglass® particles at concentrations 2.5 -10 mg

pH values of NB containing 45S5 Bioglass® and 3 mol% Ga doped BAG particles increased with the increase of particles under both static (Figure 2.5) and shaker (Figure 2.6) incubation conditions. Nutrient broth containing 45S5 Bioglass® showed a statistically significant ($p = < 0.0001$) pH rise, which rose to 8.8, 9.2 and 9.5 for 2.5, 5 and 10 mg/ml concentrations, respectively, after 24 hours under static incubation conditions. Similarly, pH values for NB containing 3 mol% Ga doped BAG particles also significantly ($p = < 0.0001$) increased to 8.8, 9.1 and 9.4 for 2.5, 5 and 10 mg/ml concentrations, respectively, in comparison to NB without particles. Enquire

Under shaker incubation conditions the pH values of the variable concentrations tested increased. The pH values significantly ($p = < 0.0001$) increased to 8.7, 9.2, and 9.6 for 45S5 Bioglass® particle concentrations 2.5, 5 and 10 mg/ml, respectively, after 24 hours. Likewise, 3 mol% Ga doped BAG particles also raised the pH of the NB to 8.8, 9.2 and 9.5 for 2.5, 5 and 10 mg/ml concentrations. A further increase in pH was not observed for either 45S5 Bioglass® and 3 mol% Ga doped BAG particles after the initial increase reported at 24 hours for static and shaker incubation conditions.

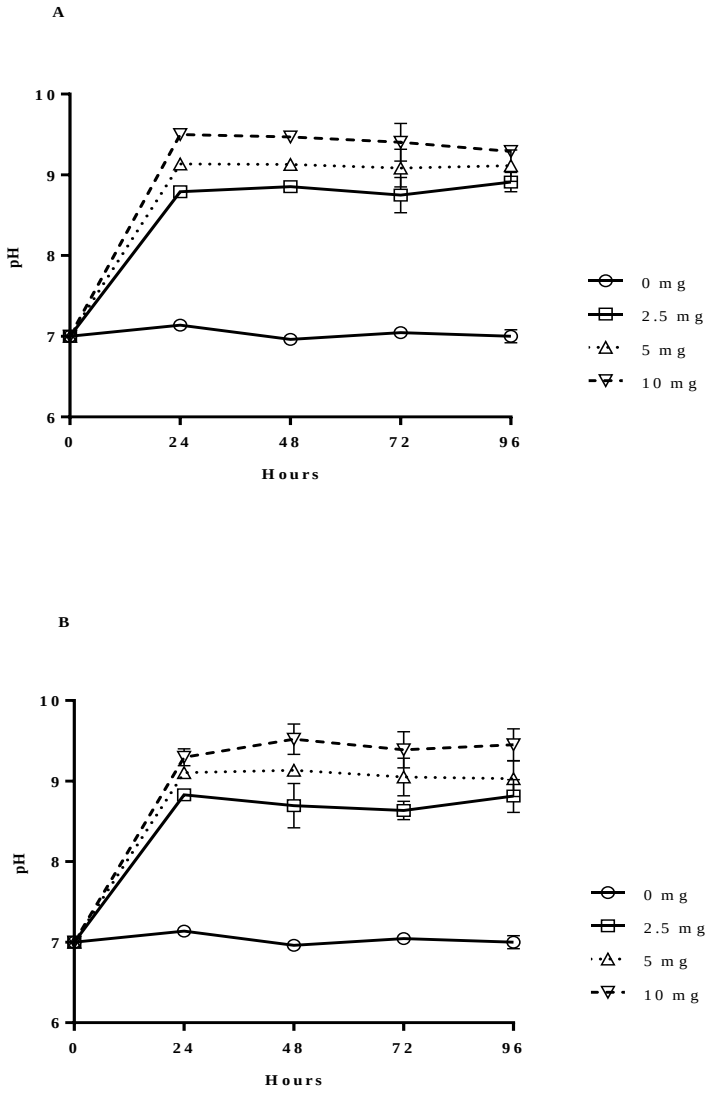

Figure 2.5 pH analysis of variable concentrations of (**A**) 45S5 Bioglass® and (**B**) 3 mol% Ga doped BAG particles immersed in NB over a 96 hour period, under static incubation conditions. Data shown are expressed as means ± SD (n=2).

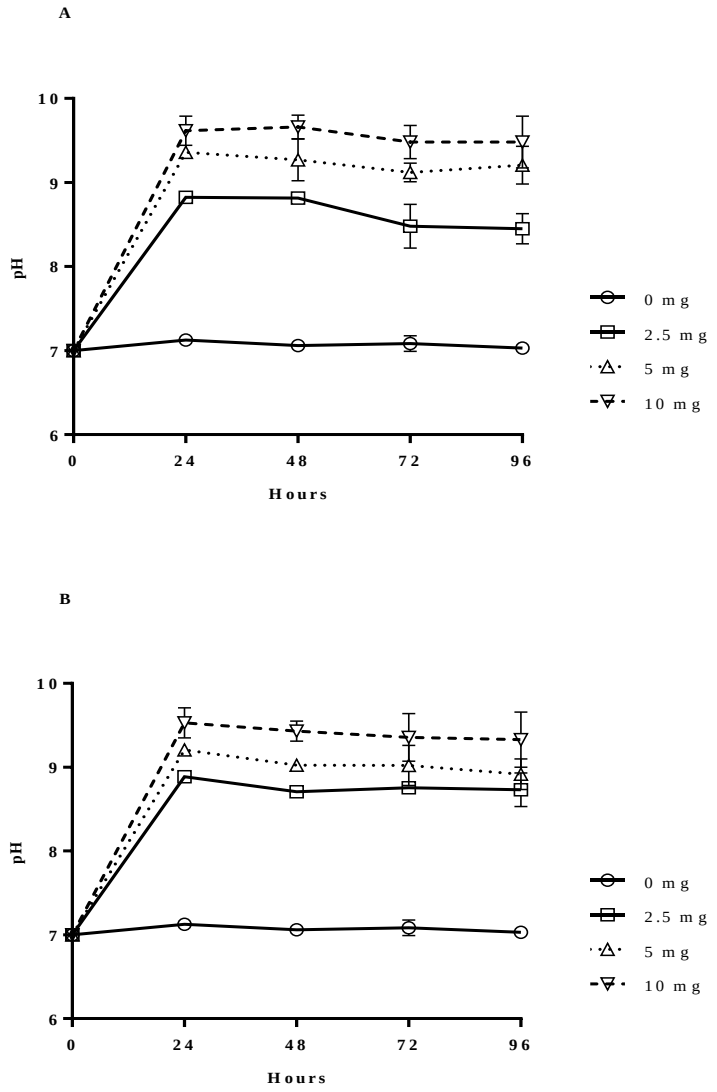

Figure 2.6 pH analysis of variable concentrations of (**A**) 45S5 Bioglass® and (**B**) 3 mol% Ga doped BAG particles immersed in NB over a 96 hour period, under shaker incubation conditions. Data shown are expressed as means ± SD (n=2).

2.4.4 Determination of the antibacterial activity of 3 mol% Ga doped BAG and 45S5 Bioglass® at concentrations 2.5-10 mg/ml

2.4.4.1 Direct contact

2.4.4.1.1 Static incubation conditions

As shown in figure 2.7, 3 mol% Ga doped BAG and 45S5 Bioglass® particles exhibited a statistically significant antibacterial effect ($p = < 0.0001$) against *E. coli* at the concentration of 10 mg/ml. A log reduction of 5.40 and 4.21 was observed at 24 hours, for *E. coli* cultured with 3 mol% Ga doped BAG ($p =< 0.0001$) and 45S5 Bioglass® ($p =< 0.0001$) particles, respectively. Despite a reduction in the number of viable cells at the earlier time points, at 96 hours a rise was observed for *E. coli* cultured with 3 mol% Ga doped BAG particles. The particles of 45S5 Bioglass® however continued to significantly reduce *E. coli* growth with a log reduction of 7.73 ($p = < 0.0001$), whereas 3 mol% Ga doped BAG particles caused a log reduction of 6.93 ($p = < 0.0001$). No statistical significant difference was observed between the two glass types.

Figure 2.8 shows the antibacterial effect of 3 mol% Ga doped BAG and 45S5 Bioglass® particles against *S. aureus*. 3 mol% Ga doped BAG and 45S5 Bioglass® particles did not display a similar antibacterial action against *S. aureus* as *E. coli*. A statistical difference was observed at 72 ($p = < 0.01$) and 96 ($p = < 0.05$) hours between control (0 mg/ml) cultures and *S. aureus* cultures containing 10 mg/ml of 45S5 Bioglass®.

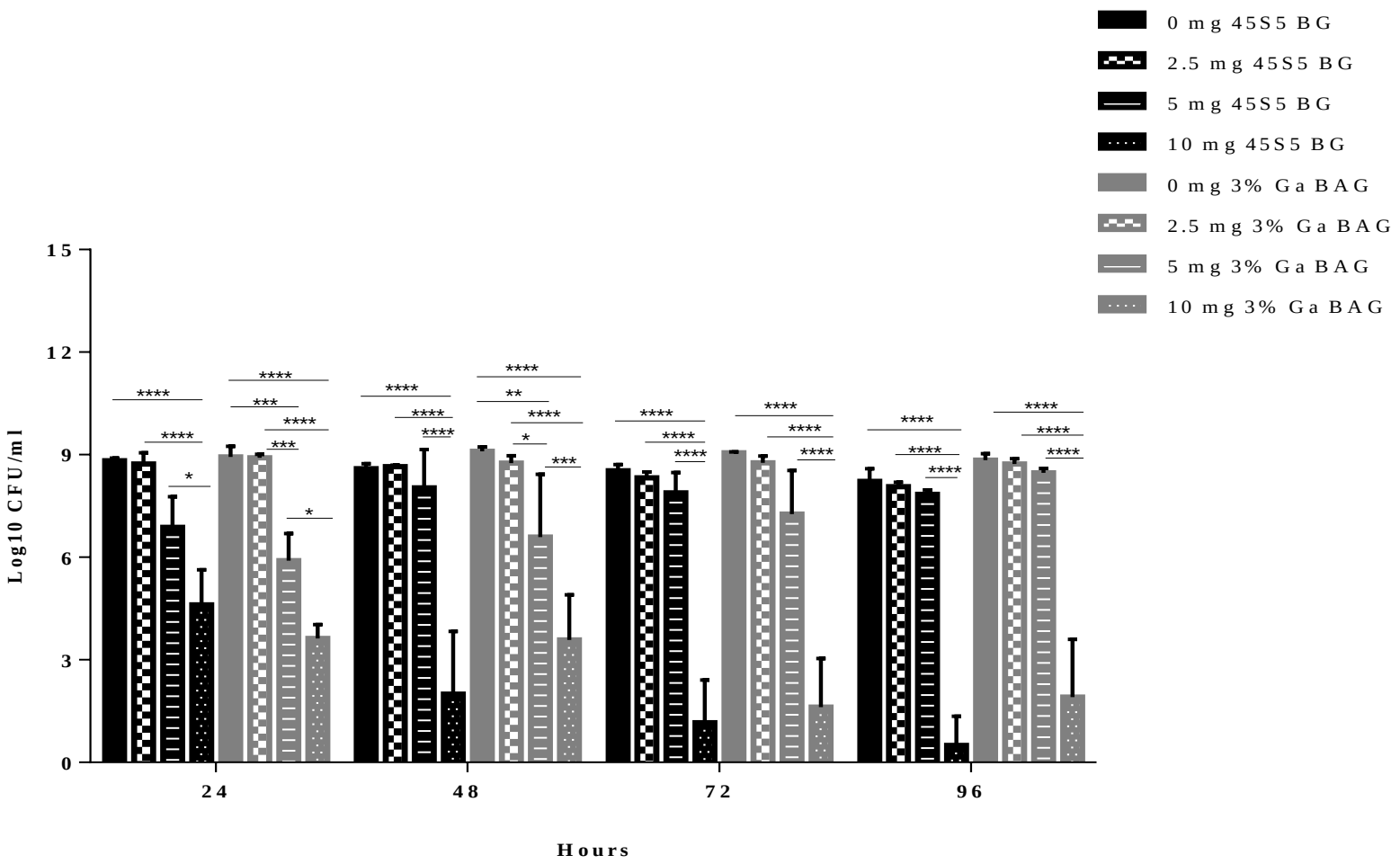

Figure 2.7 The antibacterial effect of 45S5 Bioglass® and 3 mol% Ga doped BAG particles at varying concentrations against *E. coli* under static incubation conditions, over a 96 hour period. Data shown are expressed as mean (n=3) CFU/ml.

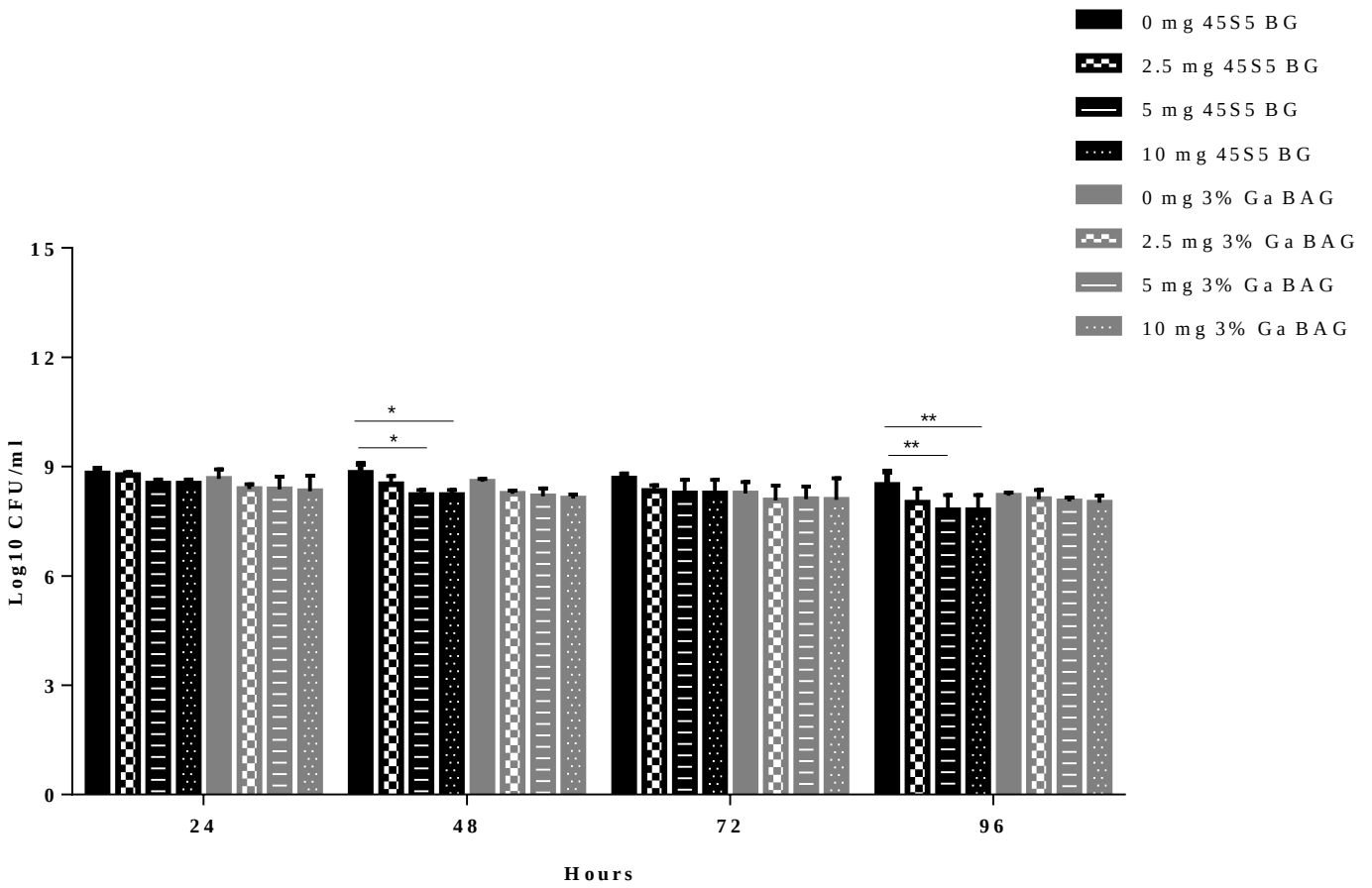

Figure 2.8 The antibacterial effect of 45S5 Bioglass® and 3 mol% Ga doped BAG particles at varying concentrations against *S.* aureus under static incubation conditions over a 96 hour period. Data shown are expressed as mean (n=3) CFU/ml.

2.4.4.1.2 Shaker incubation conditions

Under shaker incubation conditions at 10 mg/ml 3 mol% Ga doped BAG and 45S5 Bioglass® particles totally inhibited *E. coli* growth within 48 hours ($p = < 0.0001$), with a log reduction of 9.26 and 9.45, respectively (Figure 2.9). 45S5 Bioglass® revealed a significant antibacterial activity ($p = < 0.0001$) as a 1.58 log reduction was seen for 5 mg/ml at 48 hours. Lower concentrations of 3 mol % Ga doped BAG also exhibited a significant antibacterial effect at the earlier time points ($p = < 0.0001$), similarly to 45S5 Bioglass®.

3 mol% Ga doped BAG and 45S5 Bioglass® particles did not inhibit *S. aureus* under shaker incubation conditions (Figure 2.10). A statistical significant ($p = < 0.01$) reduction was observed for *S. aureus* cultures containing 10 mg/ml of 45S5 Bioglass® particles at 24 hours, but following 24 hours no further reduction was noted.

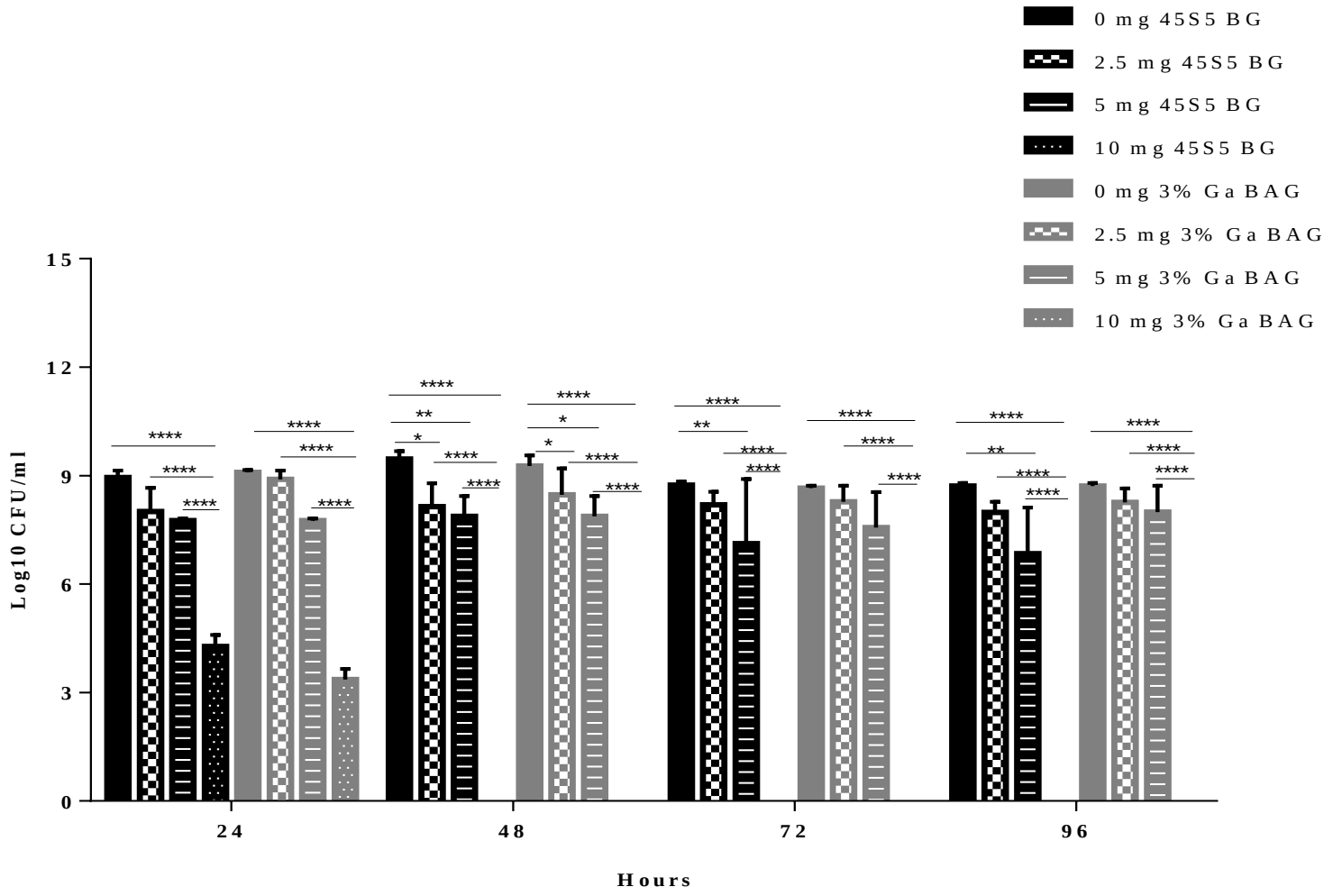

Figure 2.9 The antibacterial effect of 45S5 Bioglass® and 3 mol% Ga doped BAG particles at varying concentrations against *E.* coli under shaker incubation conditions over a 96 hour period. Data shown are expressed as mean (n=3) CFU/ml.

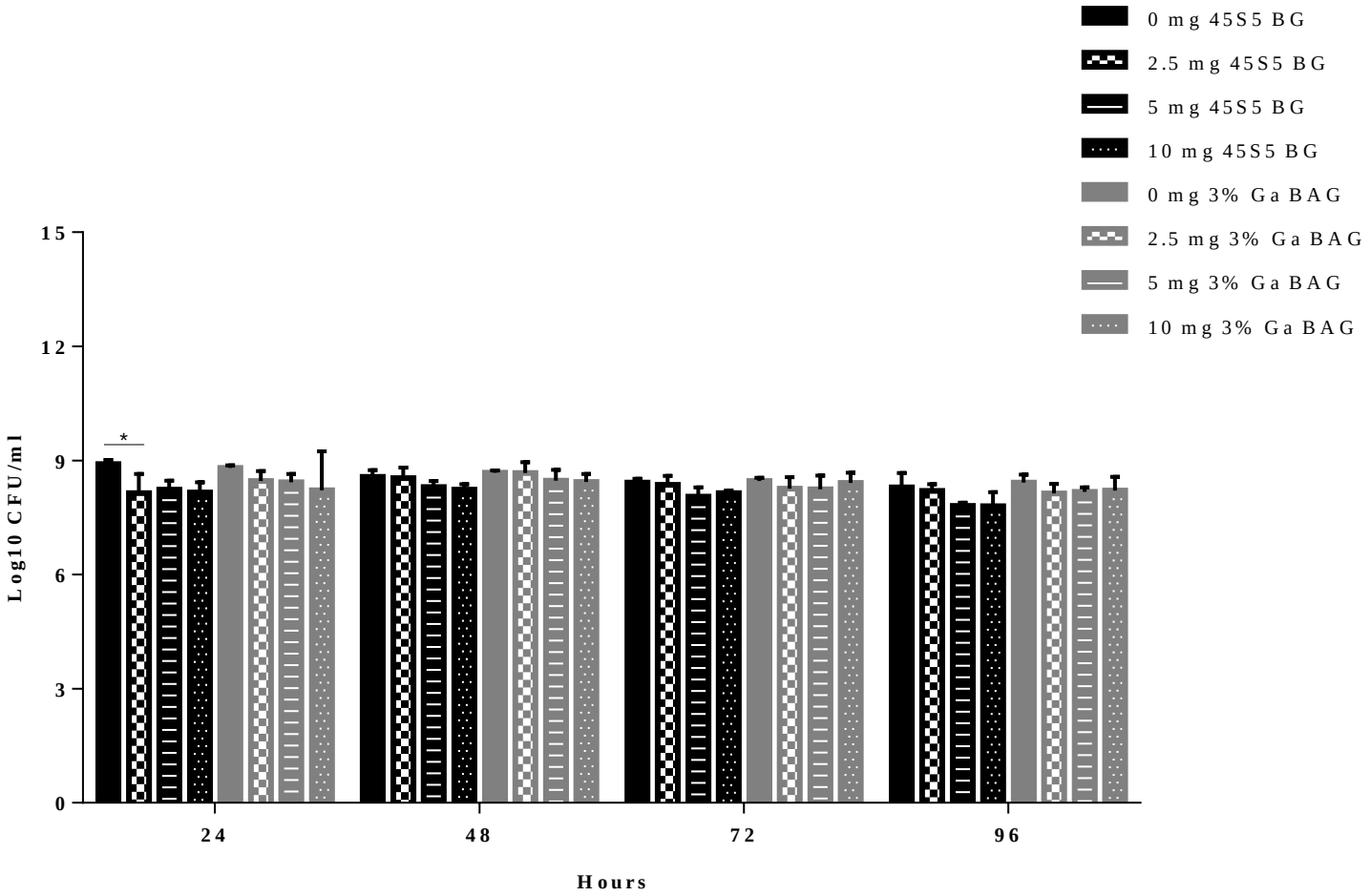

Figure 2.10 The antibacterial effect of 45S5 Bioglass® and 3 mol% Ga doped BAG particles at varying concentrations against *S. aureus* under shaker incubation conditions over a 96 hour period. Data shown are expressed as mean (n=3) CFU/m

2.4.4.2 Indirect contact

2.4.4.2.1 Static incubation conditions

Figure 2.11 shows the antibacterial effect of the dissolution products of 3 mol% Ga doped BAG and 45S5 Bioglass® when tested against *E. coli*. At 24 hours the dissolution products of 45S5 Bioglass® displayed a statistical significant antibacterial effect against *E. coli* at 5 mg/ml ($p = 0.009$) and 10 mg/ml ($p = 0.001$), with log reductions of 1.08 and 1.33 respectively. In contrast, no antibacterial effect was observed for the dissolution products of 3 mol% Ga doped BAG particles. However, at 96 hours the dissolution products of 3 mol% Ga doped BAG at 10 mg/ml exhibited a significant ($p = < 0.05$) antibacterial effect with a log reduction of 1.17, whilst 45S5 Bioglass® did not demonstrate a statistical significant reduction in the antibacterial effect with a log reduction of 1.

The antibacterial activity of the dissolution products of 3 mol% Ga doped BAG and 45S5 Bioglass® when tested against *S. aureus* can be seen in figure 2.12. It was found that at 24 hours the dissolution products of 45S5 Bioglass® demonstrated a significant antibacterial effect at 5 mg/ml and 10 mg/ml ($p = < 0.01$), whilst those of 3 mol% Ga doped BAG possessed no antibacterial activity. At 96 hours the dissolution products of 45S5 Bioglass® were unable to maintain the antibacterial effect achieved at 24 hours.

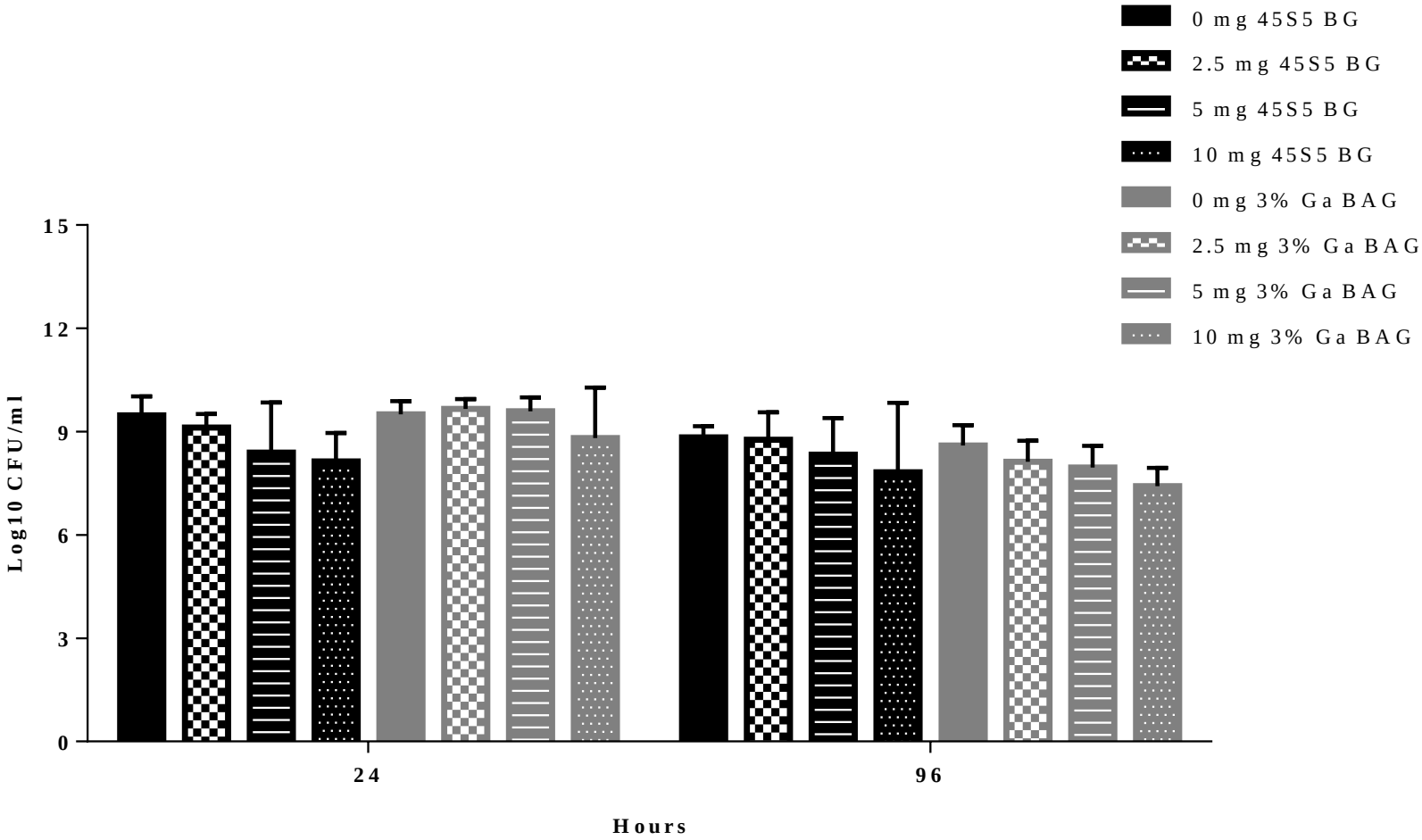

Figure 2.11 The antibacterial effect of the dissolution products of 45S5 Bioglass® and 3 mol% Ga doped BAG against *E.* coli over a 96 hour period. NB was conditioned with variable concentrations of 45S5 Bioglass® and 3 mol% Ga doped BAG particles and kept in a static incubator. Data shown are expressed as mean (n=3) CFU/ml.

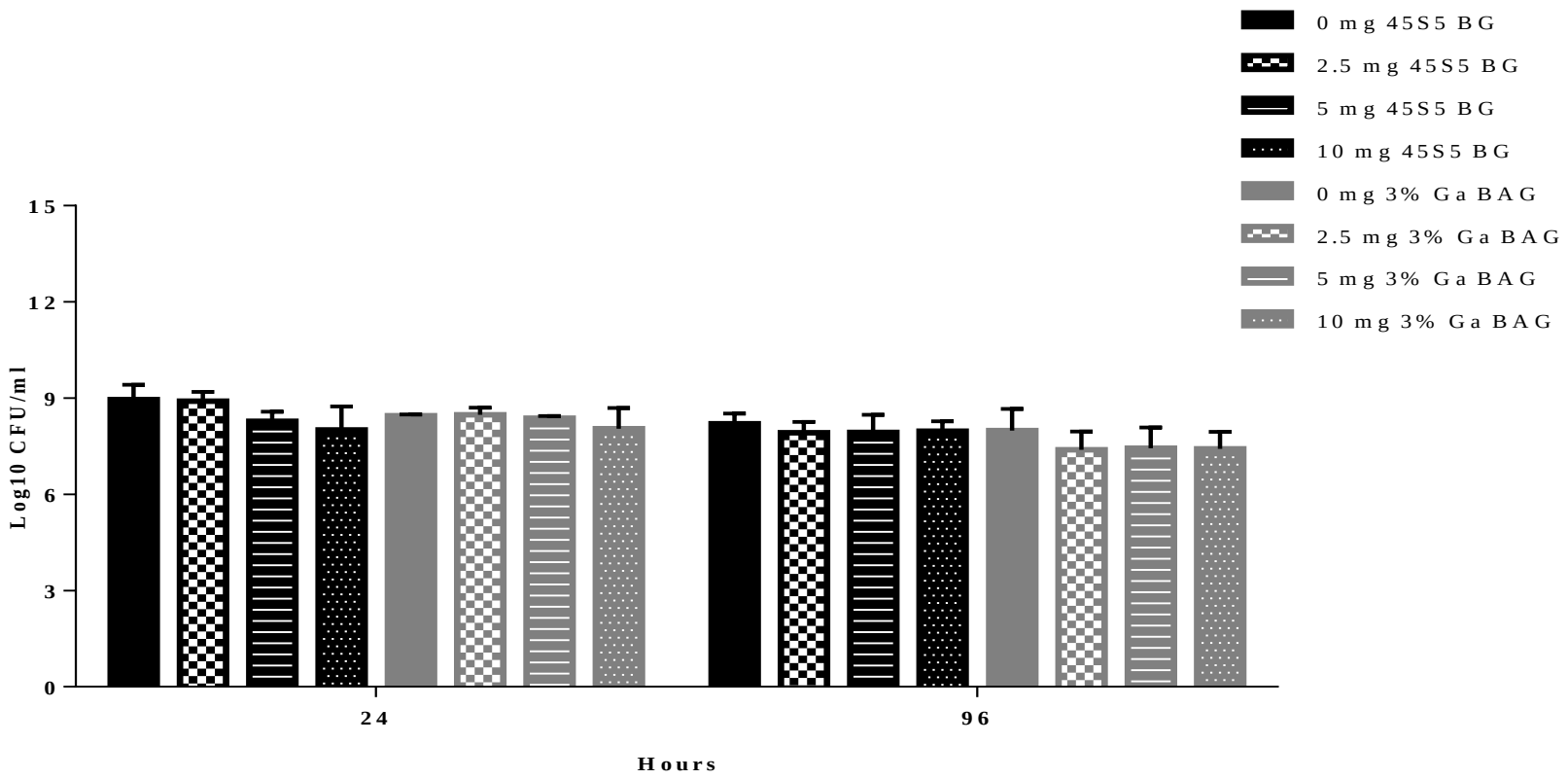

Figure 2.12 The antibacterial effect of the dissolution products of 45S5 Bioglass® and 3 mol% Ga doped BAG against *S.aureus* over a 96 hour period. NB was conditioned with variable concentrations of 45S5 Bioglass® and 3 mol% Ga doped BAG particles and kept in a static incubator. Data shown are expressed as mean (n=3) CFU/ml.

2.4.4.2.2 Shaker incubation conditions

The level of activity varied between 3 mol% Ga doped BAG and 45S5 Bioglass®, with 3 mol% Ga doped BAG dissolution products possessing a greater antibacterial action when tested against *E. coli* (Figure 2.13). This was particularly evident at 96 hours with 10 mg/ml, where a 5.24 log reduction was observed for 3 mol% Ga doped BAG ($p = 0.0001$) dissolution products and a 3.99 for 45S5 Bioglass® ($p = 0.001$). The lower concentrations investigated also demonstrated antibacterial effects. At 96 hours the dissolution products of 3 mol% Ga doped BAG ($p = < 0.01$) and 45S5 Bioglass® exhibited a significant antibacterial action at 5 mg/ml, with log reductions of 1.48 and 1.45, respectively. A statistical significant antibacterial effect was observed for 3 mol% Ga doped BAG dissolution products at 2.5 mg/ml with a log reduction of 0.78 at 96 hours ($p = 0.02$), whilst 45S5 Bioglass® possessed no antibacterial activity. It was also found that the antibacterial activity was time dependent, as the earlier time point (24 hours) represented a strong antibacterial effect whilst at 96 hours a slight antibacterial effect was observed.

As shown in figure 2.14 the dissolution products of 3 mol% Ga doped BAG had no antibacterial effect against *S. aureus*. However, the dissolution products of 45S5 Bioglass® produced a significant ($p = < 0.0001$) antibacterial effect against *S. aureus* at 5 mg/ml and 10 mg/ml (Figure 2.14). Unlike, the effect observed against *E.* coli the antibacterial activity of dissolution products when tested against *S. aureus* was not time dependent. At 10 mg/ml a 1.80 log reduction was observed at 24 hours, whilst at 96 hours the log reduction was 1.14. A similar pattern was also observed for 2.5 mg/ml and 5 mg/ml.

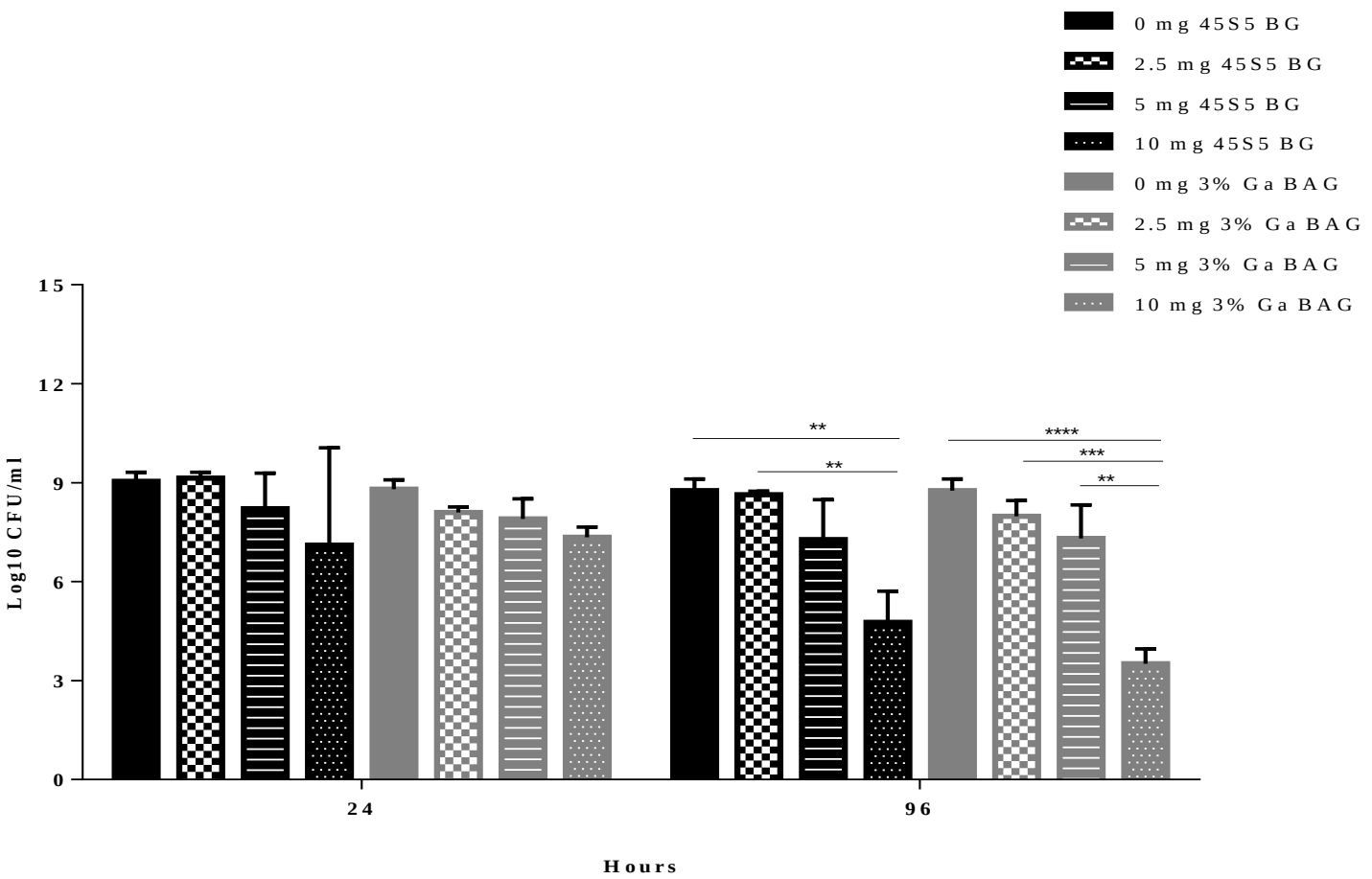

Figure 2.13 The antibacterial effect of the dissolution products of 45S5 Bioglass® and 3 mol% Ga doped BAG against *E.* coli over a 96 hour period. NB was conditioned with variable concentrations of 45S5 Bioglass® and 3 mol% Ga doped BAG particles and kept in a shaker incubator. Data shown are expressed mean (n=3) CFU/ml.

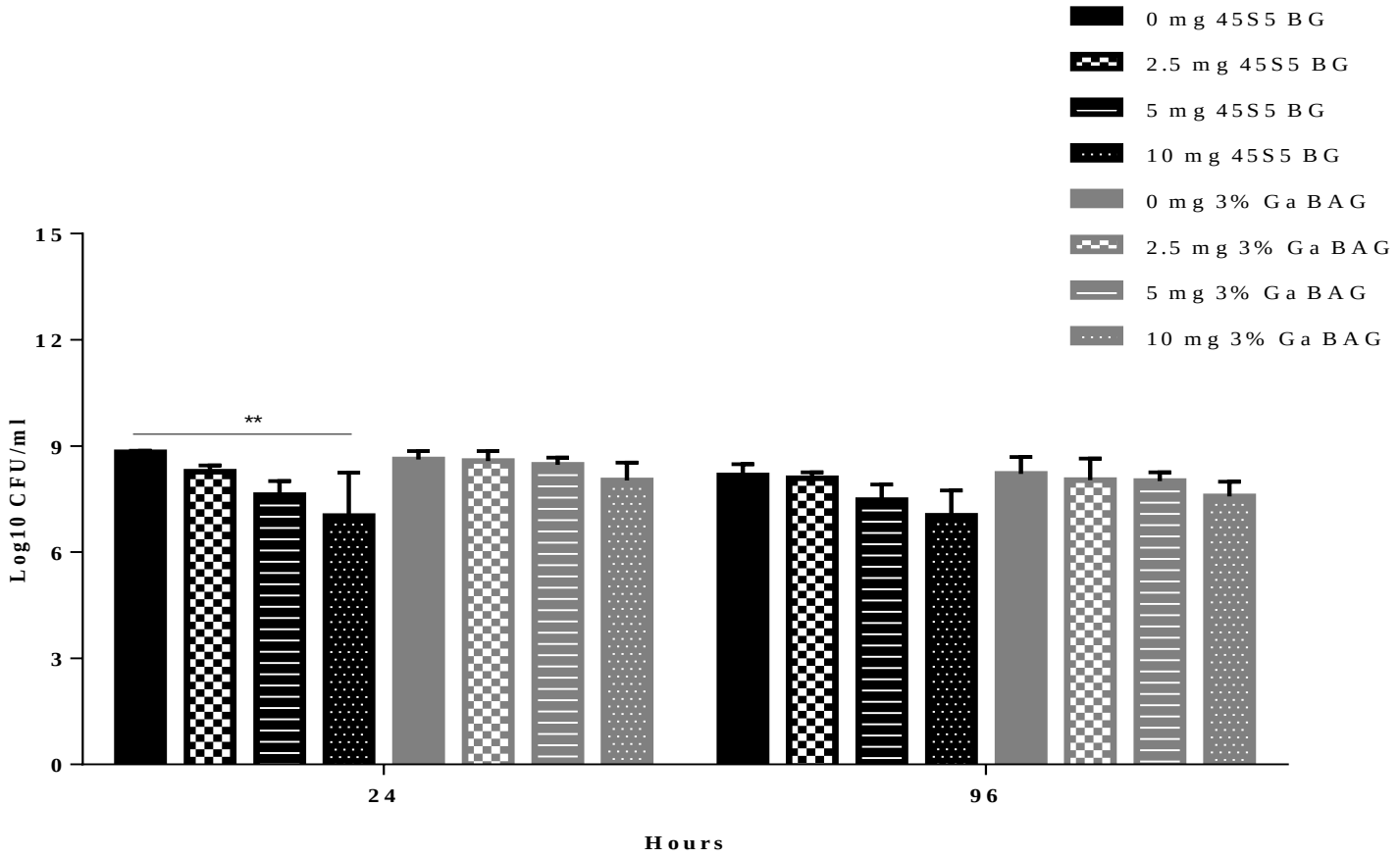

Figure 2.14 The antibacterial effect of the dissolution products of 45S5 Bioglass® and 3 mol% Ga doped BAG against *S. aureus* over a 96 hour period. NB was conditioned with variable concentrations of 45S5 Bioglass® and 3 mol% Ga doped BAG particles and kept in a shaker incubator. Data expressed as mean (n=3) CFU/ml.

2.4.5 Determination of the antibacterial activity of 3 mol% Ga doped BAG and 45S5 Bioglass® at concentrations 2.5-10 mg/ml following pH neutralisation

2.4.5.1 Direct contact

2.4.5.1.1 Static incubator conditions

At 10 mg/ml both 3 mol% Ga doped BAG and 45S5 Bioglass® particles showed no antibacterial activity against *E. coli* (Figure 2.15) and *S .aureus* (Figure 2.16) under static incubation conditions following pH neutralisation.

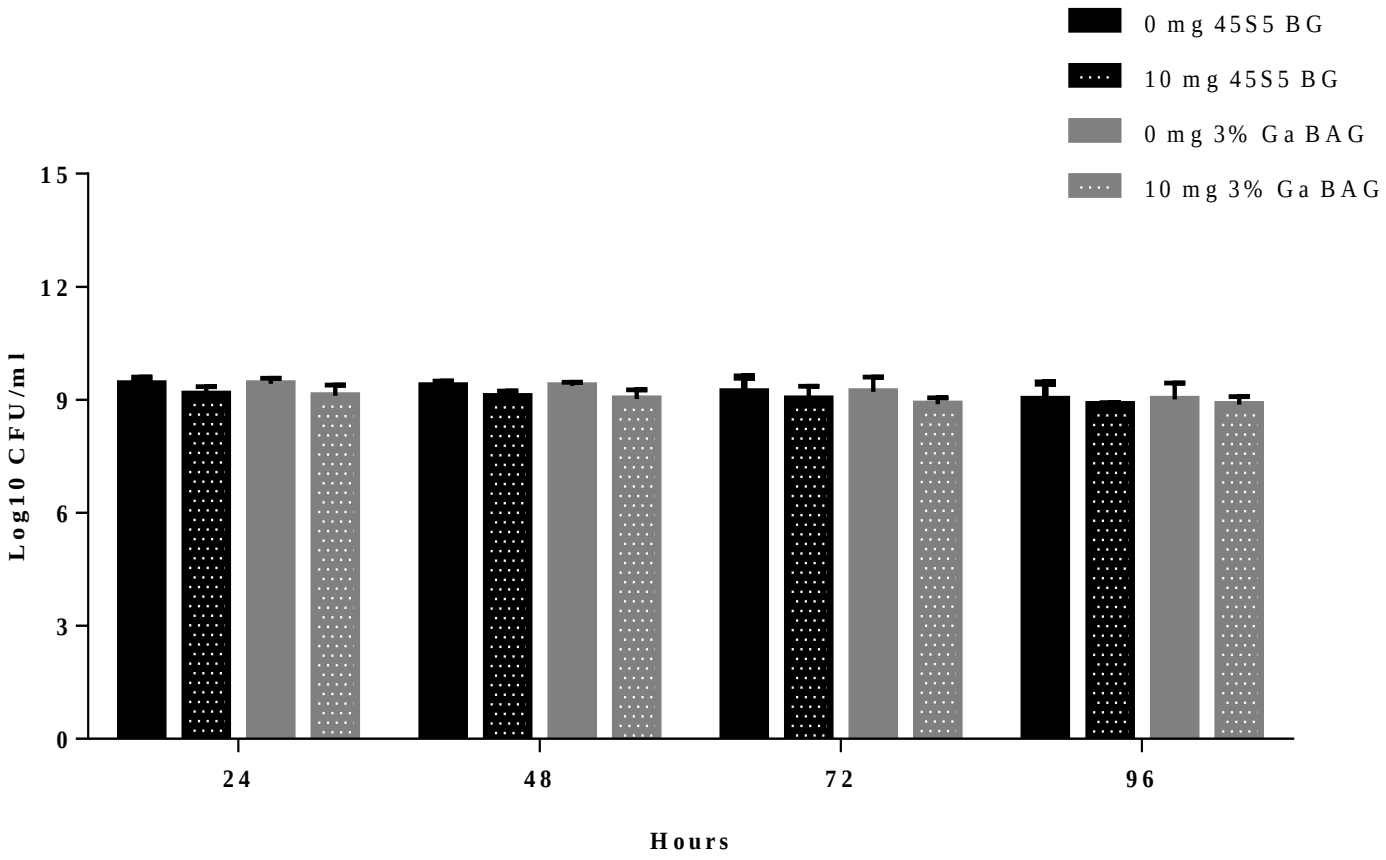

Figure 2.15 The antibacterial effect of pH neutralised 45S5 Bioglass® and 3 mol% Ga doped BAG particles at 10 mg/ml against *E.* coli over a 96 hour period, under static incubation conditions. Data shown are expressed as mean (n=3) CFU/ml.

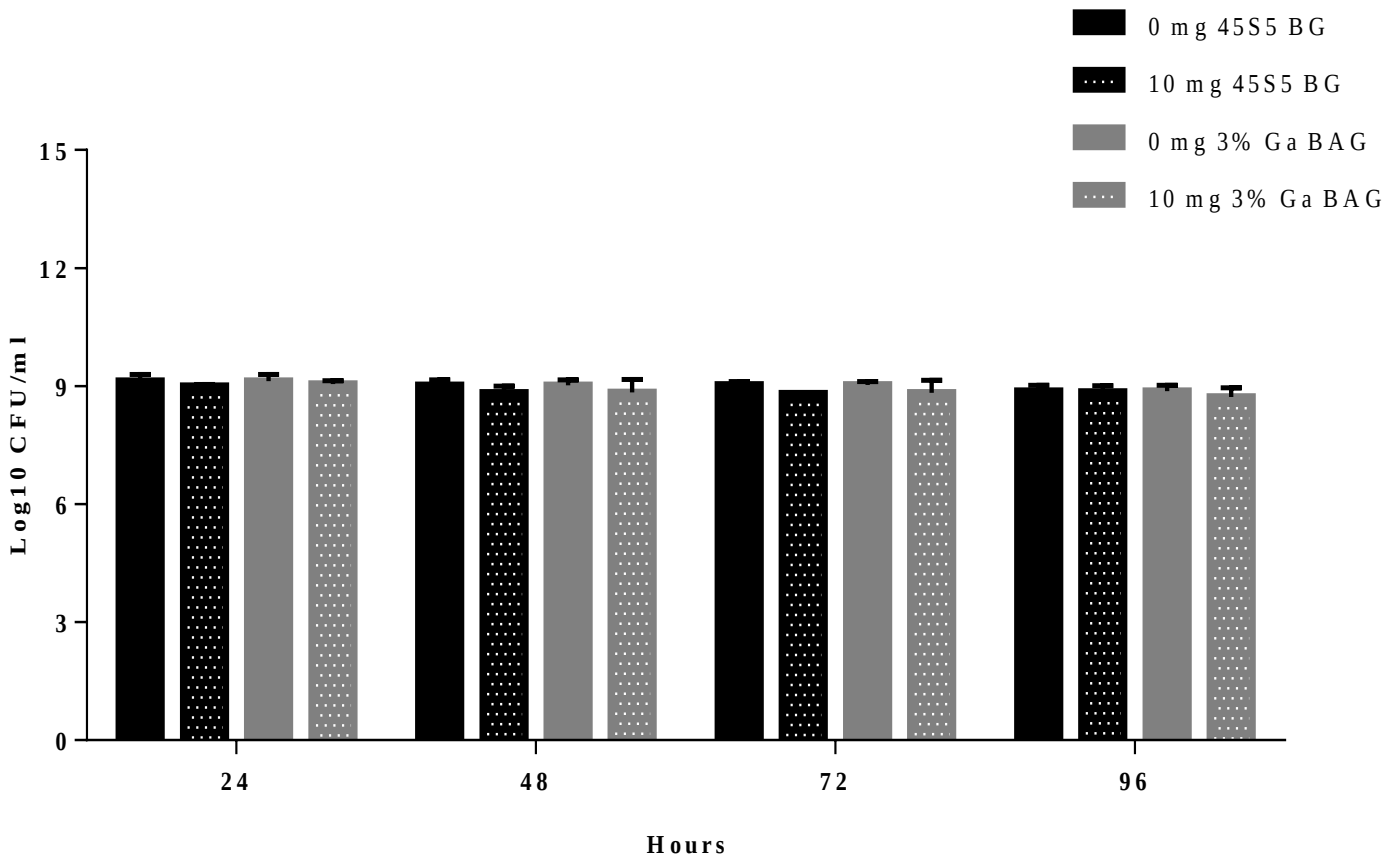

Figure 2.16 The antibacterial effect of pH neutralised 45S5 Bioglass® and 3 mol% Ga doped BAG particles at 10 mg/ml against *S. aureus* over a 96 hour period, under static incubation conditions. Data shown are expressed as mean (n=3) CFU/ml.

2.4.5.1.2 Shaker incubation conditions

Following neutralisation of the pH the particles of 3 mol% Ga doped BAG and 45S5 Bioglass® at the concentration of 10 mg/ml were unable to produce an antibacterial effect under shaker incubation conditions, against *E. coli* (Figure 2.17) and *S. aureus* (Figure 2.18).

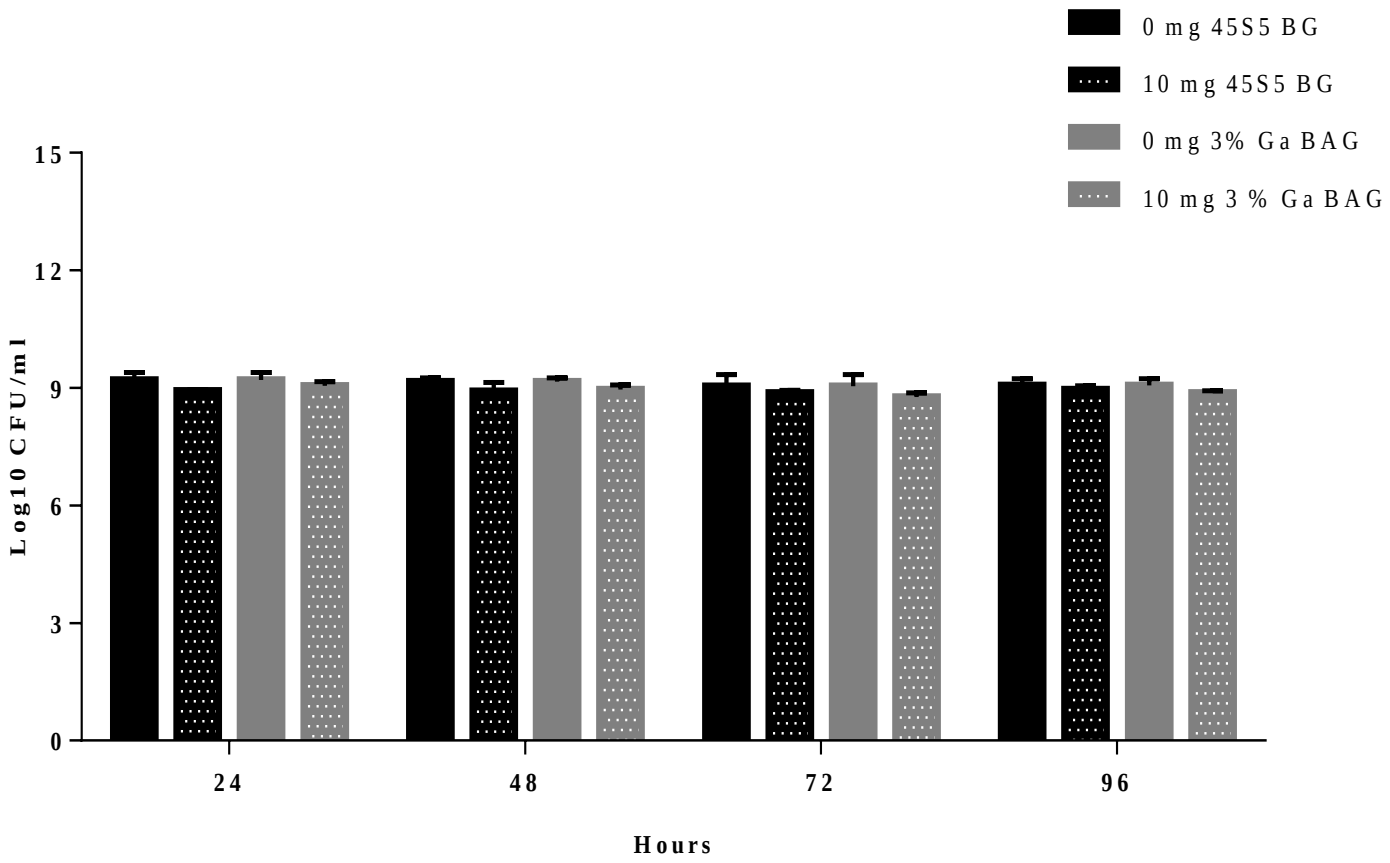

Figure 2.17 The antibacterial effect of pH neutralised 45S5 Bioglass® and 3 mol% Ga doped BAG particles at 10 mg/ml against *E.* coli over a 96 hour period, under shaker incubation conditions. Data shown are expressed as mean (n=3) CFU/ml.

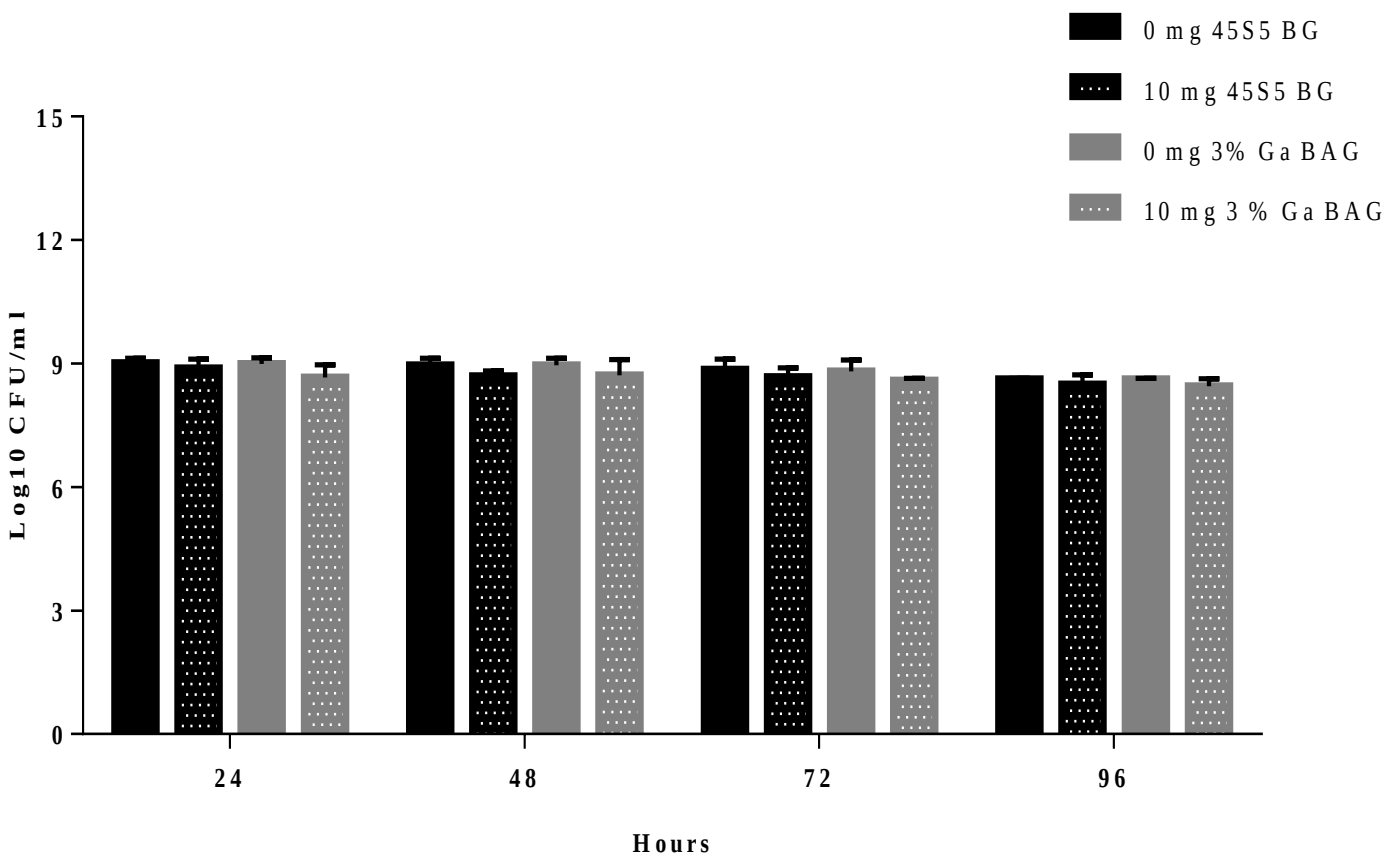

Figure 2.18 The antibacterial effect of pH neutralised 45S5 Bioglass® and 3 mol% Ga doped BAG particles at 10 mg/ml against *S.* aureus over a 96 hour period, under static incubation conditions. Data shown are expresses as mean (n=3) CFU/ml.

2.4.5.2 Indirect contact

2.4.5.2.1 Static incubation conditions

The dissolution products of 3 mol% Ga doped BAG and 45S5 Bioglass® were unable to inhibit the growth of both *E. coli* (Figure 2.19) and *S. aureus* (Figure 2.20) following pH neutralisation.

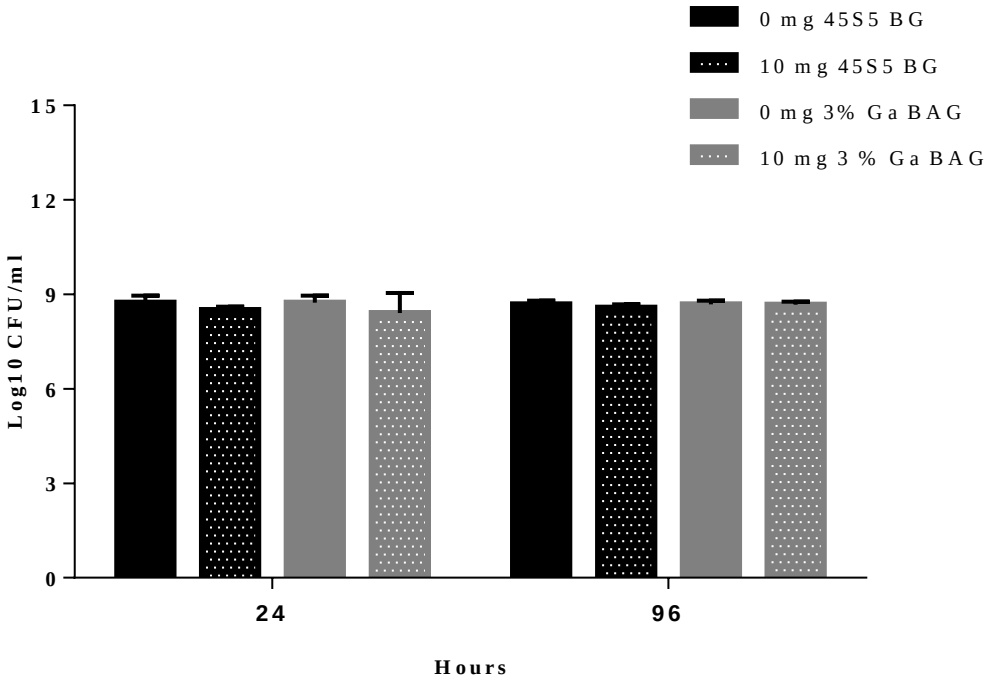

Figure 2.19 The antibacterial effect of pH neutralised 45S5 Bioglass® and 3 mol% Ga doped BAG dissolution products at 10 mg/ml against *E. coli*, over a 96 hour period, under static incubation conditions. Data shown expressed as mean (n=3) CFU/ml.

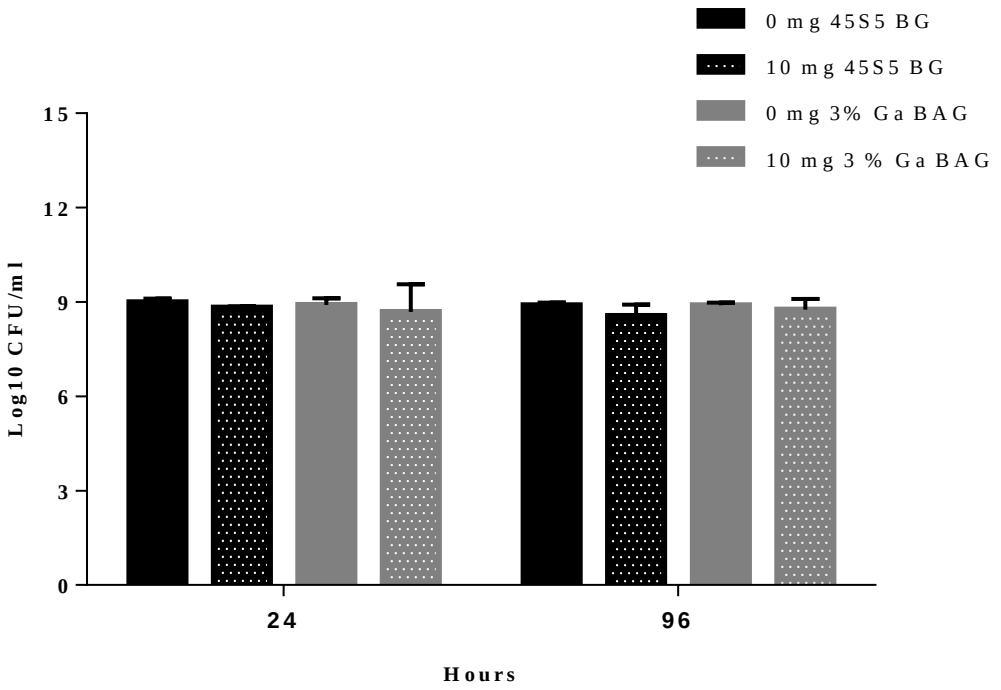

Figure 2.20 The antibacterial effect of pH neutralised 45S5 Bioglass® and 3 mol% Ga doped BAG particles at 10 mg/ml against *S.* aureus over a 96 hour period, under static incubation conditions. Data shown are expressed as mean (n=3) CFU/ml.

2.4.5.2.2 Shaker incubation conditions

Under shaker incubation conditions the neutralisation of the pH rendered the dissolution products of 3 mol% Ga doped BAG and 45S5 Bioglass® ineffective at inhibiting *E. coli* (Figure 2.21) and *S. aureus* (Figure 2.22) growth.

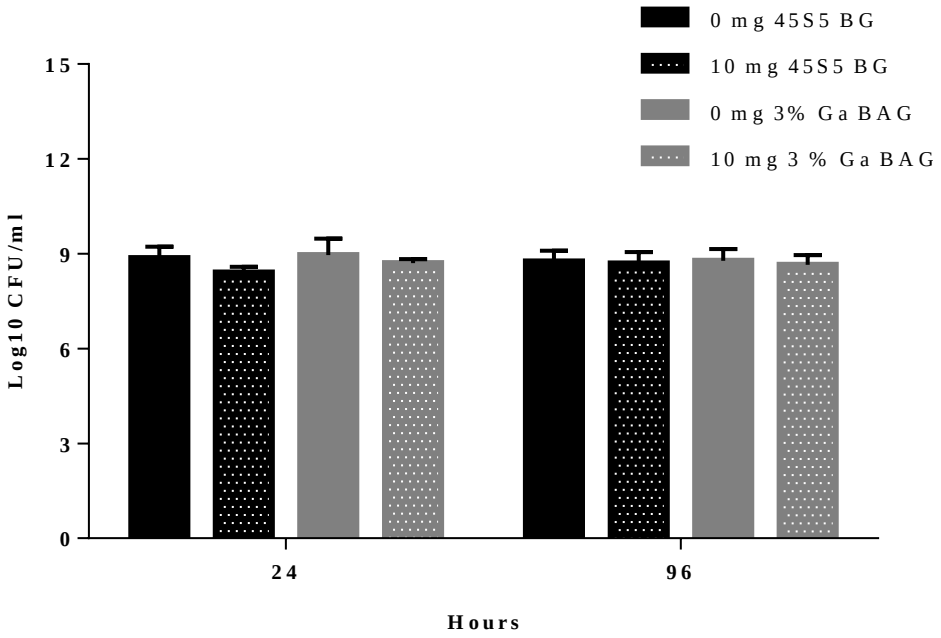

Figure 2.21 The antibacterial effect of pH neutralised 45S5 Bioglass® and 3 mol% Ga doped BAG dissolution products at 10 mg/ml against *E. coli* over a 96 hour period, under shaker incubation conditions. Data shown are expressed as mean (n=3) CFU/ml.

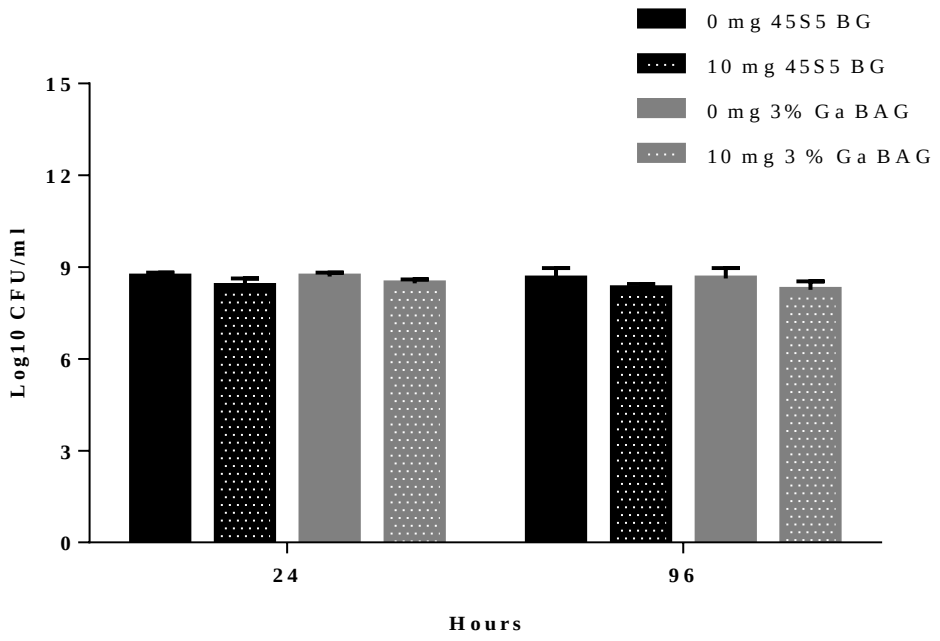

Figure 2.22 The antibacterial effect of pH neutralised 45S5 Bioglass® and 3 mol% Ga doped BAG dissolution products at 10 mg/ml against *S. aureus* over a 96 hour period, under shaker incubation conditions. Data shown are expressed as mean (n=3) CFU/ml.

2.4.6 Investigation of bacterial cell adhesion on 3 mol% Ga doped BAG and 45S5 Bioglass® particles by Scanning Electron Microscopy

The SEM images demonstrate bacterial adhesion on the surface of 3 mol% Ga doped BAG and 45S5 Bioglass® particles. However, the degree of adhesion varied between *E. coli* (Figure 2.23) and *S. aureus* (Figure 2.25). Whilst both *S. aureus* and *E. coli* were able to adhere to 3 mol% Ga doped BAG and 45S5 Bioglass® a higher level of adherence was observed with *S. aureus*. Furthermore, it was observed that relatively the same number of bacterial cells were attached onto the surface of 3 mol% Ga doped BAG and 45S5 Bioglass® particles at both 24 and 96 hours for both microorganisms tested.

The particles of 45S5 Bioglass® and 3 mol% Ga doped BAG exhibited a statistical significant antibacterial effect when tested against *E.coli* (Figure 3.24). 45S5 Bioglass® produced a log reduction of 2.1 ($p = < 0.002$), whilst a 1.6 log ($p = < 0.0007$) reduction was observed for 3 mol% Ga doped BAG at 96 hours. However, the particles of both glasses were unable to inhibit *S. aureus* growth (Figure 2.26) over a 96 hour incubation period.

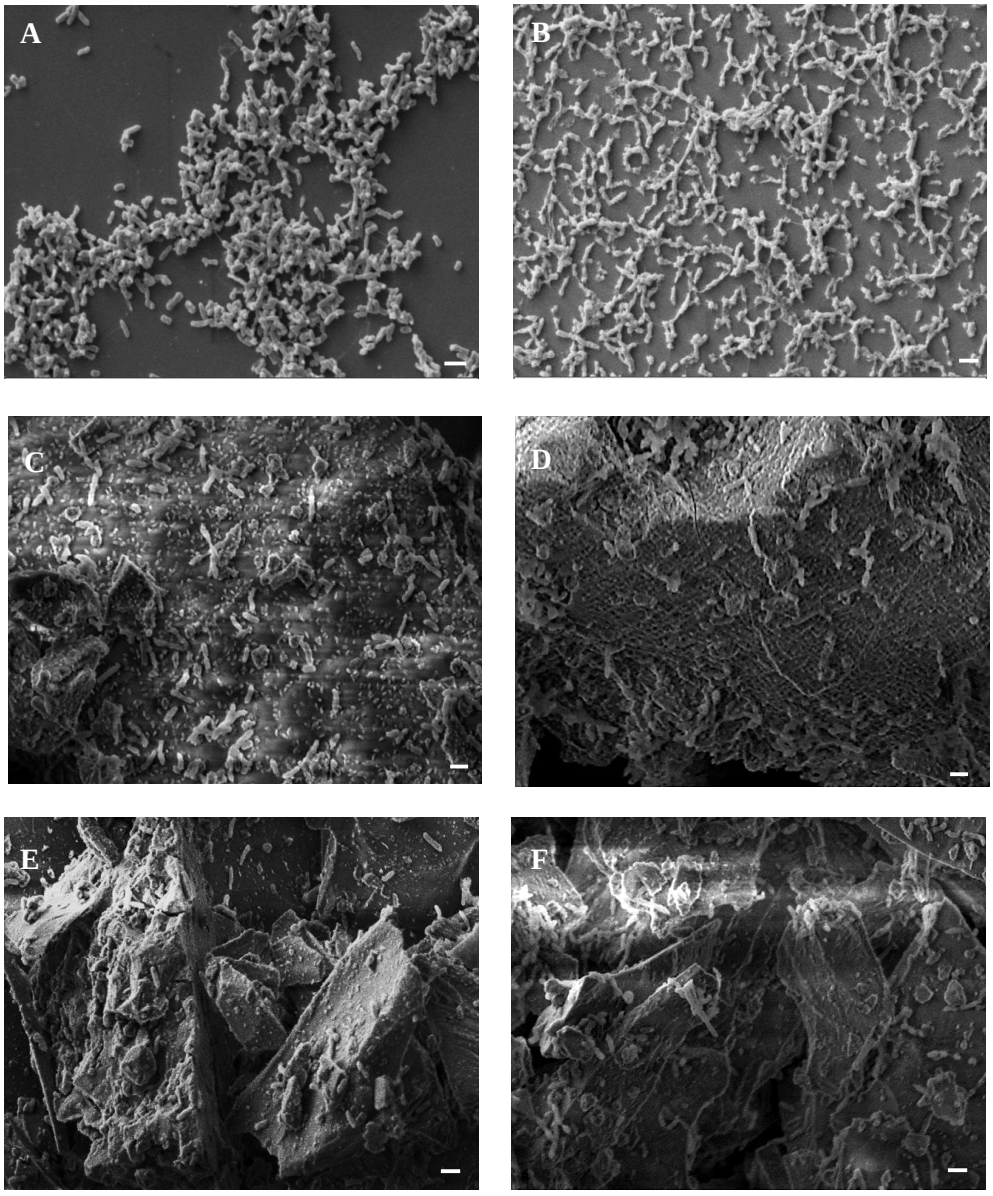

Figure 2.23 SEM images of (**A**) *E. coli* cultured onto a cover slip following a 24 hour incubation period, at 5.00 kV and WD = 7.5 mm, (**B**) *E. coli* cultured onto a cover slip following a 96 hour incubation period, at 5.00 kV and WD = 7.5 mm, (**C**) *E. coli* cultured onto 45S5 Bioglass® particles at 24 hours, at 5.00 kV and WD = 8.0 mm, (**D**) *E. coli* cultured onto 45S5 Bioglass® particles at 96 hours, at 5.00 kV and WD = 8.5 mm, (**E**) *E. coli* cultured onto 3 mol% Ga doped BAG particles at 24 hours, at 5.00 kV and WD = 7.5 mm, and (**F**) *E. coli* cultured onto 3 mol% Ga doped BAG particles at 96 hours, at 5.00 kV and WD = 7.5 mm. Bar represents 2 µm.

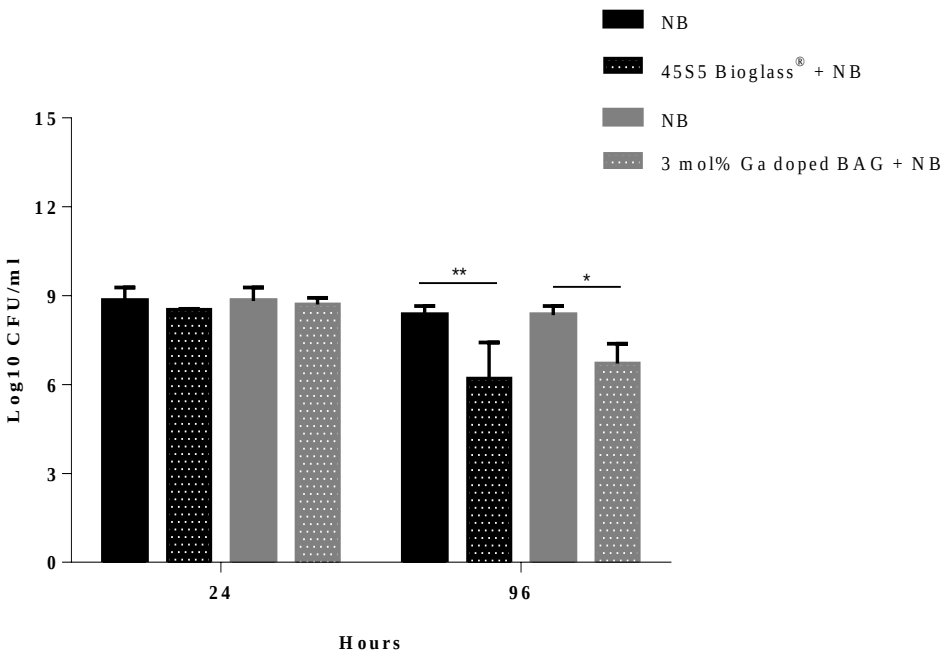

Figure 2.24 Mean CFU/ml (n=3) of *E. coli* cultured onto glass cover slip (0 mg/ml), 45S5 Bioglass® and 3 mol% Ga doped BAG particles (10 mg/ml) following a 24 and 96 hour incubation period, for SEM analysis.

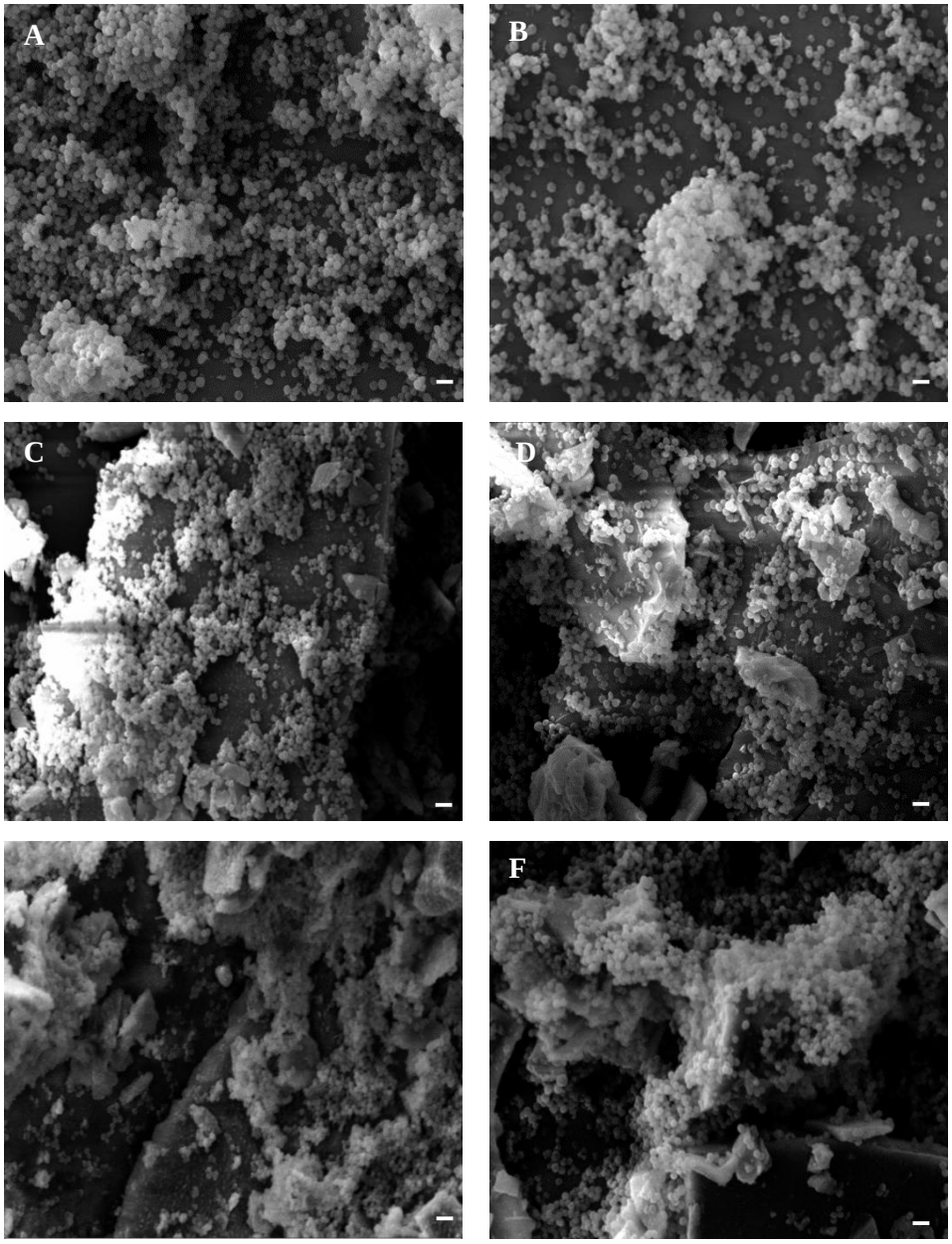

Figure 2.25 SEM images of *S. aureus* cultured onto 45S5 Bioglass® and 3 mol% Ga doped BAG particles following 24 and 96 hours incubation, at 15.00 kV and WD = 6.5 mm. (**A**) *S. aureus* cultured onto a cover slip following a 24 hour incubation period, (**B**) *S. aureus* cultured onto a cover slip following a 96 hour incubation period, (**C**) *S. aureus* cultured onto 45S5 Bioglass® particles at 24 hours, (**D**) *S. aureus* cultured onto 45S5 Bioglass® particles at 96 hours, (**E**) *S. aureus* cultured onto 3 mol% Ga doped BAG particles following 24 hours, at 15.00 kV and WD = 6.0 mm, and (**F**) *S. aureus* cultured onto 3 mol% Ga doped BAG particles following 96 hours, at 15.00 kV and WD = 6.0 mm. Bar represents 2 µm.

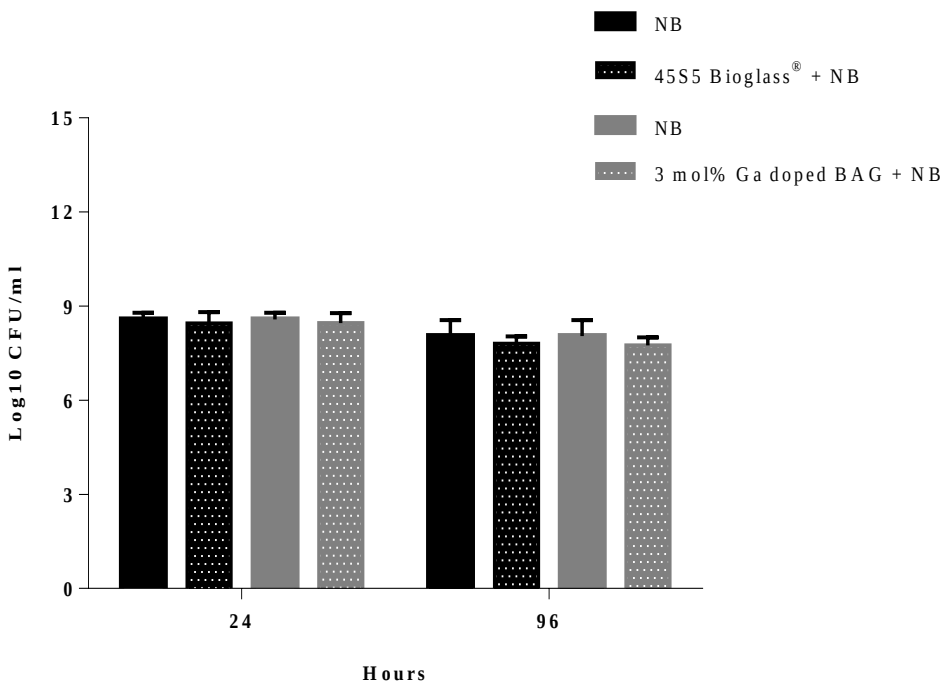

Figure 2.26 Mean CFU (n=3) of *S. aureus* cultured onto glass cover slip (0 mg/ml), 45S5 Bioglass® and 3 mol% Ga doped BAG particles(10 mg/ml) following a 24 and 96 hour incubation period, for SEM analysis.

2.5 DISCUSSION

A growing body of data demonstrates that Ga^{3+} compounds are antibacterial as are Ga^{3+} doped PBG systems. However, the antibacterial efficacy of Ga^{3+} ions when incorporated within a silicate-based glass system has not been investigated. In this study the antibacterial action of silicate-based glass system doped with 3 mol% Ga^{3+} was investigated using *E. coli* and *S. aureus*. Furthermore, the antibacterial efficacy of 45S5 Bioglass® was also investigated and compared.

The results for this study demonstrated that 3 mol% Ga doped BAG produced a similar antibacterial effect as 45S5 Bioglass® particles. The antibacterial effect was concentration dependent, as reduced survival was observed at the highest concentrations tested. 45S5 Bioglass® and 3 mol% Ga doped BAG at 50 mg/ml and 100 mg/ml inhibited *E. coli* growth but could only inhibit *S. aureus* at 100 mg/ml. The results of the current study are consistent with previous findings, which have demonstrated concentration-dependent kill. Munukka *et al*. (2008) investigated the antibacterial efficacy of eight BAGs against 29 clinically important bacterial species. They demonstrated that all BAGs had a growth-inhibitory effect at the highest concentration tested, 100 mg/ml. In addition, Hu *et al*. (2009) reported that bacterial kill over 98% could be achieved for *E.* coli, *S. aureus* and *S. epidermidis* at the 45S5 Bioglass® concentrations of 50 mg/ml and 100 mg/ml. When BAGs are immersed into aqueous solutions Ca^{2+}, Na^{+}, PO_4^{3-} and Si^{4+} ions are released and as a result elevate the pH and osmotic pressure of the environment. Jones *et al*. (2001) reported that the dissolution of Ca^{2+}, Na^{+}, PO_4^{3-} and Si^{4+} ions into solution increased as glass particle concentration in solution increased. This may explain the growth inhibition at the highest concentrations, as the pH values measured ranged from 10 – 11. However, the antibacterial effect was found to vary between the bacterial species, as both BAGs at 100 mg/ml inhibited *E.coli* growth within 24 hours of culture, whereas reduced survival for *S. aureus* occurred at 96 hours.

The initial glass concentrations (25 mg/ml, 50 mg/ml and 100 mg/ml) in this study were chosen based on previous studies (Mannukka *et al*., 2008; Hu *et al*., 2009; Allan *et al*., 2001; Mortazavi *et al.,* 2010; Leppäranta *et al*., 2008; Zhang *et al*., 2010) however, these concentrations were found to exhibit cytotoxic effects against osteoblast-like Saos-2 cells and bone marrow derived MSCs (see chapter 3), and therefore lower concentrations (2.5 mg/ml, 5 mg/ml and 10 mg/ml) were chosen. The difference between *E. coli* and *S. aureus* was also observed at the lower concentrations tested. It was evident from the direct contact experiments that both 3 mol% Ga doped BAG and 45S5 Bioglass® did not exhibit broad-spectrum antibacterial properties, as reduced survival could only be demonstrated for *E. coli* but not for *S. aureus*.

In agreement with the results presented here, Valappil *et al*. (2008) reported that the zones of inhibitions were larger for *E. coli* and *P. aeruginosa* than *S. aureus*, when investigating the antibacterial action of Ga^{3+} doped PBGs. The difference has also been observed with Ga^{3+} compounds, such as Ga^{3+} (III) protoporphyrin IX (PPIX) complex (Ga (III)-PPIX), which has demonstrated potent antibacterial activity against both Gram-negative and Gram–positive bacteria. However, the antibacterial effect of Ga^{3+} (III)-PPIX was markedly greater for *E. coli* with a minimum inhibitory concentration (MIC) of <0.5 µg/ml, whilst the effective concentration doubled for *S. aureus* with a MIC of 1.0-2.5 µg/ml (Minandri *et al*., 2014). Similar findings were also observed for 45S5 Bioglass® in a study conducted by Hu *et al*. (2009), in which a significant difference was seen between Gram-negative bacterium (*E. coli*) and Gram-positive bacteria (*S. aureus* and *S. epidermidis*) at the lowest concentration tested, 10 mg/ml.

The difference observed between *S. aureus* and *E. coli* could be attributed to their cell structures. The cell wall of Gram-positive bacteria is primarily composed of a thick peptidoglycan layer however it also contains large amounts of teichoic and lipotechoic acids. Doyle *et al*. (1980) and Hughes *et al*. (1972) demonstrated that the teichoic acids (which

provide highly charged anionic clusters) contribute to the binding of metal ions such as Na^+ and Ca^{2+} ions to the cell wall. Beveridge and Murray, (1976) suggested that the carboxyl groups of peptidoglycan were also responsible for the interactions between cell walls and cations. It has been suggested by Stoor *et al.* (1996) that BAGs are subject to bacterial adhesion due to the presence of Ca^{2+} ions in the Si-rich layer. This could explain why no reduced survival was observed for *S. aureus*. The metal binding sites present in the cell wall probably mediated the binding of *S. aureus* onto the surface of 3 mol% Ga doped BAG and 45S5 Bioglass® particles. Moreover both BAGs are known to produce a Si-rich layer in an aqueous environment and release Ca^{2+} and Na^+ ions. The SEM images of this study also support these findings, as greater numbers of *S. aureus* were seen on the surface of both 3 mol% Ga doped BAG and 45S5 Bioglass® particles. Gorriti *et al*. (2009) reported *S. aureus* adhesion on 45S5 Bioglass® scaffold, and furthermore it was unable to significantly affect the viability of *S. aureus*. However, this does not apply to *E.* coli, which is a Gram-negative bacterium. The cell wall of *E.* coli is composed of a thin peptidoglycan layer with no teichoic acids enclosed within its outer membrane. Hu *et al*. (2009) reported that needle like BAG debris was adsorbed onto the surface of *E.* coli, which led to the destruction of the cell wall. In addition, the higher local pH value measured on the surface of the Bioglass® particles was believed to potentiate the antibacterial effect of Bioglass® particles by destroying the bacterial structure. The SEM images show very few numbers of *E. coli* on the surface of both 3 mol% Ga doped BAG and 45S5 Bioglass® particles.

Indirect contact experiments were conducted to elucidate whether the dissolution products would be sufficient to inhibit cell growth, and also if particle presence is necessary for bacterial inactivation. The results of the indirect contact experiments show that 3 mol% Ga doped BAG and 45S5 Bioglass® particles were only effective at the highest concentrations tested at reducing bacterial growth, particularly *E. coli* growth. There was a noticeable difference between the two incubation conditions, as *E. coli* growth was greatly reduced under shaker incubation

conditions. It was also evident that the dissolution products of 3 mol% Ga doped BAG produced a greater antibacterial action than those of 45S5 Bioglass®, under shaker incubation conditions. Similarly, at 25 mg/ml the particles of 3 mol% Ga doped BAG demonstrated a significant inhibitory effect against *E. coli*.

It can be inferred that the inclusion of Ga^{3+} ions within the BAG system enhances its antibacterial action. It has been reported that Ga^{3+} ions target bacterial iron metabolism by exploiting the chemical similarities between Fe^{3+} ions and Ga^{3+} ions (Chitamber, 2010; Valappil *et al*., 2008). The ability of Ga^{3+} ions to easily substitute for Fe^{3+} ions, allows it to interfere with many iron-requiring enzymes, including ribonucleotide reductase, which catalyses the first step in DNA synthesis, and superoxide dismutase and catalase which protect against oxidative stress (Valappil *et al*., 2008). Despite the presence of Ga^{3+} ions the antibacterial effect could also have been attributed to the Ca^{2+} and Na^{+} ions, which increase aqueous pH. As small concentrations of Ga^{3+} ions are released from Ga^{3+} doped BAGs. Franchini *et al*. (2012) reported that after 24 hours the concentration of Ga^{3+} ions was 4.3 ppm whereas 101 and 3490 ppm was observed for Ca^{2+} and Na^{+} ions respectively, which were released from 3.5 mol% Ga doped silicate-based BAG. However, this Ga^{3+} ion concentration should be sufficient to exert an antibacterial activity as concentrations as low as 0.007-1.4 ppm were reported to disrupt *P. aeruginosa* iron metabolism (Kaneko *et al*., 2007).

The dissolution products did not only reduce the growth of *E. coli* as growth reduction was also observed for *S. aureus* but the degree of reduction varied. The outer membrane of *E. coli* is embedded with porins, which are nonspecific pores or channels that allow the passage of small hydrophilic molecules across the outer membrane (Nikaido, 2013). Calcium and Na^{+} are small hydrophilic ions and could therefore utilise the porin pathway to enter *E. coli* and once inside elevate the intracellular pH, resulting in cell death. Furthermore, elevated pH levels of the medium attributed to the alkali ions, can alter the pH gradient present in the cytoplasmic

membrane of bacteria, which is important for the movement of nutrients into the cell. Therefore, by influencing the transfer and permeability of the cytoplasmic membrane, the high pH can induce inhibition and toxic effects on the bacteria (Xie *et al*., 2008). *S. aureus* lacks an outer membrane and its cell wall binds Ca^{2+} and Na^{+} ions, therefore the dissolution products did not display a similar level of antibacterial efficacy. Moreover, Cutinelli and Galdiero. (1967) demonstrated that an increased pH (of 9) increased the amount of ions bound by *S. aureus* cell wall. In this study the concentration of 10 mg/ml caused alkalisation of NB with values as high as 9. An increased pH deprotonates functional groups within the cell wall, resulting in an increasing number of sites available for metal adsorption (Fowle and Fein, 1999). However, 100 mg/ml demonstrated a significant antibacterial efficacy against *S. aureus*, which could be attributed to the high levels of dissolution products present in the media. It can therefore be assumed that *S. aureus* is able to survive in a mildly alkaline environment produced by the lower concentrations of BAGs, but cannot tolerate an extreme alkaline environment. These results indicate that the presence of bioactive glass particles play an important role in the antibacterial effect against *E. coli* but not *S. aureus*.

Only one *in vivo* study has been conducted to evaluate the antibacterial activity of BAGs and it showed that particulate Bioglass® does not exhibit antibacterial activity *in vivo*. Xie *et al*. (2008) suggested that the inactivity of particulate Bioglass® *in vivo* was due to the '*big buffer system'* in body fluid, which could swiftly exchange dissolution products with nearby blood and other body fluid, so the ionic concentration and pH in body fluid at the site of implantation cannot increase to sufficient high levels required to inhibit bacterial growth. In this current study the pH was neutralised to investigate the effect of pH adjustment on the antibacterial activity of 3 mol% Ga doped BAG and 45S5 Bioglass®. It was found that following pH neutralisation, 3 mol% Ga doped BAG and 45S5 Bioglass® were ineffective at inhibiting *E. coli* and *S. aureus* growth. The results for the neutralised experiments are consistent with the *in vitro* study conducted by Allan *et al*. (2001) in which no difference was reported between

the control group and pH adjusted Bioglass® supernates. It has been suggested that a reduction in the pH may alter the solubilities of particular ions present in the BAG which at a higher pH could be responsible for the antibacterial effect (Allan *et al*., 2001). The results of the neutralisation experiments provide evidence that pH alone may be responsible for the antibacterial activity.

Incubation conditions influenced the antibacterial effect of the particles. The particles significantly inhibited *E. coli* growth under shaking incubation conditions. This could be contributed to the fact that particles under shaking conditions are suspended in solution. Therefore, are far more likely to come into contact with the solution resulting in increased dissolution. Under static incubation conditions particles on the top layer are more likely to be exposed to the solution. However, even under shaking conditions 45S5 Bioglass® particles were unable to exhibit a strong antibacterial effect against *S. aureus*. This could be a result of *S. aureus* adhering onto the surface of the particles, and reducing the dissolution rate. The dissolution products are therefore unable to penetrate through the layer of cells in close contact to the particles that may have protected the cells in suspension. When investigating the attachment of *E. coli* and *S. aureus* on the surface of glass particles the total viable CFU count was also determined. The results for *S. aureus* were similar to those obtained for the direct contact experiments, however significant growth reduction was not observed for *E. coli*. This could be because the particles formed a dome when immersed into NB, shielding the particles under the dome from the solution and hence reducing dissolution. Therefore, the release of dissolution products is required to produce an antibacterial effect against *E. coli*.

2.6 CONCLUSION

3 mol% Ga doped BAG possesses similar antibacterial properties to 45S5 Bioglass®, and neither exhibit broad-spectrum antibacterial activity, as total growth inhibition was only observed for *E. coli* at the highest concentrations. This study illustrates that possibly two aspects are involved in the antibacterial effect of 3 mol% Ga doped BAG and 45S5 Bioglass® particles against *E. coli*, the high aqueous pH and contact between particles and bacterial cells, however even in the presence of particles the BAGs are ineffective at inhibiting *S. aureus* growth. The neutralisation experiments demonstrate that the antibacterial action is primarily driven by pH. The fact that the bacterial cells could withstand the antibacterial effect of the particles following pH neutralisation raises the question whether the two BAGs investigated would be effective antibacterial agents *in vivo*. These results highlight the importance of pH neutralisation *in vitro,* and also that results obtained will largely be influenced by the method and concentrations selected, glass composition and bacterial strains.

CHAPTER THREE

The Effects of Gallium doped Bioactive Glass and 45S5 Bioglass® on the Growth and Viability of Human Mesenchymal Stem Cells and Osteoblast-like Cells *In Vitro*

3.1 INTRODUCTION

Bioactive glasses have the ability to form a strong bond with living tissue due to the formation of a HCA layer on their surface and have been used clinically to repair craniofacial, maxillofacial and periodontal tissues (Hench *et al*., 2006; Hench. 2010). Existing research has established that BAGs allow adhesion, proliferation and differentiation of healthy osteoblasts on their surfaces *in vitro* (Xynos *et al*., 2000; Labbaf *et al*., 2011; Mayr-Wohlfart *et al*., 2000; Silver *et al*., 2001; Valerio *et al*., 2003; El-Ahmed *et al*., 1995; Christodoulou *et al*., 2005). Similarly, *in vivo* studies have reported gradual degradation of implanted BAGs with subsequent bone formation at the implant surface (Hamadouche *et al*., 2001; Livingston *et al*., 2002; Vogel *et al*., 2001; Heikkilae *et al*, 1995). These findings suggest that BAGs have potential in bone repair, e.g. to enhance bone formation following fracture or following resections of bone tumours.

Initial studies investigating the antineoplastic activity of Ga^{3+} revealed that patients with advanced malignant lymphoma receiving Ga^{3+} nitrate frequently became hypocalcaemic (the presence of low serum Ca^{2+} levels in the blood). This observation led to further investigations which evaluated the role Ga^{3+} played in bone metabolism. It was found that Ga^{3+} would suppress bone resorption by inhibiting osteoclast action without evidence of cytotoxic effects on osteoblasts (bone forming cells) (Bockman *et al*., 1990). This antiresorptive activity has led to its clinical use in the treatment of hypercalcaemia (presence of high serum Ca^{2+} levels in the blood) of malignancy and other metabolic bone disorders characterised by increased bone resorption by osteoclasts (Chitamber, 2010; Warrell, 1997; Bernstein, 2013). In addition to acting on osteoclasts to inhibit bone resorption, Ga^{3+} has also been reported to stimulate bone formation by acting directly on osteoblasts (Bernstein *et al*., 1998). Several authors have demonstrated that Ga^{3+} increases the expression of type-I collagen and OCN in osteoblasts, proteins which are involved in differentiation and bone mineralisation (Jenis. 1993; Bockman. 1993). Furthermore, Ga^{3+} doped silicate-based glass systems maintain the ability of HCA formation *in vitro* when immersed into physiological fluids (Franchini *et al*., 2012; Lusvardi *et*

al, 2013). Gallium could therefore be used to dope silicate-based glass systems, in order to manufacture a material that would combine the bone bonding properties of silicate-based glass systems with the antiresorptive and anabolic properties of Ga^{3+}, and may act as an effective material for bone regeneration.

Previous *in vitro* studies examining osteogenic properties of BAGs have utilised primary human osteoblasts as well as osteoblast-like cell lines, such as Saos-2 cells as the prototypes for osteoblastic cells. The osteosarcoma tumour cell line, Saos-2 which has been isolated from an 11 year old Caucasian female in 1975 has been used to investigate the cytocompatibility of various BAGs (Mayr-Wohlfart *et* al., 2001; Alcaide *et* al., 2010; Gentleman *et al*., 2010; Gao *et al*., 2001). Despite being a tumour cell line, Saos-2 cells exhibit many osteoblastic traits such as high levels of ALP activity and the ability to synthesise OCN and collagen type I which are characteristic of bone forming cells (Czekanska *et al*., 2012). Furthermore, these cells are highly proliferative and can be cultured to perform a large number of experiments over a relatively short period of time. Several *in vitro* studies have reported osteogenic effects of various BAG compositions on animal and human MSCs (Radin *et al*., 2004; Reilly *et al*., 2007; Doostmohammadi *et al*., 2011; Labbaf *et al*., 2011). Mesenchymal stem cells are precursors to osteoblast cells; hence the effect of BAG particles and dissolution products is critical. Therefore, MSCs are an important cell type to use to test the biocompatibility of BAGs. However, there is no published information concerning the cytotoxic effect of Ga doped BAG particles on the proliferation of human MSCs and or osteoblasts.

3.2 AIMS

The aims of this study were to:

- Investigate and compare the cytotoxic effects of 3 mol% Ga doped BAG and 45S5 Bioglass® on osteoblasts, using the Saos-2 cell line as a model system.
- Investigate and compare the effects of 3 mol% Ga doped BAG and 45S5 Bioglass® on non-transformed human MSCs.

Several aspects of the activity of both BAGs were tested. These included:

- Assessment of the effects of the particles (direct contact) of both BAGs with each cell type.
- Assessment of the effects of the dissolution products (indirect contact) of both BAGs on each cell type, using media which had been incubated with the BAG particles under static and shaker incubation conditions.
- Assessment of the influence of pH.

3.3 METHODSAND MATERIALS

3.3.1 Glass preparations

See section 2.3.5 in chapter 2.

3.3.2 pH analysis

To determine the aqueous pH value of 3 mol% Ga doped BAG and 45S5 Bioglass® at concentrations of 2.5 mg/ml, 5 mg/ml and 10 mg/ml, triplicate stock solutions were prepared in 5 ml Dulbecco's modified Eagle's medium/Ham's-F12 (DMEM/Ham's-F12) (PAA, Yeovil, Somerset, UK), supplemented with 10% (v/v) foetal bovine serum (FBS) (PAA, Yeovil, Somerset, UK), and 1% (v/v) penicillin (50U/ml) and streptomycin (P/S) (50µg/ml). Culture media without glass particles served as the control. The stock solutions and controls were incubated over night at 37°C in static and shaker (with a shaking speed of 100 rpm) incubators. The pH of the stock solutions and controls was measured using the Mettler Toledo pH probe (Fisher Scientific, Loughborough, UK) following 24, 48, 72 and 96 hours of incubation.

3.3.3 Determination of Bioactive glass surface characteristics

Glass cover slips (12mm) (Fisher Scientific, Loughborough, UK) were placed into the wells of a 24 well plate (Fisher Scientific, Loughborough, UK), onto which were placed 3 mol% Ga doped BAG and 45S5 Bioglass® particles, followed by the addition of 1 ml DMEM /Hams's-F12. Following a 24 and 96 hour incubation period at 37°C the culture medium was removed from each well, and the particles were washed with PBS (x3) (PAA, Yeovil, Somerset, UK) before being dried overnight at 37°C. Following the 24 hour incubation period the glass cover slips containing particles were removed and mounted onto stubs, gold-sputtered prior to observation with a Carl Zeiss EVO MA10 scanning electron microscope (SEM).

3.3.4 Maintenance of mesenchymal stem cell stock culture

Primary bone marrow derived human mesenchymal stem cells (MSCs) were provided already culture-expanded from bone marrow aspirates, by Dr Karina Wright at the Robert and Agnes Hunt (RJAH) Orthopaedic Hospital, Oswestry, UK. Bone marrow derived MSCs were cultured and maintained in DMEM/Ham's-F12, supplemented with 10% (v/v) FBS, and 1% (v/v) penicillin (50U/ml) and streptomycin (50μg/ml) in a humidified atmosphere at 37^0C with 5% CO_2. Upon reaching ~70-75% confluence, cultures were passaged using 0.25% trypsin-1 mM EDTA (PAA, Yeovil, Somerset, UK) and a viable cell count was performed by trypan blue exclusion (see section 3.3.7). The MSCs for the experiments outlined below were isolated from three different donors and were referred to as BMMSC058, BMMSC028 and BMMSC101.

3.3.5 Maintenance of Saos-2 stock cell culture

Saos-2, (ATCC HTB-85) the human osteosarcoma cell line was cultured and maintained in DMEM/Ham's/F12 supplemented with 10% (v/v) FBS and 1% (v/v) P/S. Cell cultures were incubated at 37ºC and 5% CO_2. Once the cells became ~70-75% confluent they were passaged using 0.25% trypsin-1 mM EDTA and a viable cell count was performed by trypan blue exclusion (see section 3.3.7).

3.3.6 Passaging of cells

Once the cells reached ~70-75% confluency they were trypsinised, this involved washing the cells in PBS, which was then discarded. The cells were then incubated at 37ºC for 5 minutes in 0.25% trypsin-EDTA (PAA, Yeovil, Somerset, UK), to lift the cells off the tissue culture flask surface. Once the cells had dislodged, culture media was added to stop 0.25% trypsin-EDTA activity and the resultant dislodged cells were then harvested by centrifugation at 1000 rpm for 10 minutes. The supernatant was discarded, the resulting pellet was re-suspended in 1 ml of culture media and a viable cell count was performed by trypan blue exclusion. The cells were then either seeded into new tissue culture flasks or used for experiments.

3.3.7 Viable cell counts by trypan blue exclusion

Cell viability was measured by using the trypan blue dye, which only penetrates non-viable cells that have perforated cell membranes and as a result the cells appear blue. In order to perform a viable cell count, 20µl of cell suspension was added to 20µl of 0.4% (w/v) trypan blue solution (Sigma Aldrich, Dorset, UK). This suspension was mixed throughly before being loaded onto a haemocytometer (Fisher Scientific. Loughborough, Leicester, UK). The number of viable and non-viable cells were then determined.

3.3.8 Characterisation of MSCs

To verify that the culture-expanded cells were indeed MSCs, phenotypic characterisation was performed on BMMSC028 and BMMSC101. Mesenchymal stem cells at passage 4-5 were harvested by trypsinisation, centrifuged at 1000 rpm for 10 minutes and re-suspended in PBS containing 2% bovine serum albumin (BSA) (Sigma Aldrich, Dorset, UK). Cell count was performed via trypan blue exclusion (see section 3.3.7), following which the cells were blocked with 10% normal human immunoglobulin (Ig) (Grifols, Cambridge, UK) solution. The cells were then incubated with the following phycoerythrin (PE) conjugated mouse monoclonal anti-human antibodies: CD34, CD45, CD105 (Immunotools, Friesoythe, Germany), CD73 and CD90 (BD Biosciences, Oxford, UK) (Dominici *et al*., 2006). Non-specific fluorescence was determined by incubating cells with isotype-matched control PE-conjugated antibodies IgG2a and IgG1 (Immunotools, Friesoythe, Germany). The immunoreactivity for each cluster of differentiation (CD) surface antigen was measured by flow cytometry using a Beckman Coulter FC500 Flow Cytometer and the data was analysed using Kaluza® Analysis 1.3 Software.

3.3.9 Determination of the cytotoxic effects of 3 mol% Ga doped BAG and 45S5 Bioglass® on human MSCs and Saso-2 cells.

3.3.9.1 Direct contact

To evaluate the cytotoxic effect, MSCs and Saos-2 cells were seeded onto either 3 mol% Ga doped BAG or 45S5 Bioglass® UV sterilised (see section 2.3.7.1 of chapter 2) particles. Initially for each concentration (2.5 mg/ml, 5 mg/ml, 10 mg/ml and 100 mg/ml), 3 mol% Ga doped

BAG and 45S5 BG® particles were placed into triplicate wells of a 24 well plate (Fisher Scientific, Loughborough, UK). One ml of DMEM/Hams-F-12 supplemented with 10% (v/v) FBS and 1% (v/v) P/S was then added to each well containing glass particles. Bone marrow derived MSCs and Saos-2 cells were then seeded at a cell density of 1 x 10^4 into each well, and incubated at 37ºC and 5% CO_2 for 96 hours. To visualise the number of viable and non-viable cells, LIVE/DEAD staining was performed. The staining solution was prepared with Calcein-AM and Propidium iodide (Sigma-Aldrich, Dorset, UK) as stated in the manufacturer's instructions. Once the staining solution was prepared, 1 ml was added to each well and the plate was incubated at 37ºC for 30 minutes. After 30 minutes the staining solution was removed and DMEM/Hams-F-12 culture media was added to the wells. Fluorescence microscopy (wavelength of 490 nm) was used to score the number of live (green) and dead (red) cells.

Calcein-AM is highly lipophilic and cell membrane permeable, but is not a fluorescent molecule. However, the calcein generated from Calcein-AM by esterase in viable cells emits a strong green fluorescence and therefore only stains viable cells. Nuclei staining dye, Propidium iodide cannot pass through a viable cell membrane. It enters the cell by passing through disordered areas of dead cell membrane, and intercalates with the DNA double helix of the cell to emit red fluorescence.

3.3.9.2 Indirect contact

For the indirect contact experiment, DMEM/Ham's-F12 culture media supplemented with 10% (v/v) FBS and 1% (v/v) P/S was conditioned with the UV sterilised (see section 2.3.7.1 of chapter 2) particles of either 3 mol% Ga BAG and 45S5 Bioglass® at the concentration of 2.5 mg/ml, 5 mg/ml, 10 mg/ml (lower concentrations), 25 mg/ml, 50 mg/ml and 100 mg/ml (higher concentrations). The conditioned medium was then incubated at 37°C for 72 hours in either a shaking incubator (100 rpm) or a static incubator. After the incubation period, conditioned medium was filtered using a 0.45 micron syringe filter (Sartorius Stedim Biotech, Goettingen, Germany) and pH readings were recorded using the Mettler Toledo pH probe. The filtered

conditioned media was divided equally into two separate sterile universals for each concentration. The pH of the media in one of the universals was not neutralised and it remained alkaline (pH ranging from 9 to >9), however the pH for the media in the other universal was neutralised to a pH of 7.5. This was achieved through the use of pH strips (Life Technologies, Paisley, UK) and the addition of 0.1M of HCl (Fisher Scientific, Loughborough, UK). Once the neutralisation process was completed, MSCs and Saos-2 cells were harvested via trypsinisation (see section 3.3.7). Cell counts were performed via trypan blue exclusion (see section 3.3.4), following which the cells were seeded into a 96 well plate (Fisher Scientific, Loughborough, UK), containing 200 µls of conditioned DMEM/Ham's-F12 culture media, at a density of 5 x 10^3 per well of a 96 well plate in triplicates. The cells were incubated at 37ºC and 5% CO_2 for 96 hours. During the 96 hour period the cells were treated once (at 48 hours) with the conditioned DMEM/Ham's-F12 culture media. Following the 96 hours of incubation, cell viability was determined using the MTT test (Milford, Haarlem, Netherlands) assay.

Cell viability was determined using the MTT (Milford, Haarlem, Netherlands) assay. NAD(P)H dependent cellular oxidoreductase enzymes present within viable cells reduce the tetrazolium dye, MTT 3-(4,5-dimethylthiazol-2-yl)-2,5-diphenyltetrazolium bromide to insoluble formazan crystals. The insoluble formazan is solubilised with dimethyl sulfoxide (DMSO) (Sigma Aldrich, Dorset, UK) and the absorbance can be determined as a direct measure of cell viability. The MTT solution was prepared on the day of its use. Hundred µl of 5mg/ml MTT was diluted per 1 ml PBS supplemented with 4.5g/l glucose (Molekula, Gillingham, Dorset, UK). Following the 96 hour incubation period, media was removed from each well and replaced with 100 µl of PBS/Glucose + MTT solution (Milford, Haarlem, Netherlands). The 96 well plate was incubated in the dark at 37ºC with 5% CO_2 for 4 hours. At the end of the incubation period, the solution was carefully removed and the plate was left to air dry for 10 minutes. Hundred µl of DMSO (Sigma-Aldrich, UK) was added to each well and the plate was mixed for 20 seconds on a shaker to dissociate cell debris. The absorbance was read using an Ascent MultiScan FX Spectrophotometer (Fisher Scientific, Loughborough, UK)

at 590nm and background at 690nm. The absorbance values obtained were corrected for background and normalised to the control.

3.3.10 To investigate the effect of the dissolution products of 3 mol% Ga doped BAG and 45S5 Bioglass® on cellular adhesion and morphology.

Stock solutions were prepared for UV sterilised (see section 2.3.7.1 of chapter 2) 3 mol% Ga doped BAG and 45S5 Bioglass at 2.5 mg/ml, 5 mg/ml and 10 mg/ml in DMEM/Ham's-F12 culture media supplemented with 10% (v/v) FBS and 1% (v/v) P/S. Culture medium without particles served as the control. The stock solutions and controls were incubated at 37°C in a static incubator and shaker (100 rpm) incubator for 72 hours. Following 72 hour incubation period the stock solutions were filtered using a 0.45 micron syringe filter and pH values measured using a Mettler Toledo pH probe. Refer to section 3.3.9.2 for the neutralisation of the filtered conditioned media. Once the neutralisation process was completed, MSCs and Saos-2 cells were harvested via trypsinisation (see section 3.3.7). Cells were seeded at a density of 5 x 10^3 per well of a 96 well plate in triplicate. The cells were incubated at 37ºC and 5% CO_2 for 96 hours. During the 96 hour period the cells were treated once (at 48 hours) with conditioned DMEM/Ham's-F12 culture media. At 96 hours phase contrast images were taken using a Jenoptik ProgRes CF Microscope (Microscope World, Carlsbad, USA).

3.3.11 Statistical analysis

Two-way ANOVA was carried out to determine statistical significances (GraphPad Prism 6.0). If a significant difference was detected a Tukey test and a Sidak's test were carried out to determine which values were significantly different. Differences were considered statistically significant at a level of $P < 0.05$.

3.4 RESULTS

3.4.1 Characterisation of MSCs.

To confirm that the culture-expanded bone marrow MSCs maintained their phenotype, they were stained for a set of cell surface (CD) markers. As shown in figure 3.1, the majority of the MSCs were positive for CD73 (88.0% ± SD 9.19), CD90 (87.8% ± SD 12.0) and CD105 (90.7% ± SD 1.37), but were negative for CD34 (99.5% ± SD 0.04) and CD45 (99.4% ± SD 0.07), suggesting that the culture-expanded MSCs were not of haematopoietic origin and had pluripotent differentiation potential. Therefore, under the right conditions they could differentiate into osteoblasts, chondrocytes and adipocytes.

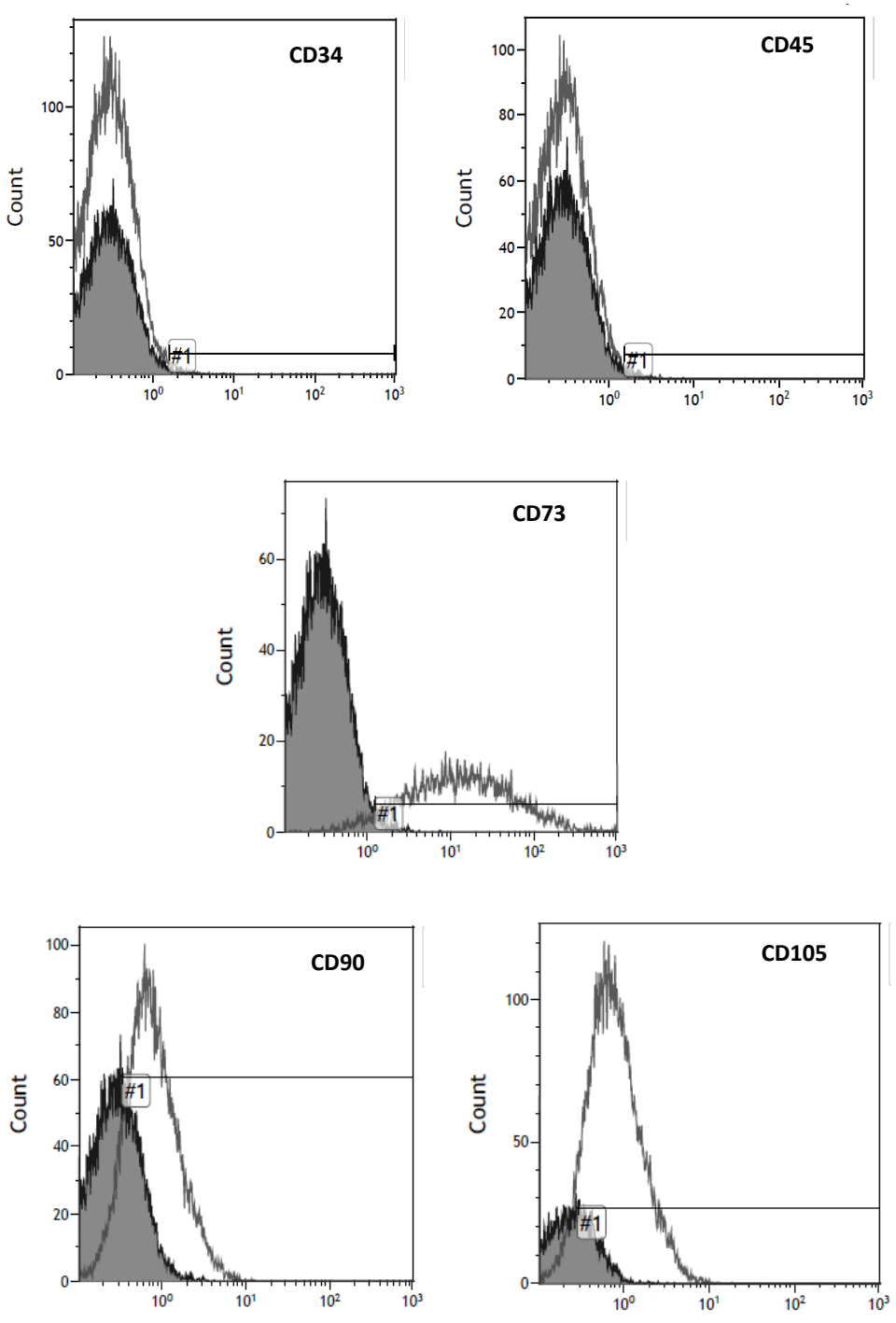

Figure 3.1 The CD profile of MSCs. MSCs were subjected to flow cytometry analysis after they were stained with antibodies for the negative CD markers CD34 and CD45 (top), and positive markers CD73 (middle), CD90 and CD105 (bottom). In each histogram the isotype-control Ig are shown in grey, and the CD marker in white.

3.4.2 Surface characteristics of 3 mol% Ga doped BAG and 45S5 Bioglass® particles

Figure 3.2 shows the SEM images of 3 mol% Ga doped BAG and 45S5 Bioglass® particles. The particles of both 3 mol% Ga doped BAG and 45S5 Bioglass® appear to be angular and irregular shaped. The surfaces of unreacted 45S5 Bioglass® and 3 mol% Ga doped BAG particles in figure 3.2 (A and D) appear smooth and are covered by flakes of smaller particles. Figures 3.2B and 3.2E show the surfaces of 45S5 Bioglass® and 3 mol% Ga doped BAG, respectively, revealing a relatively smooth surface with smaller particles scattered on top. Following 96 hours of soaking, the presence of small nodule-like speckles can be seen on the surface of 45S5 Bioglass® (Figure 3.2C). Figure 3.2F shows the surface of 3 mol% Ga doped BAG after 96 hour immersion in DMEM/Ham's-F12 culture media, revealing a smooth surface peppered with smaller particles.

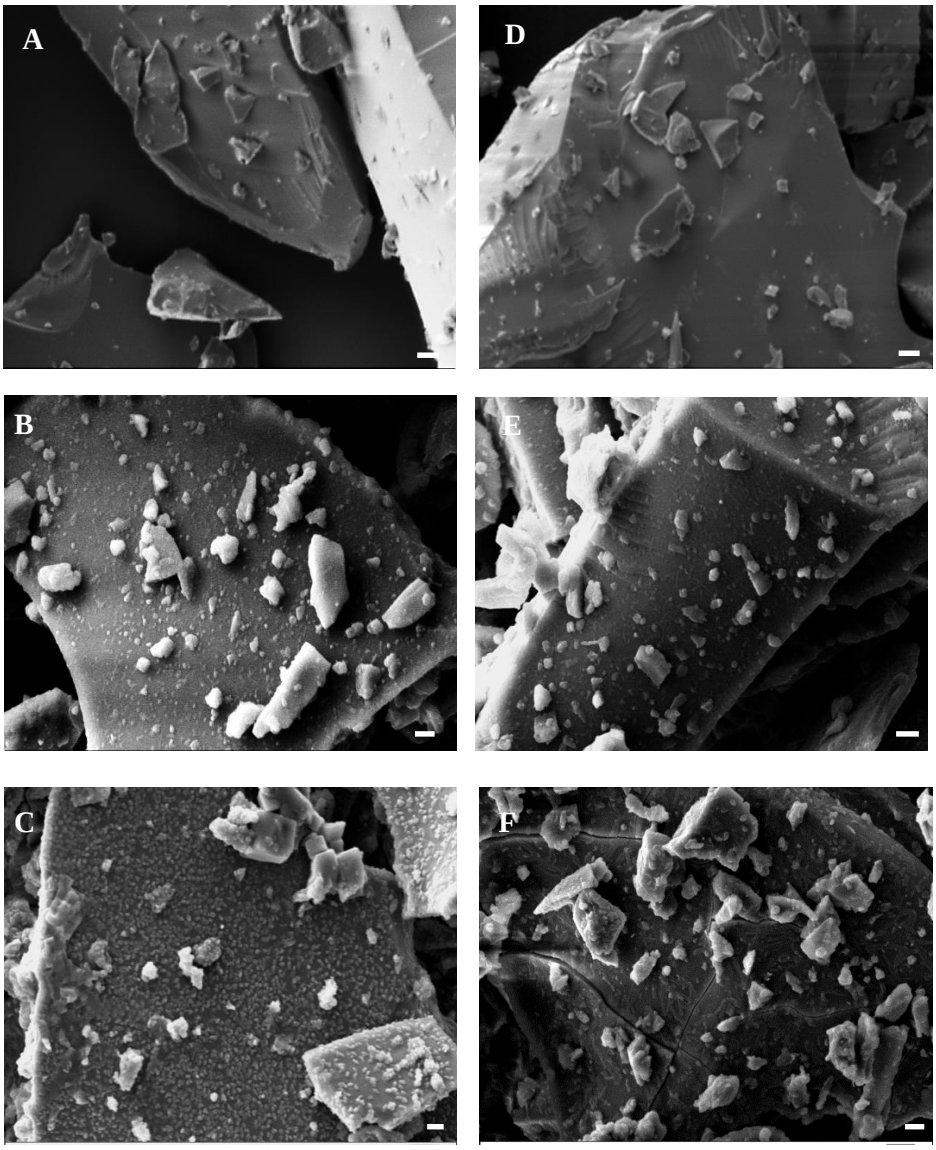

Figure 3.2 SEM images of the surfaces of (**A**) 45S5 Bioglass® particles at 0 hours at 5.00 kV and WD = 9.5 mm, (**B**) 45S5 Bioglass® particles after soaking in DMEM/Ham's-F12 media for 24 at 15.00 kV and WD = 5 mm, and (**C**) 96 hours at 10.95 kV and WD = 6.5 mm, (**D**) 3 mol% Ga doped BAG at 0 hours at 5.00 kV and WD = 8.00 mm, (**E**) 3 mol% Ga doped BAG particles after soaking in DMEM/Ham's-F12 media for 24 at 15.00 kV and WD = 4.5 mm, and (**F**) 96 hours at 10.95 kV and WD = 4.5 mm. Bar represents 2µm.

3.4.3 The cytotoxic effect of 3 mol% Ga doped BAG and 45S5 Bioglass® at concentrations 25 - 100 mg/ml on Saos-2 cell viability.

LIVE/DEAD staining was performed to evaluate the cytotoxic effects of 3 mol% Ga doped BAG and 45S5 Bioglass® particles. Following exposure to the particles over a 96 hour period, viable (green) and non-viable (red) Saos-2 cells could not be seen on the particles, which appeared to have taken up the staining solution (see figure A.3 in appendix).

MTT assay was performed to assess Saos-2 cell viability following exposure to higher concentrations of 45S5 Bioglass® and 3 mol% Ga doped BAG dissolution products. The results were calculated as percentages of respective controls. As shown in figure 3.3 the dissolution products of 45S5 Bioglass® and 3mol% Ga doped BAG demonstrated a significant cytotoxic effect against Saso-2 cells in comparison to the non-treated control. At all the concentrations tested 45S5 Bioglass® exhibited significant cytotoxicity ($p = < 0.0001$) with cell viability of 16.9%, 9.08%, and 7.91% for 25mg/ml, 50 mg/ml and 100 mg/ml, respectively. Dissolution products of 3 mol% Ga doped BAG ($p = < 0.0001$) were similar to 45S5 Bioglass® in their action, with cell viability of 13.8%, 5.87% and 6.89% at 25 mg/ml, 50 mg/ml and 100 mg/ml, respectively. No statistical significant difference was observed between 45S5 Bioglass® and 3 mol% Ga doped BAG at all concentrations tested.

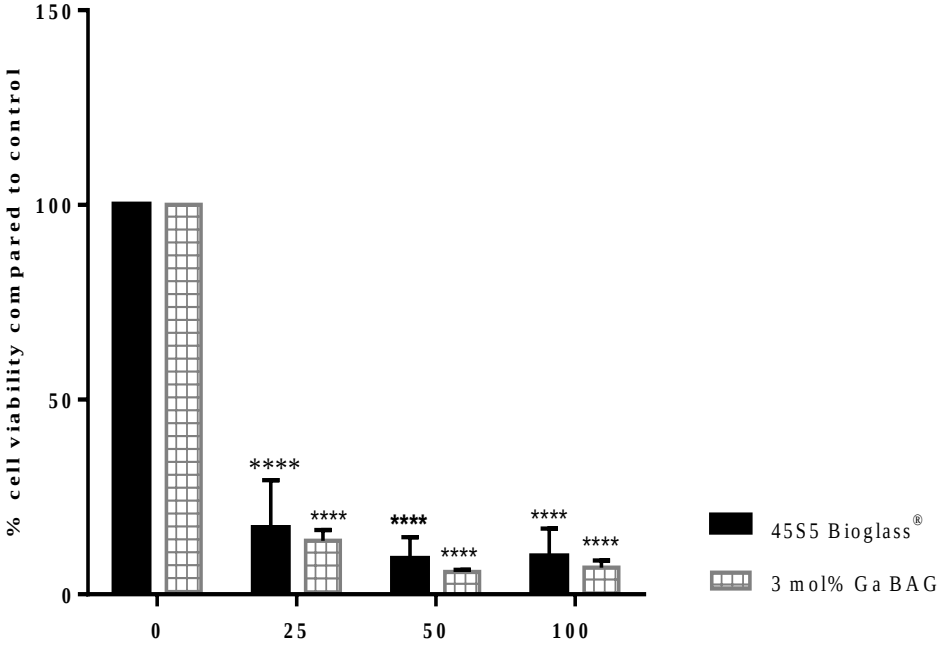

Figure 3.3 The effect of the dissolution products of 45S5 Bioglass® and 3 mol% Ga doped BAG on Saos-2 cells. MTT assays were used to assess Saos-2 cell viability following 96 hours incubation in BAG conditioned medium. Data shown are expressed as means ± SD (n=3) and reported at a significant level of $p < 0.0001$ (****).

3.4.4 pH analysis of 3 mol% Ga doped BAG and 45S5 Bioglass® at concentrations 2.5-10 mg/ml

pH values of DMEM/Hams-F12 culture medium containing either 45S5 Bioglass® or 3 mol% Ga doped BAG particles increased with the increase of particle concentration under both static (Figure 3.4) and shaker (Figure 3.5) incubation conditions. Culture medium containing 45S5 Bioglass® showed a statistically significant ($p = < 0.0001$) rise in pH, which increased to 8.6 (± SEM 0.08), 8.6 (± SEM 0.14) and 9.2 (± SEM 0.03) for 2.5, 5 and 10 mg/ml concentrations, respectively, after 24 hours under static incubation conditions. Similarly, pH values for DMEM/Hams-F12 media containing 3 mol% Ga doped BAG particles also significantly ($p = < 0.0001$) increased to 8.5, 8.6 and 9.1 for 2.5, 5 and 10 mg/ml concentrations, respectively, in comparison to culture medium without particles at 24 hours. A further increase in pH was not observed for either 45S5 Bioglass® or 3 mol% Ga doped BAG particles after the initial increase reported at 24 hours for static incubation conditions.

Under shaker incubation conditions, pH values of the variable concentrations tested increased. The pH values significantly ($p = < 0.0001$) increased to 9.0, 9.4, and 9.5 for 45S5 Bioglass® particle concentrations 2.5, 5 and 10 mg/ml, respectively, after 24 hours. Likewise, 3 mol% Ga doped BAG particles also significantly ($p = 0.0001$) increased the pH of the culture medium to 8.9, 9.2 and 9.5 for 2.5, 5 and 10 mg/ml concentrations.

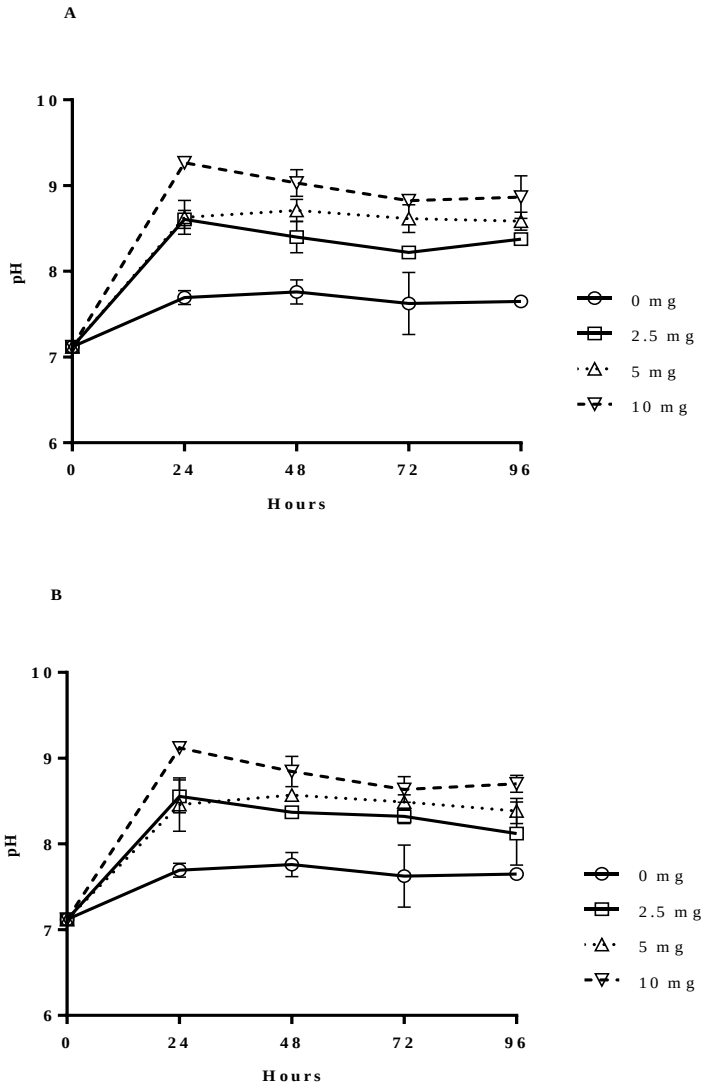

Figure 3.4 pH analysis of variable concentrations of (**A**) 45S5 Bioglass® and (**B**) 3 mol% Ga doped BAG particles immersed in DMEM/Ham's-F12 media over a 96 hour period, under static incubation conditions. Data shown are expressed as means ± SD (n=2).

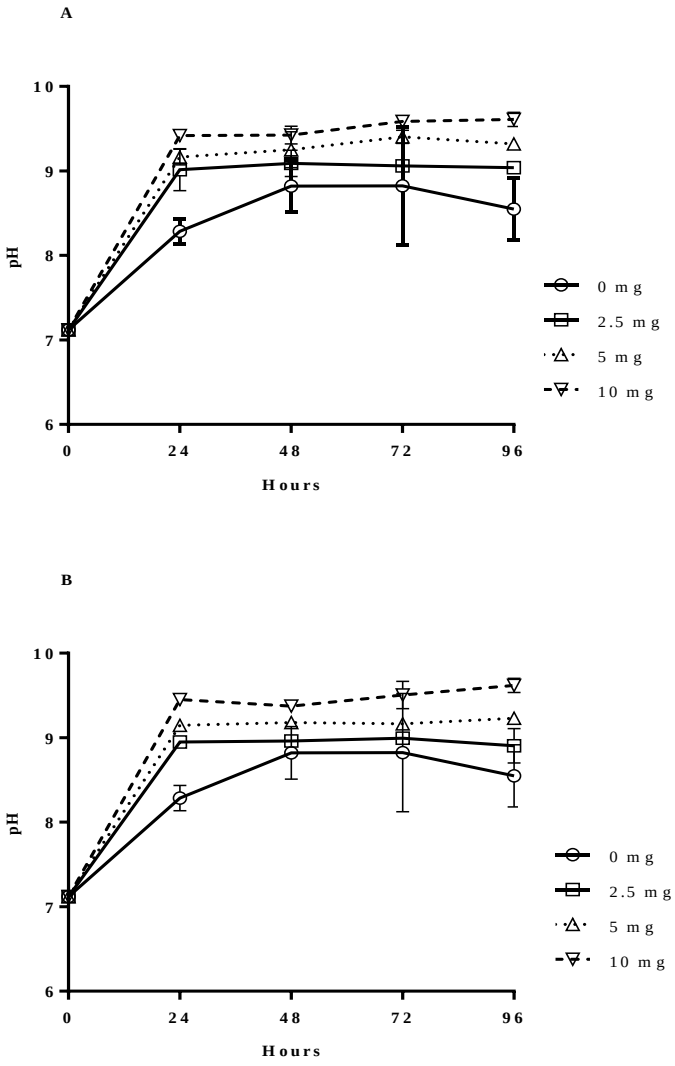

Figure 3.5 pH analysis of variable concentrations of (**A**) 45S5 Bioglass® and (**B**) 3 mol% Ga doped BAG particles immersed in DMEM/Ham's-F12 media over a 96 hour period, under shaker incubation conditions. Data shown are means ± SD (n=2).

3.4.5 Direct contact of 3 mol% Ga doped BAG and 45S5 Bioglass® particles at concentrations 2.5 – 10 mg/ml with Saos-2 cells and MSCs

3.4.5.1 Saos-2 cells

The viability of Saos-2 cells was compromised as the concentration of 45S5 Bioglass® and 3 mol% Ga doped BAG particles increased. A high number of cells in group's 0mg/ml, 2.5 mg/ml and 5 mg/ml were stained with Calcein-AM (green – live) with very few cells stained with Propidium iodide (red – dead). However, at 10 mg there were a higher number of cells stained with Propidium iodide. This was observed for 45S5 Bioglass® (Figure 3.6) and 3 mol% Ga doped BAG (Figure 3.7) after 96 hours.

Figure 3.8 also shows that 2.5 mg/ml was the most effective concentration for both 45S5 Bioglass® (Figure 3.4A) and 3 mol% Ga doped BAG (Figure 3.4B) particles, with a viability of 90.4% and 85.1%, respectively. Moreover, 5 mg/ml of 45S5 Bioglass® exhibited a similar effect, as a significant difference ($p = 0.05$) was observed between 0 mg/ml. A statistically significant reduction in the viability of Saos-2 cells was observed after exposure to 3 mol% Ga doped BAG ($p = < 0.001$) particles at 10 mg/ml, compared to 0 mg/ml. The percentage viability at 10 mg/ml for 3 mol% Ga doped BAG particles was 51.2%, whereas for 45S5 Bioglass® particles was 61.4%.

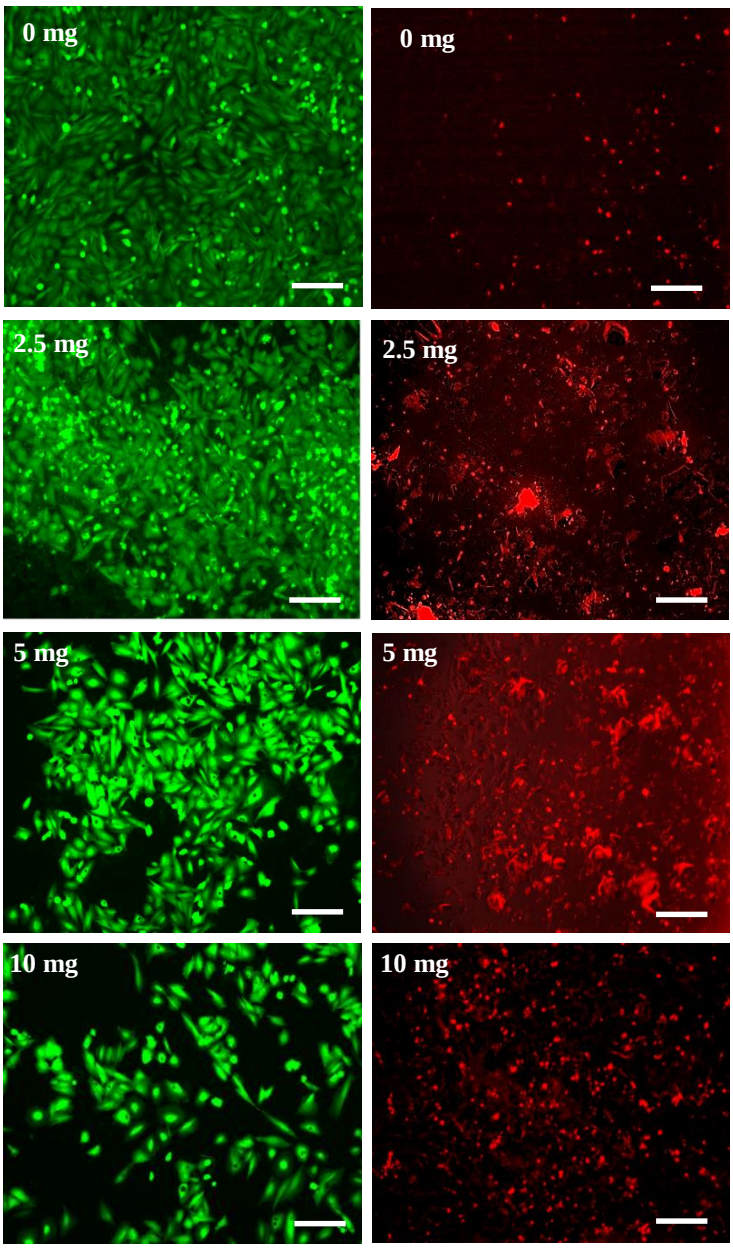

Figure 3.6 Same field of view fluorescent microscopy images at x10 objective are shown for LIVE/DEAD staining of Saos-2 cells cultured with and without 45S5 Bioglass® particles at variable concentrations for 96 hours. Green indicates live cells and red dead cells. Bar indicates 100 µm.

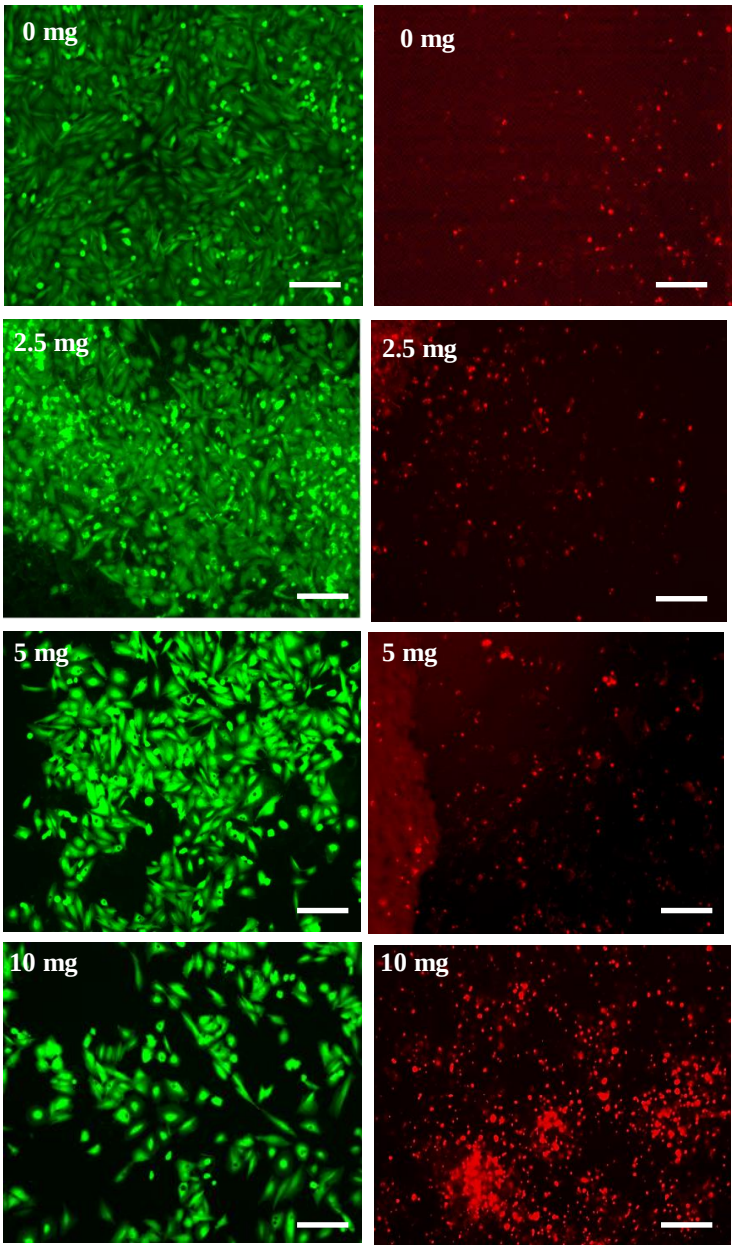

Figure 3.7 Same field of view fluorescent microscopy images at x10 objective are shown for LIVE/DEAD staining of Saos-2 cells cultured with and without 3 mol% Ga doped BAG particles at variable concentrations, for 96 hours. Live cells are green and dead cells are red. Bar indicates 100µm.

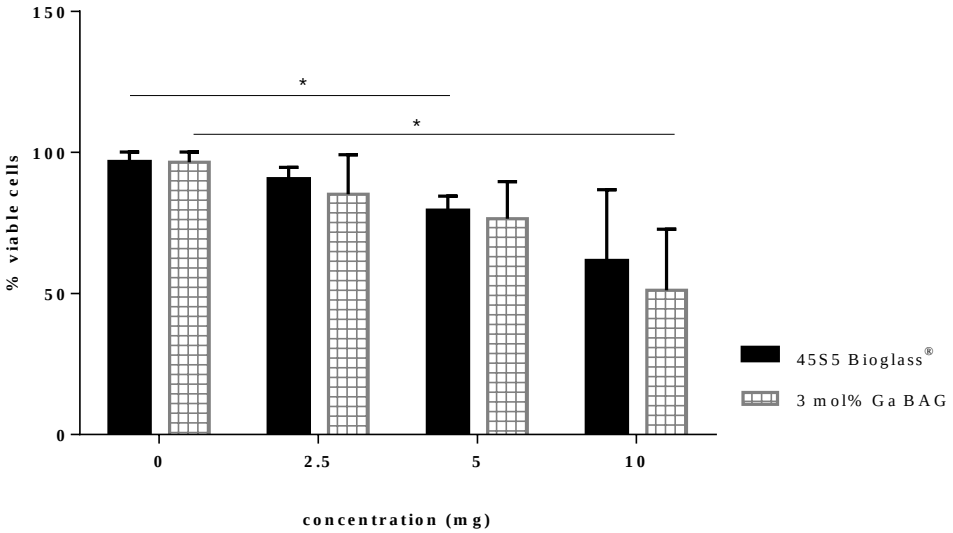

Figure 3.8 The proportion of viable and non-viable cells were determined following LIVE/DEAD staining of Saos-2 cells cultured with 45S5 Bioglass® and 3 mol% Ga doped BAG particles at variable concentrations, over a 96 hour incubation period. Viable cells of Saos-2 cells cultured with (**A**) 45S5 Bioglass® and **(B**) 3 mol% Ga doped BAG particles. Data shown are expressed as means ± SD (n=3) and reported at a significant level of p = < 0.05 (*).

3.4.5.2 MSCs

LIVE/DEAD staining demonstrated that particles of 45S5 Bioglass® (Figure 3.9) and 3 mol% Ga doped BAG (Figure 3.10) were non-cytotoxic with live (green) cells visible in all concentrations with very few dead (red) cells, after 96 hours in culture. However, figure 3.11 shows a slight but progressive reduction in MSC viability with increasing particle concentration for both 45S5 Bioglass® (Figure 3.11A) and 3 mol% Ga doped BAG (Figure 3.11B). Despite the slight reduction in cell viability no statistical significance was observed. Nevertheless at 10 mg/ml the percentage of viable MSCs following exposure to 45S5 Bioglass® particles was 73.2% and a similar effect was exhibited by 3 mol% Ga doped BAG particles, with a cell viability percentage of 73.3%.

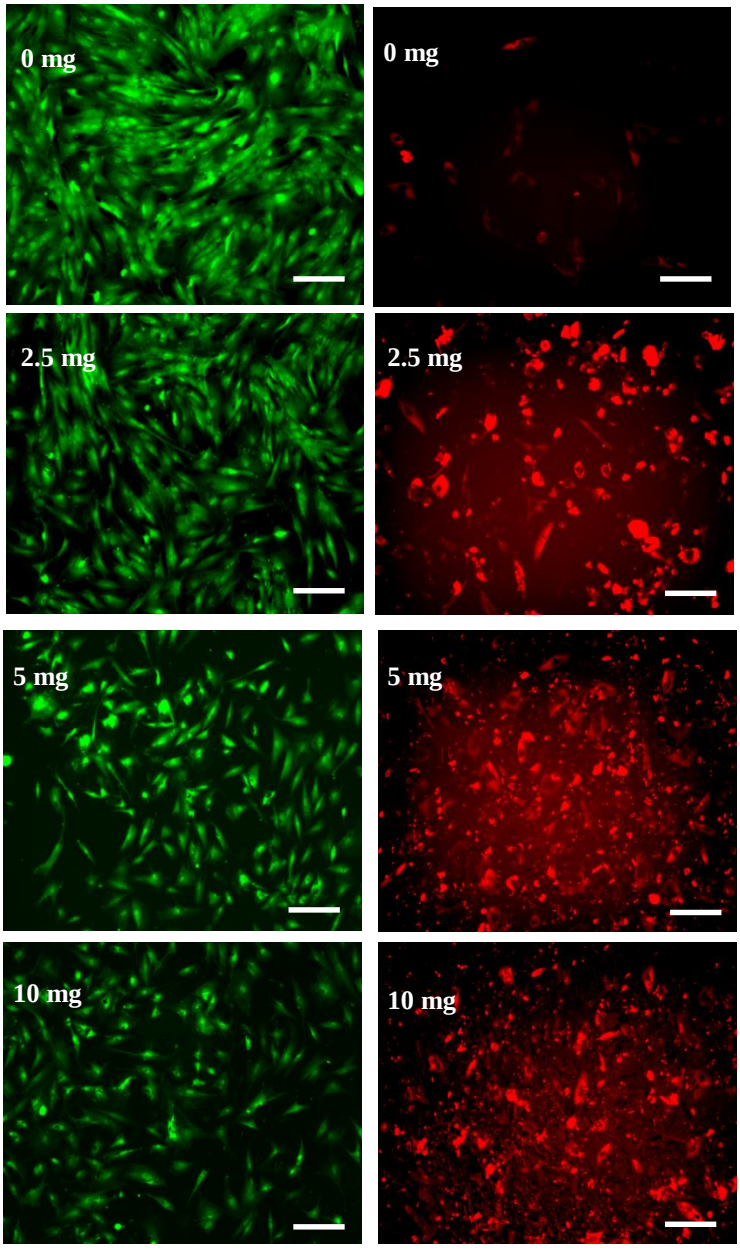

Figure 3.9 Same field of view fluorescent microscopy images at x10 objective are shown for LIVE/DEAD staining of MSCs cells cultured with and without 45S5 Bioglass® particles for 96 hours. Live cells are green and dead cells are red. Bar indicates 100µm.

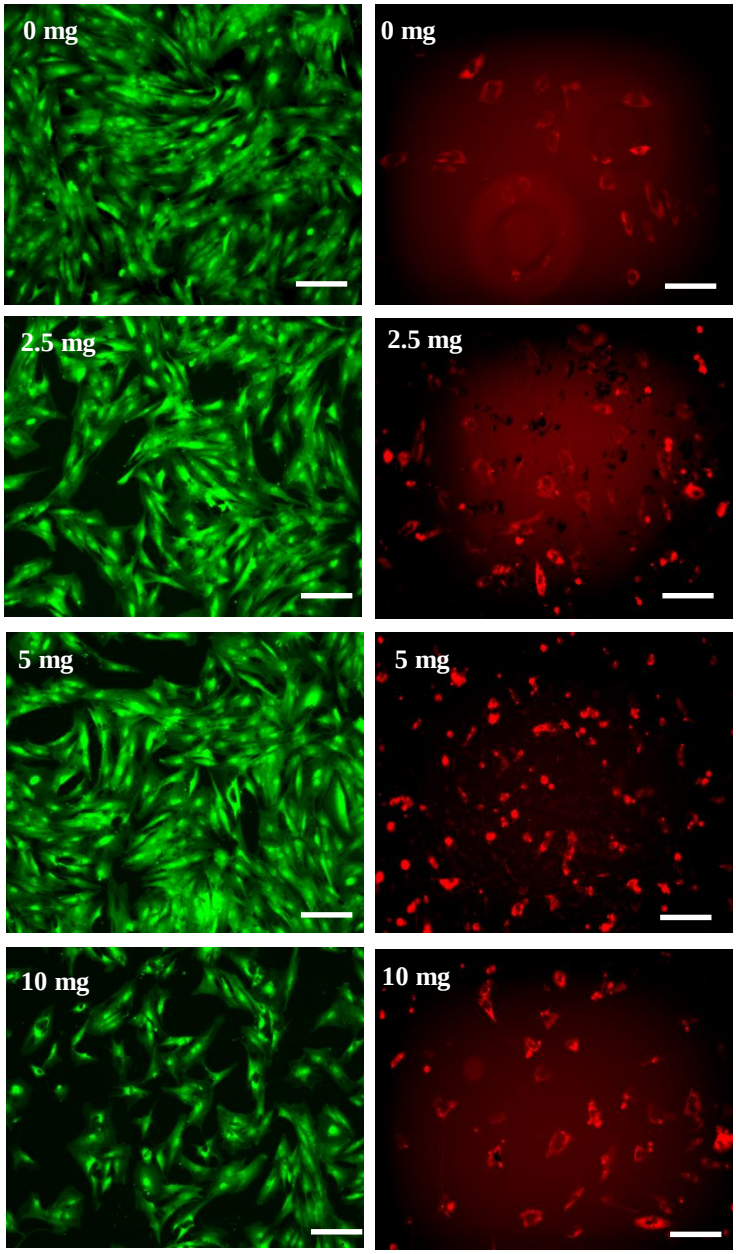

Figure 3.10 Same field of view fluorescent microscopy images are shown for LIVE/DEAD staining of MSCs cells cultured with variable concentrations and without 3 mol% Ga doped BAG particles, for 96 hours. Live cells are green and dead cells are red. Bar indicates 100µm.

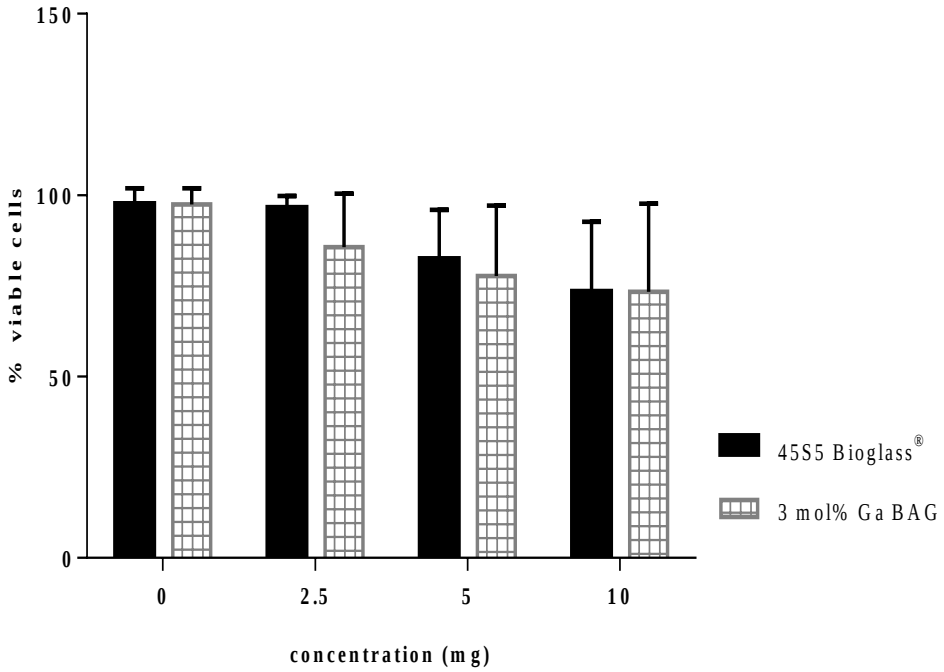

Figure 3.11 The proportion of viable or non-viable cells were determined following LIVE/DEAD staining of MSCs cultured with 45S5 Bioglass® and 3 mol% Ga doped BAG particles at variable concentration, over a 96 hour incubation period. Viable cells of MSCs cultured with (**A**) 45S5 Bioglass® and, (**B**) 3 mol% Ga doped BAG particles. Data shown are expressed as means ± SD (n=3).

3.4.6 Cytotoxic effect of 3 mol% Ga doped BAG and 45S5 Bioglass® dissolution products at concentrations 2.5 -10 mg/ml on Saos-2 cell and MSC viability

3.4.6.1 The cytotoxic effect of the dissolution products of 3 mol% Ga doped BAG and 45S5 Bioglass® on Saos-2 cells

The MTT assay was used to assess the viability of Saos-2 cells cultured in 45S5 Bioglass® and 3 mol% Ga doped BAG conditioned medium generated under static and shaker incubating conditions. The results were calculated as percentages of respective controls. As shown in figure 3.12 (A) under static incubation conditions the dissolution products of 45S5 Bioglass® and 3 mol% Ga doped BAG were cytotoxic, with 45S5 Bioglass® exhibiting greater cytotoxicity. A statistical significant reduction in Saos-2 cell viability was observed following exposure to 45S5 Bioglass® ($p = 0.05$) and 3 mol% Ga doped BAG ($p = 0.05$) dissolution products at 10 mg/ml, compared to control (0 mg/ml). The percentage viability at 10 mg/ml for 45S5 Bioglass® was 67%, and for 3 mol% Ga doped BAG 68.6%.

The dissolution products from 45S5 Bioglass® and 3 mol% Ga doped BAG conditioned DMEM/Ham's-F12 culture medium generated under shaker incubating conditions decreased the number of viable Saos-2 cells (Figure 3.12B). Moreover, the cytotoxicity of the dissolution products was concentration dependent, as the highest concentration of 10 mg/ml exhibited the strongest cytotoxic effect. A statistically significant reduction in Saos-2 cell viability was observed after exposure to the dissolution products of 45S5 Bioglass® at 10 mg/ml with a cell viability of 4.78% ($p = 0.0001$), whilst 18.4% ($p = 0.0001$) was observed for 3 mol% Ga doped BAG, compared to the control. The dissolution products of 45S5 Bioglass® ($p = 0.001$) demonstrated a greater cytotoxic effect with a cell viability of 38.4% whereas 72.7% was observed for 3 mol% Ga doped BAG, at 5 mg/ml.

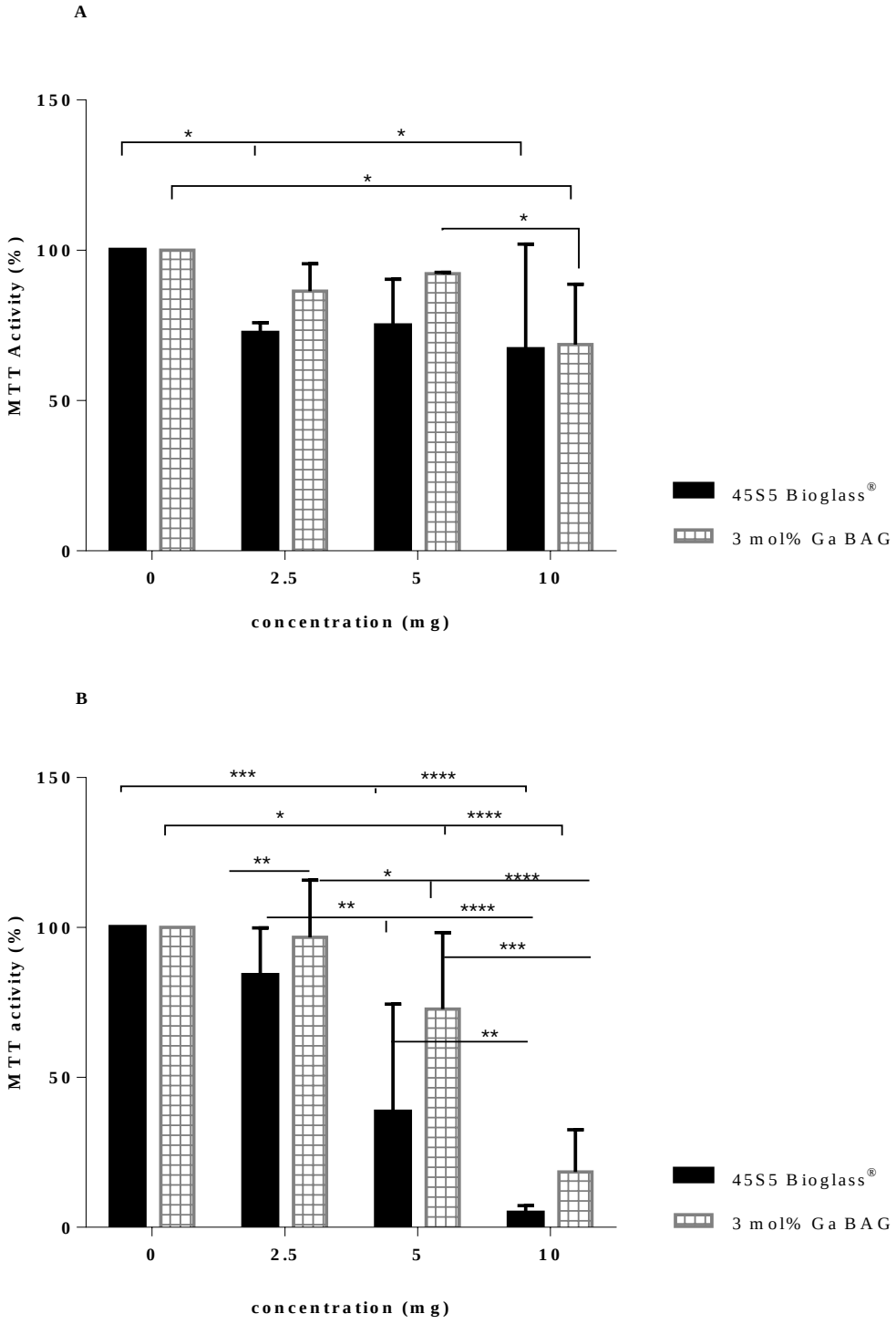

Figure 3.12 The effect of the dissolution products of 45S5 Bioglass® and 3 mol% Ga doped BAG on Saos-2 cells. MTT assays were used to assess Saos-2 cell viability following 96 hours incubation in BAG conditioned medium generated under static (**A**) and shaker (**B**) incubating conditions. Data shown are expressed as means ± SD (n=3) and reported at a significant level of p = 0.05 (*), p = 0.0097 (**), p = 0.0009 (***) and p = 0.0001 (****).

3.4.6.2 The cytotoxic effect of pH neutralised dissolution products of 3 mol% Ga doped BAG and 45S5 Bioglass® on Saos-2 cells

Following pH neutralisation of conditioned DMEM/Ham's-F12 culture medium, which had been generated in a static incubator the dissolution products of 45S5 Bioglass® and 3 mol% Ga doped BAG were non-cytotoxic at the concentrations tested (Figure 3.13A). The dissolution products of 45S5 Bioglass® at 2.5 mg/ml increased ($p = 0.03$) cell viability, which was 108.3 %, whereas cell viability of 88% in comparison to the non-treated control was observed for the dissolution products of 3 mol% Ga doped BAG.

The pH neutralisation of conditioned culture medium generated under shaker incubating conditions, which consisted of dissolution products from 45S5 Bioglass® and 3 mol% Ga doped BAG demonstrated a cytotoxic effect at 10 mg/ml (Figure 3.13B). 45S5 Bioglass® dissolution products exhibited a slightly greater cytotoxicity with cell viability of 30.8%, than 3 mol% Ga doped BAG dissolution products (46.1%). Although, no statistical significant difference was observed the cytotoxic effect of the dissolution products on Saos-2 cells appeared to be concentration dependent.

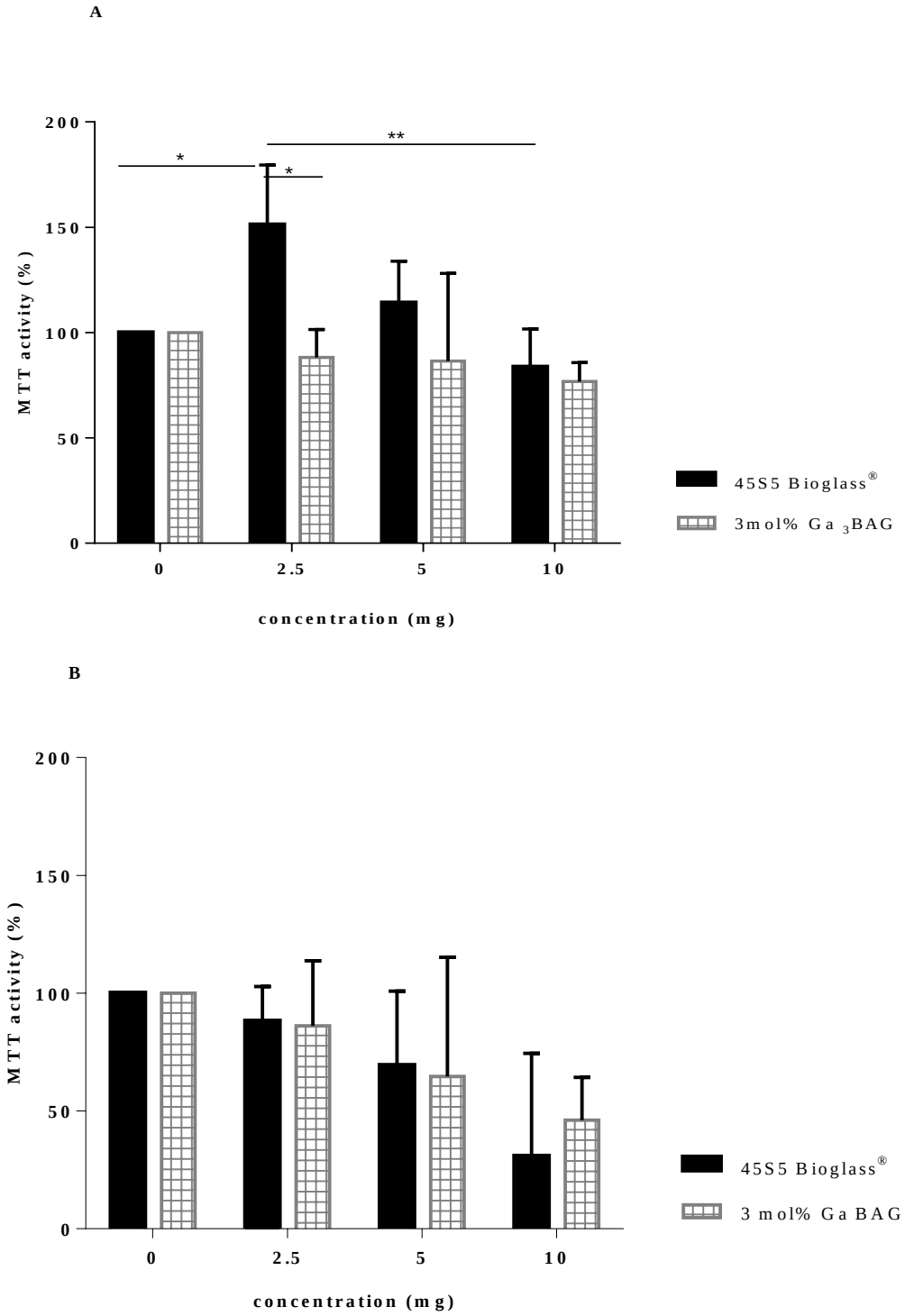

Figure 3.13 The effect of dissolution products of 45S5 Bioglass® and 3 mol% Ga doped BAG following pH neutralisation on Saos-2 cells. MTT assays were used to assess Saos-2 cell viability following 96 hours incubation in BAG conditioned medium generated under static (**A**) and shaker (**B**) incubating conditions. . Data shown are expressed as means ± SD (n=3) and are reported at a significant level of p = 0.03 (*), and p = 0.001 (**).

3.4.6.3 The cytotoxic effect of the dissolution products of 3 mol% Ga doped BAG and 45S5 Bioglass® on MSCs

Under static incubating conditions the culture medium generated with dissolution products from 45S5 Bioglass® and 3 mol% Ga doped BAG demonstrated a concentration dependent cytotoxic effect on MSC viability (Figure 3.14A). A statistically significant reduction ($p = 0.05$) in the viability of MSCs was observed after exposure to the dissolution products of 45S5 Bioglass® at 10 mg/ml, compared to the non-treated control. Although, no statistical significant difference was observed between 45S5 Bioglass® and 3 mol% Ga doped BAG dissolution products at 10 mg/ml, the dissolution products of 45S5 Bioglass® exhibited greater cytotoxicity with a cell viability of 46.6%, whilst the cell viability observed for 3 mol% Ga doped BAG was 58%.

Culture medium consisting of dissolution products from 45S5 Bioglass® and 3 mol% Ga doped BAG generated under shaker incubation conditions demonstrated a concentration dependent cytotoxicity (Figure 3.13B). At the highest concentration tested, 10 mg/ml exhibited statistically significant cytotoxicity for both 45S5 Bioglass® ($p = 0.001$) and 3 mol% Ga doped BAG ($p = 0.01$), compared to 0 mg/ml. Additionally, the dissolution products of 45S5 Bioglass® and 3 mol% Ga doped BAG at 5 mg/ml also demonstrated a statistical significance of $p = 0.05$, compared to 0 mg/ml. Despite no statistical significant difference being observed between the two glass groups, 45S5 Bioglass® ($p = 0.001$) demonstrated greater cytotoxicity at 10 mg/ml with a reduction in cell viability of 16.4%, whilst 3 mol% Ga doped BAG ($p = 0.01$) displayed a cell viability of 33.5%.

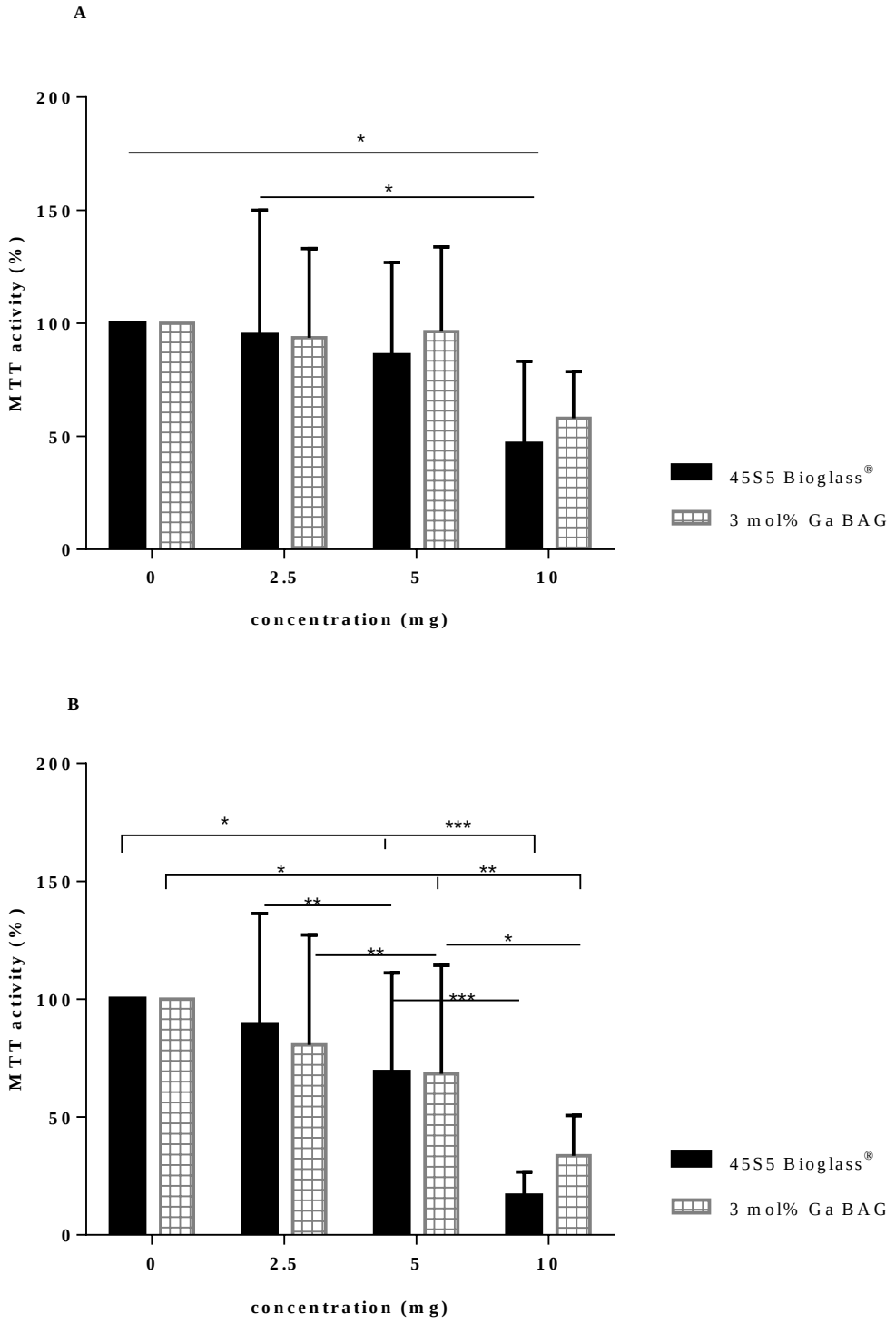

Figure 3.14 The effect of the dissolution products of 45S5 Bioglass® and 3 mol% Ga doped BAG on MSCs cells. MTT assays were used to assess MSCs viability following 96 hours incubation in BAG conditioned medium generated under static (**A**) and shaker (**B**) incubating conditions. Data shown are expressed as means ± SD (n=3) and reported at a significant level of p 0.05 (*), p = 0.01 (**) and p = 0.001 (***).

3.4.6.4 The cytotoxic effect of pH neutralised dissolution products of 3 mol% Ga doped BAG and 45S5 Bioglass® on MSCs

As shown in figure 3.15 (A) the dissolution products of 45S5 Bioglass® and 3 mol% Ga doped BAG conditioned medium generated under static incubating conditions, demonstrated a non-cytotoxic effect on MSCs. The viability of MSCs significantly increased at 2.5 mg/ml and 5 mg/ml for 45S5 Bioglass® with cell viability of 151.9% and 125.7%, respectively. Additionally, statistical significance ($p = 0.05$) was observed between 2.5 mg/ml and the higher concentrations. The dissolution products of 3 mol% Ga doped BAG did not increase the viability of MSCs however they also did not exhibit cytotoxicity at the lower concentrations tested. 3 mol% Ga doped BAG demonstrated cytotoxicity at the highest concentration of 10 mg/ml in comparison to the non-treated control, with cell viability of 71.3%, whereas a reduction in cell viability of 89.8% was observed for 45S5 Bioglass®.

Figure 3.15 (B) demonstrates that the cytotoxic effect of 45S5 Bioglass® and 3 mol% Ga doped BAG dissolution products present in conditioned culture media generated under shaker incubating conditions, had a concentration dependent cytotoxic effect on MSCs. 2.5 mg/ml exhibited the least cytotoxic effect with a cell viability of 105.1% and 106.5% for 45S5 Bioglass® and 3 mol% Ga doped BAG, respectively. However, a statistically significant reduction in MSCs viability was observed at 10 mg/ml for 45S5 Bioglass® ($p = 0.05$) and 3 mol% Ga doped BAG ($p = 0.01$), compared to 0 mg/ml. Furthermore, at 10 mg/ml 3 mol% Ga doped BAG dissolution products exerted a slightly greater cytotoxic effect than 45S5 Bioglass® with a cell viability of 48.8% and 59.9%, respectively.

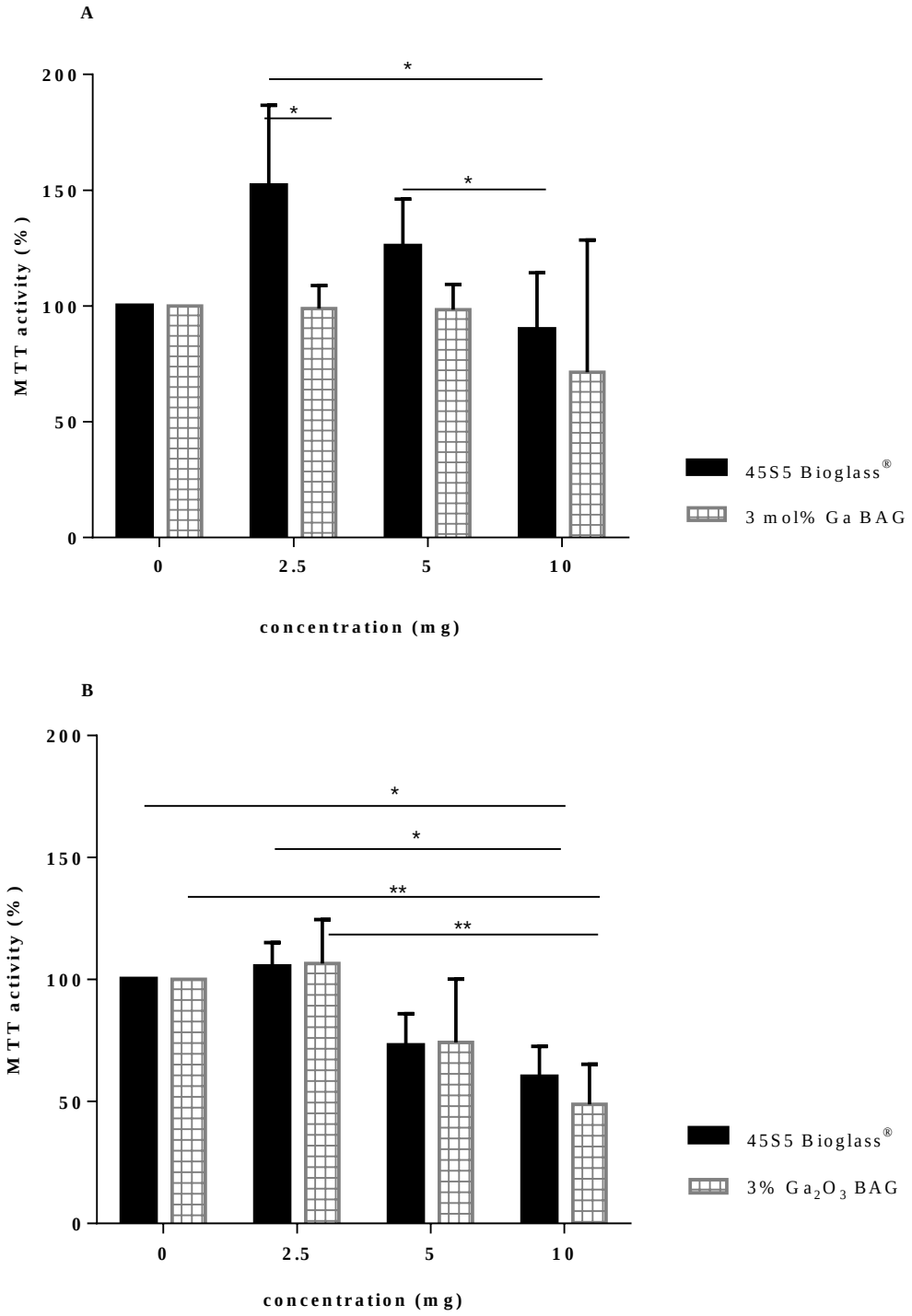

Figure 3.15 The effect of dissolution products of 45S5 Bioglass® and 3 mol% Ga doped BAG following pH neutralisation on MSCs. MTT assays were used to assess Saos-2 cell viability following 96 hours incubation in BAG conditioned medium generated under static (**A**) and shaker (**B**) incubating conditions. Data shown are expressed as means ± SD (n=3) and reported at a significant level of p 0.05 (*) and p 0.01 (**).

3.4.7 Cell Morphology and adhesion studies – at concentrations 2.5-10 mg/ml

3.4.7.1 The effect of the dissolution products from 3 mol% Ga doped BAG and 45S5 Bioglass® on Saos-2 cells

The morphology and the shape of Saos-2 cells cultured with the dissolution products of 45S5 Bioglass® and 3 mol% Ga BAG were examined by light microscopy. The conditioned culture medium with the dissolution products of 45S5 Bioglass® and 3 mol% Ga doped BAG was generated under static and shaker incubating conditions. Figures 3.16 and 3.17 show that as the concentration of the dissolution products from both glasses increased, the typical cube shape of Saos-2 cells transformed into a rounded shape and detached themselves from the surface of the well. This transformation appears more prominent for Saos-2 cells treated with culture media conditioned with 10 mg/ml of 45S5 Bioglass® and 3 mol% Ga doped BAG under shaker incubation conditions. As the concentration of the dissolution products increased, the number of viable cells viewed under the microscope decreased, compared to the non-treated control.

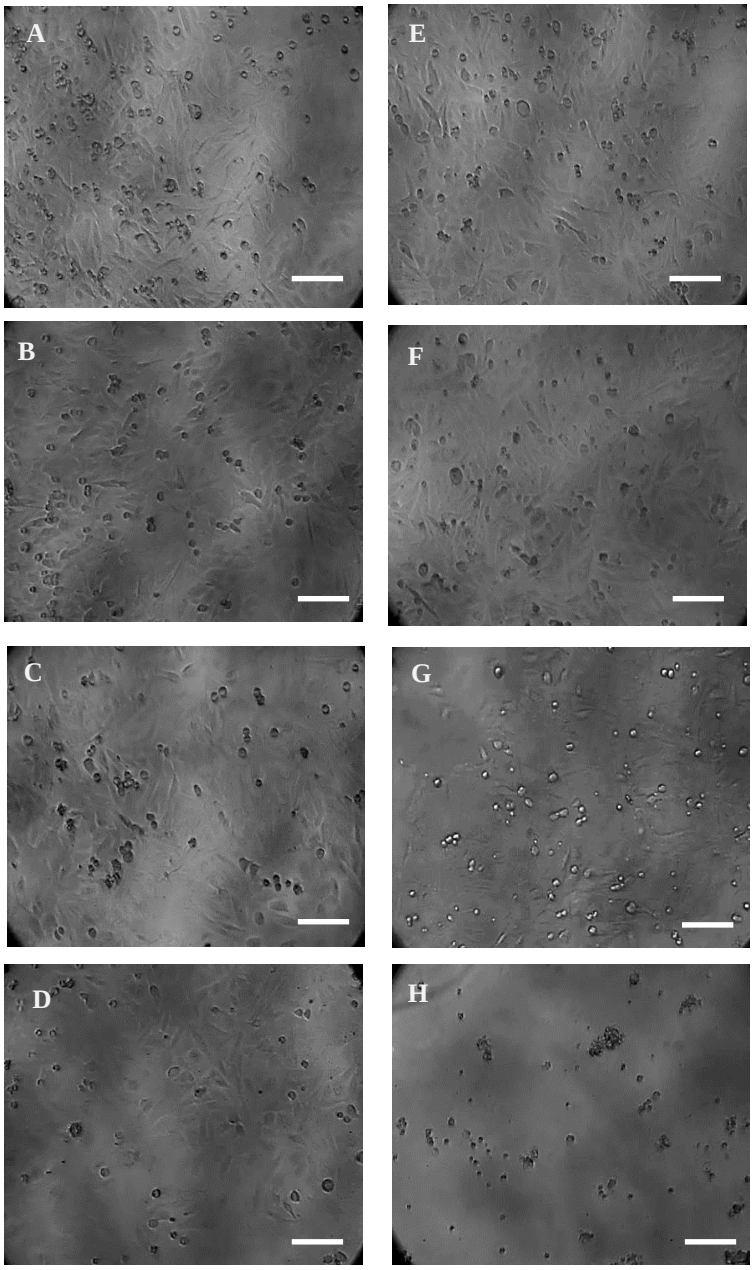

Figure 3.16 Phase contrast images at x10 objective of Saos-2 cells treated with 45S5 Bioglass® conditioned media following a 96 hour incubation period. Saos-2 cells were treated with conditioned media generated under static incubation conditions at 0 mg/ml (**A**), 2.5 mg/ml (**B**), 5 mg/ml (**C**) and 10 mg/ml (**D**). Saos-2 cells were treated with conditioned media generated under shaker incubation conditions at 0 mg/ml (**E**), 2.5 mg/ml (**F**), 5 mg/ml (**G**) and 10 mg/ml (**H**). Bar indicates 100µm.

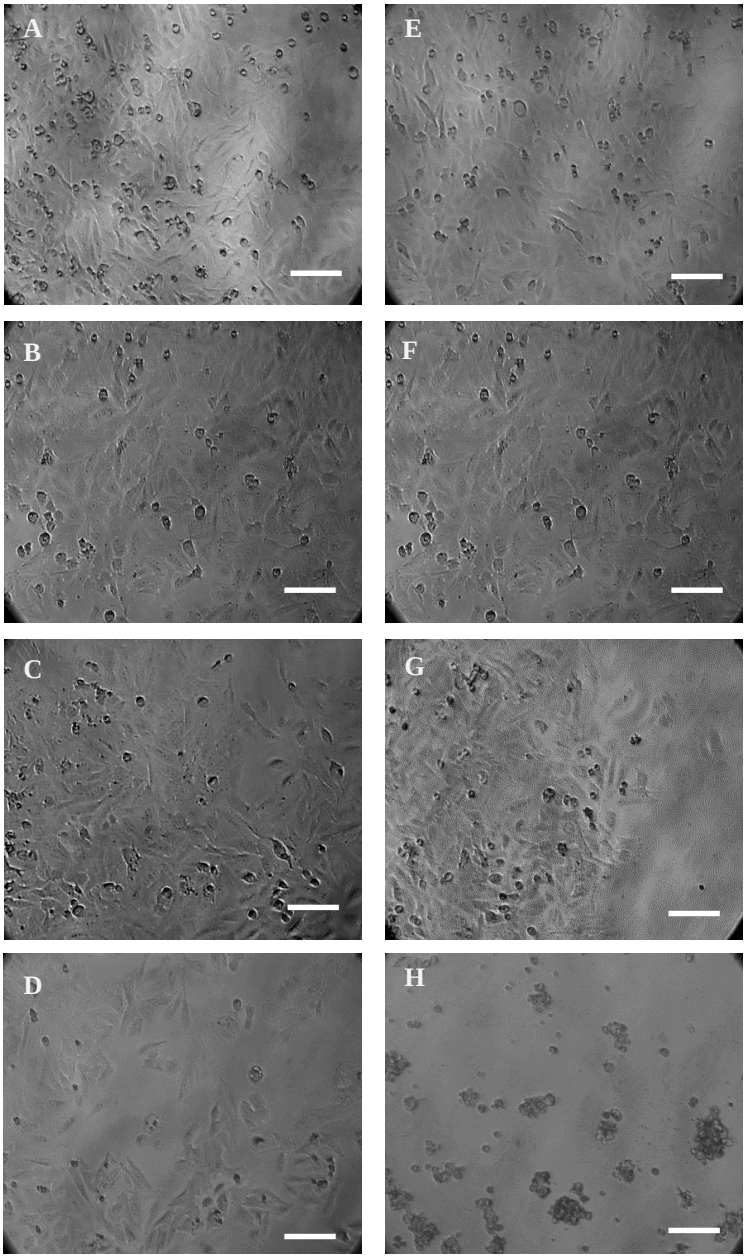

Figure 3.17 Phase contrast images at x10 objective of Saos-2 cells treated with 3 mol% Ga doped BAG conditioned media following a 96 hour incubation period. Saos-2 cells were treated with conditioned media generated under static incubation conditions at 0 mg/ml (**A**), 2.5 mg/ml (**B**), 5 mg/ml (**C**) and 10 mg/ml (**D**). Saos-2 cells were treated with conditioned media generated under shaker incubation conditions at 0 mg/ml (**E**), 2.5 mg/ml (**F**), 5 mg/ml (**G**) and 10 mg/ml (**H**). Bar indicates 100µm.

3.4.7.2 The effect of pH neutralised dissolution products of 3 mol% Ga doped BAG and 45S5 Bioglass® on Saos2 cells

Following pH neutralisation of culture medium conditioned with 45S5 Bioglass® and 3 mol% Ga doped BAG, generated under static and shaker incubating conditions; the media was used to treat Saos-2 cells for 96 hours. Figures 3.18 and 3.19 demonstrate that the morphology of Saos-2 cells cultured with conditioned media generated under static incubation conditions was similar to Saos-2 cells treated with media without dissolution products. However, an increase in the concentration of the dissolution products resulted in a progressive reduction of viable cells.

The lower concentrations of 45S5 Bioglass® and 3 mol% Ga doped BAG conditioned culture medium generated under shaker incubation conditions did not affect the morphology of Saos-2 cells. At 10 mg/ml predominantly non-viable Saos-2 cells were observed which appeared rounded in shape and had detached from the well.

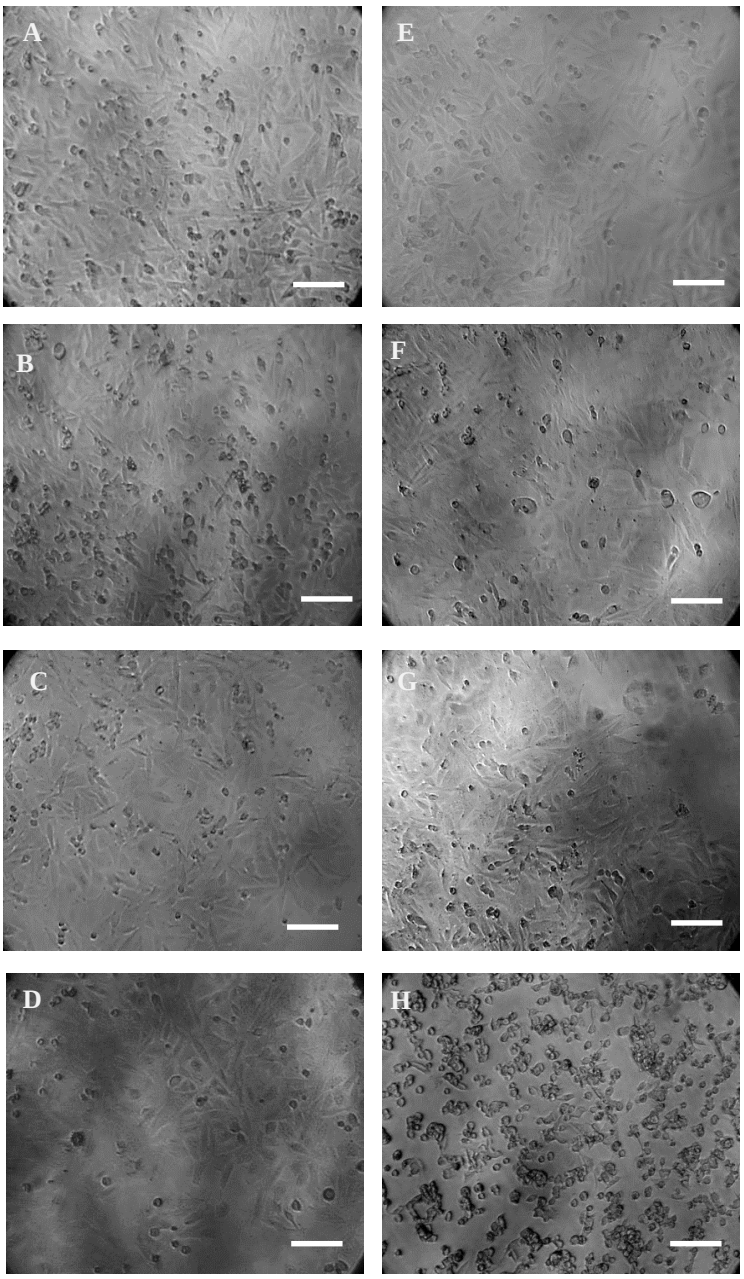

Figure 3.18 Phase contrast images at x10 objective of Saos-2 cells treated with 45S5 Bioglass® conditioned media following pH neutralisation, over a 96 hour incubation period. Saos-2 cells were treated with conditioned media generated under static incubation conditions at 0 mg/ml (**A**), 2.5 mg/ml (**B**), 5 mg/ml (**C**) and 10 mg/ml (**D**). Saos-2 cells were treated with conditioned media generated under shaker incubation conditions at 0 mg/ml (**E**), 2.5 mg/ml (**F**), 5 mg/ml (**G**) and 10 mg/ml (**H**). Bar indicates 100µm.

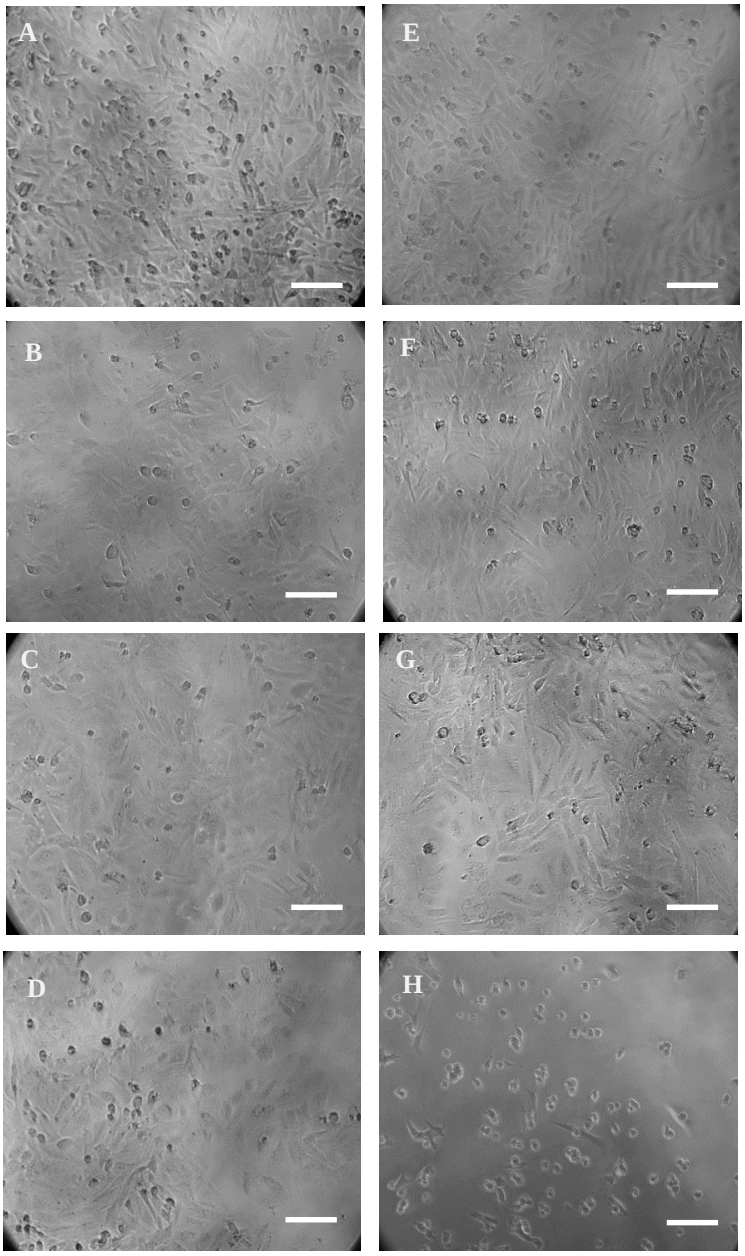

Figure 3.19 Phase contrast images at x 10 objective of Saos-2 cells treated with 3 mol% Ga doped BAG conditioned media following pH neutralisation, over a 96 hour incubation period. Saos-2 cells were treated with conditioned media generated under static incubation conditions at 0 mg/ml (**A**), 2.5 mg/ml (**B**), 5 mg/ml (**C**) and 10 mg/ml (**D**). Saos-2 cells were treated with conditioned media generated under shaker incubation conditions at 0 mg/ml (**E**), 2.5 mg/ml (**F**), 5 mg/ml (**G**) and 10 mg/ml (**H**). Bar indicates 100µm.

3.4.7.3 The effect of the dissolution products from 3 mol% Ga doped BAG and 45S5 Bioglass® on MSCs

Bone marrow derived MSCs cultured in 45S5 Bioglass® and 3 mol% Ga doped BAG conditioned culture medium generated under static incubating conditions had a similar morphology of long, thin, and widely dispersed, to MSCs cultured in the absence of dissolution products (Figures 3.20 and 3.21). Bone marrow MSCs cultured in lower concentrations of shaker conditioned medium of 45S5 Bioglass® and 3 mol% Ga doped BAG also presented a similar morphology as the MSCs grown in 0 mg/ml. The highest concentration of conditioned culture media for both 45S5 Bioglass® and 3 mol% Ga doped BAG reduced the number of viable MSCs, which appeared rounded. Additionally, extremely thin MSCs not widely dispersed were also observed at 10 mg/ml for both 45S5 Bioglass® and 3 mol% Ga BAG conditioned media, generated under shaker incubating conditions.

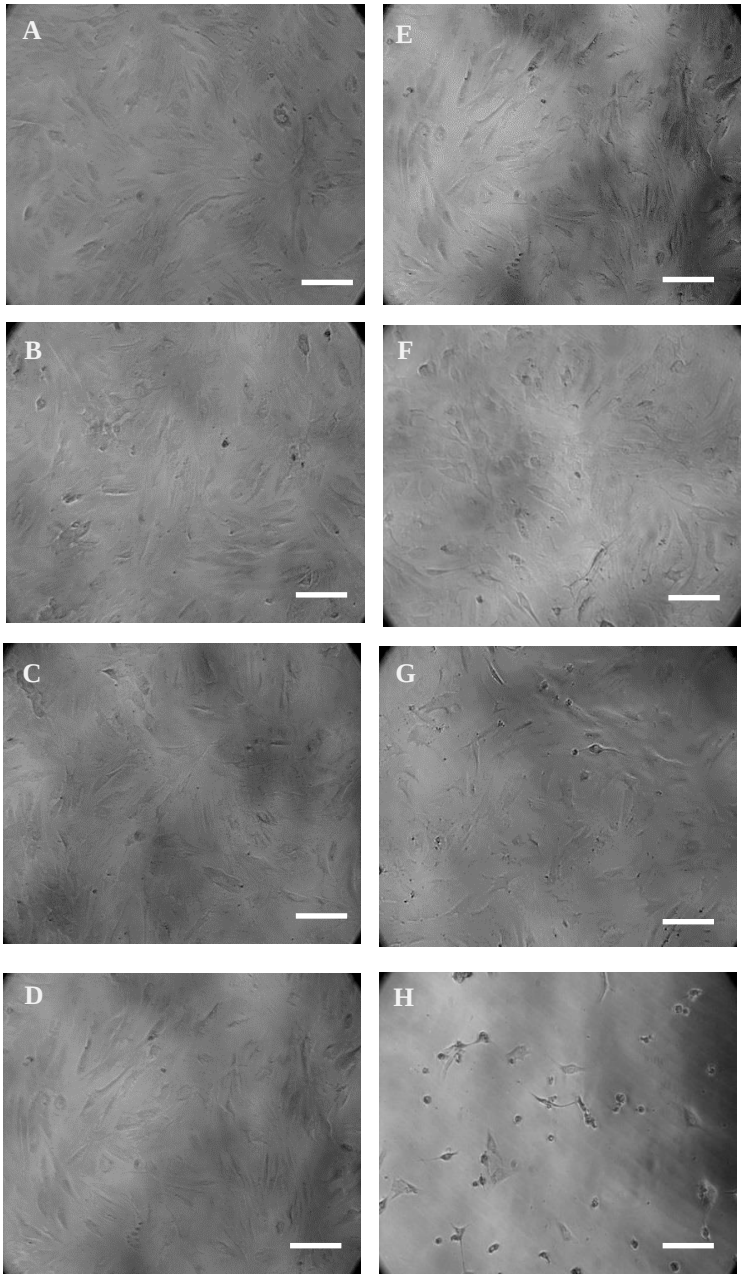

Figure 3.20 Phase contrast images at x10 objective of MSCs treated with 45S5 Bioglass® conditioned media following a 96 hour incubation period. MSCs were treated with conditioned media generated under static incubation conditions at 0 mg/ml (**A**), 2.5 mg/ml (**B**), 5 mg/ml (**C**) and 10 mg/ml (**D**). MSCs were treated with conditioned media generated under shaker incubation conditions at 0 mg/ml (**E**), 2.5 mg/ml (**F**), 5 mg/ml (**G**) and 10 mg/ml (**H**). Bar indicates 100µm.

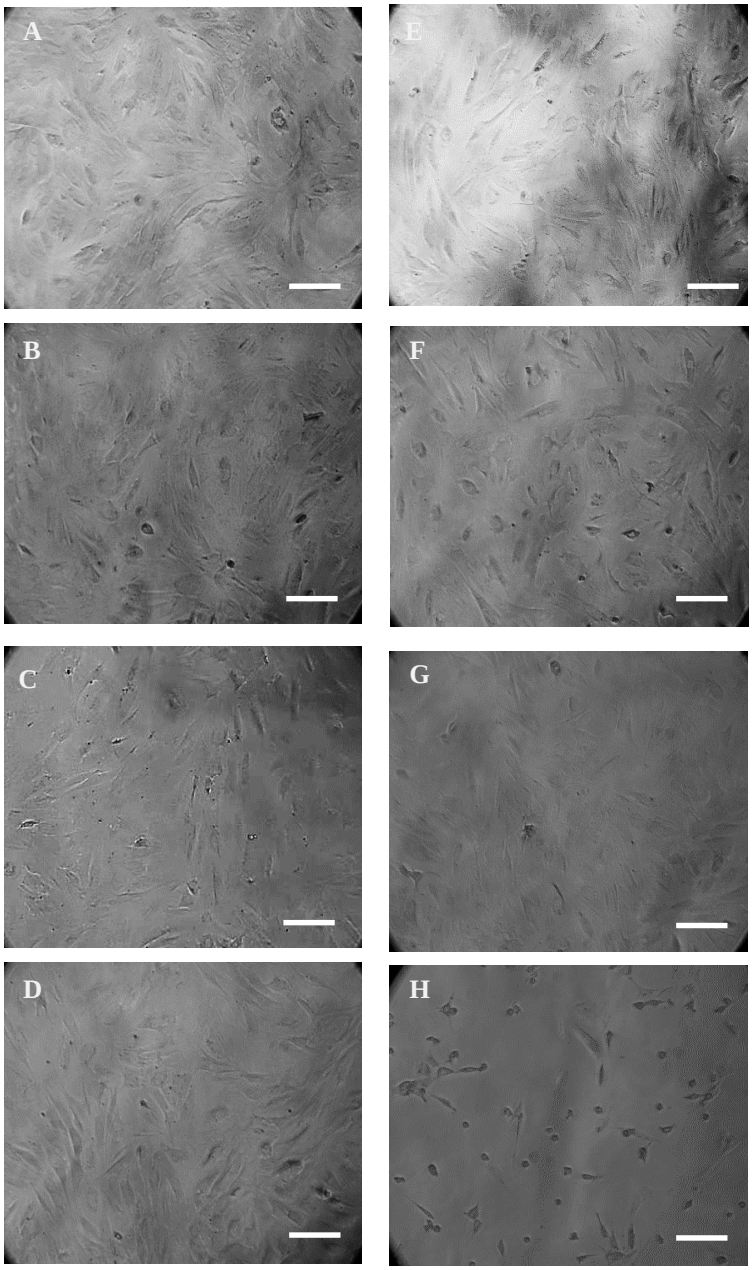

Figure 3.21 Phase contrast images of MSCs treated with 3 mol% Ga doped BAG on BMMSC conditioned media following a 96 hour incubation period. MSCs were treated with conditioned media generated under static incubation conditions at 0 mg/ml (**A**), 2.5 mg/ml (**B**), 5 mg/ml (**C**) and 10 mg/ml (**D**). MSCs were treated conditioned media generated under shaker incubation conditions at 0 mg/ml (**E**), 2.5 mg/ml (**F**), 5 mg/ml (**G**) and 10 mg/ml (**H**) of. Bar indicates 100μm.

3.4.7.4 The effect of pH neutralised dissolution products of 3 mol% Ga doped BAG and 45S5 Bioglass® on MSCs

The morphology of MSCs cultured in 45S5 Bioglass® and 3 mol% Ga doped BAG conditioned media generated under shaker incubation conditions, at 10 mg/ml appeared extremely thin and were not widely dispersed (Figures 22 and 23). Furthermore, a reduction in size and number was also observed. However, MSCs treated with the lower concentrations had a similar morphology to those grown in 0 mg/ml. Bone marrow MSCs treated with 45S5 Bioglass® and 3 mol% Ga doped BAG conditioned media generated under static incubation conditions, retained their typical long and thin morphology, even at the highest concentration of 10 mg/ml.

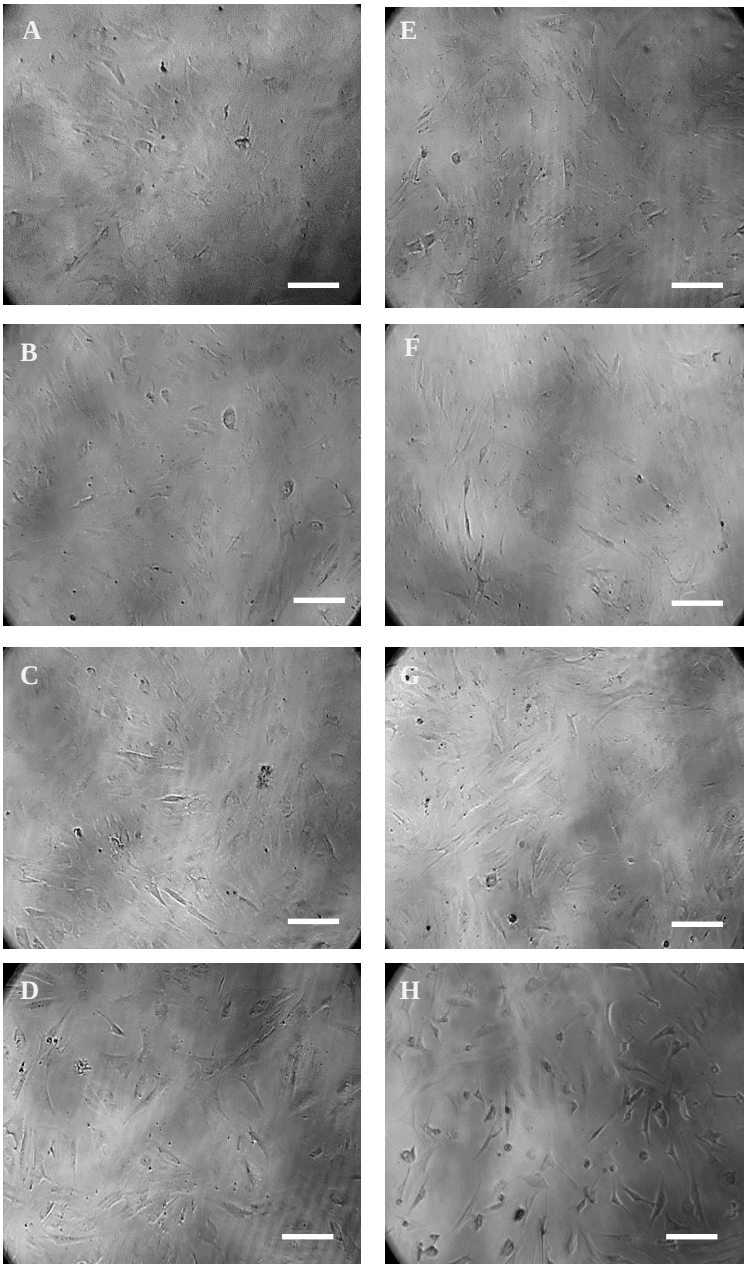

Figure 3.22 Phase contrast images at x10 objective of MSCs treated with 45S5 Bioglass® conditioned media following pH neutralisation over a 96 hour incubation period. MSCs were treated with conditioned media generated under static incubation conditions at 0 mg/ml (**A**), 2.5 mg/ml (**B**), 5 mg/ml (**C**) and 10 mg/ml (**D**). MSCs were treated with conditioned media generated under shaker incubation conditions at 0 mg/ml (**E**), 2.5 mg/ml (**F**), 5 mg/ml (**G**) and 10 mg/ml (**H**). Bar indicates 100µm.

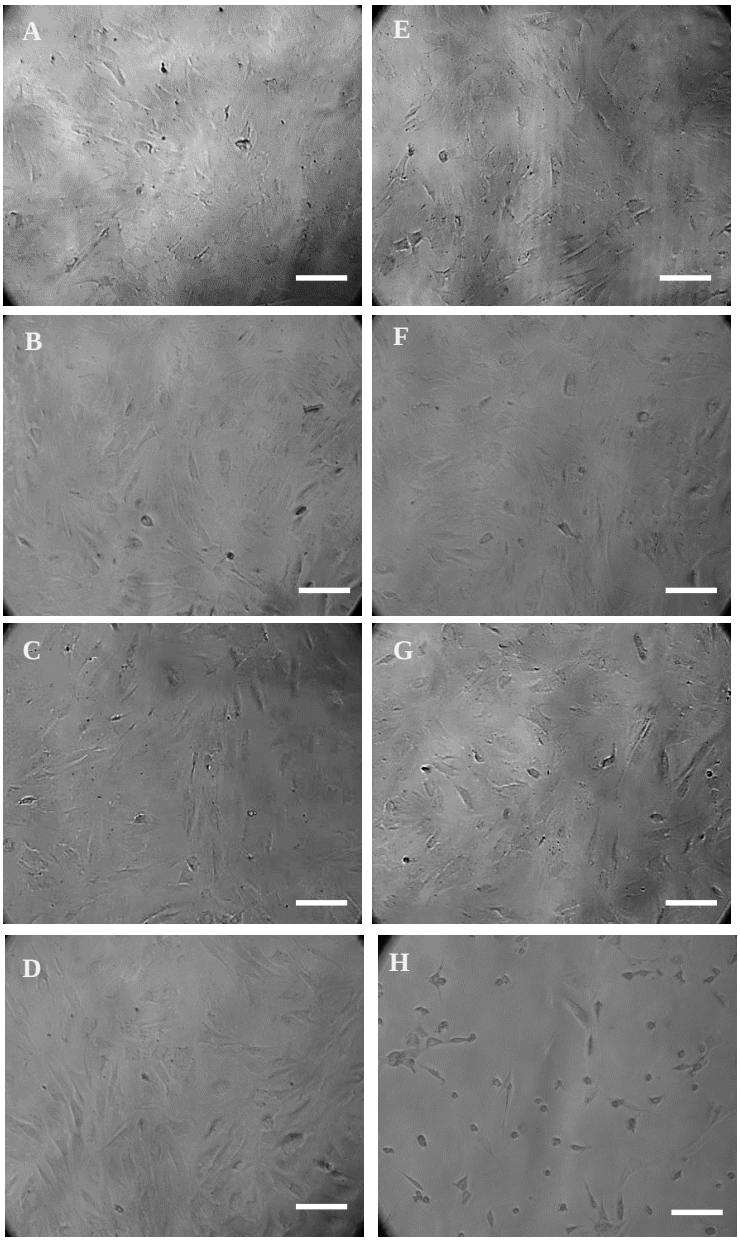

Figure 3.23 Phase contrast images at x10 objective MSCs treated with 3 mol% Ga doped BAG conditioned media following pH neutralisation after 96 hour incubation period. MSCs were treated with conditioned media generated under static incubation conditions at 0 mg/ml (**A**), 2.5 mg/ml (**B**), 5 mg/ml (**C**) and 10 mg/ml (**D**). MSCs were treated with conditioned media generated under shaker incubation conditions at 0 mg/ml (**E**), 2.5 mg/ml (**F**), 5 mg/ml (**G**) and 10 mg/ml (**H**). Bar indicates 100µm.

3.5 DISCUSSION

Osteogenesis is not only dependent upon the action of BAG dissolution products on osteoprogenitor cells, but also on the formation of a HCA layer, which provides a surface suitable for osteogenic cell attachment and proliferation. Bone bonding to the HCA layer is thought to involve protein adsorption, cell attachment, cell proliferation and differentiation, secretion of extracellular matrix and its mineralisation (Jones, 2013). Matsuura *et al*. (2000) reported that serum proteins such as vitronectin and fibronectin were adsorbed onto hydroxyapatite discs that mediated osteoblast adhesion onto the hydroxyapatite surface. *In vitro* studies have demonstrated that 45S5 Bioglass® and Ga doped BAG do form a HCA layer (Sepulveda *et al*., 2001; Jones *et al*., 2001; Franchini *et al*., 2012; Lusvardi *et al*., 2013).

In this study the cytotoxic effects of 3 mol% Ga doped BAG particles on the growth and viability of human bone marrow derived MSCs and osteoblast-like Saos-2 cells were investigated. Although the osteogenic effects of 45S5 Bioglass® are well established, the cytotoxic effects of 45S5 Bioglass® were also investigated and compared. Initially, the concentrations chosen were 25 mg/ml, 50 mg/ml and 100 mg/ml based on existing literature, which reported that BAGs at these concentrations exhibited antibacterial efficacy against a range of pathogens. Even though these concentrations were found to exhibit antibacterial efficacy against *E. coli* (see chapter 2) they were also cytotoxic. The dissolution products at 25 mg/ml, 50 mg/ml and 100 mg/ml significantly reduced Saos-2 cell viability in comparison to non-treated cells, for both BAGs. Furthermore, viable and non-viable cells could not be observed via LIVE/DEAD staining following exposure to 3 mol% Ga doped BAG and 45S5 Bioglass® particles. The prevention of bacterial colonisation is essential for the survivability of orthopaedic implants, but not at the expense of damaging host cells. Therefore, lower concentrations (2.5 mg/ml, 5 mg/ml and 10 mg/ml) were chosen in the hope that the BAGs would maintain their antibacterial properties without adverse effects on human cells. Henceforth, results obtained with the lower concentrations will be discussed.

The results for the direct contact experiments, where 1 x 10^4 MSCs and Saos-2 cells were seeded onto varying concentrations of both 45S5 Bioglass® and 3 mol% Ga doped BAG particles, demonstrated that cell viability of both cell types was dependent on concentration. An increase in particle concentration resulted in decreased number of viable (green) cells assessed by LIVE/DEAD staining (figures 3.6, 3.7, 3.9 and 3.10). This decrease in cell viability could be attributed to the decreased formation of a HCA layer in solution. Jones *et al*., (2001) found that as 45S5 Bioglass® concentration increased the concentration of active ions increased but the rate of HCA layer formation decreased, and instead calcium carbonate (calcite) was detected on the surface. Calcite formation is due to the increased calcium to phosphorous ratio, which causes an increase in pH of the solution (Jones *et al*., 2001; Sepulveda *et al*., 2001).

In vitro studies have reported HCA (apatite like) formation on the surface of 45S5 Bioglass® following 22 hours of soaking in stimulated body fluid (SBF) and minimum essential medium alpha medium (αMEM) supplemented with 10% FBS and 1% penicillin and streptomycin (Jones *et al*., 2001; Sepulveda *et al*., 2001), however in this study the SEM images show that no significant differences were observed between the dry 45S5 Bioglass® particles and those immersed in DMEM-Hams/F12 media for 24 hours. At 96 hours small nodules can be seen on the surface of 45S5 Bioglass® particles, which could be HCA formation or calcite as the concentration of the particles immersed in media was the highest concentration tested, 10 mg/ml. Additionally, the particles of 3 mol% Ga doped BAG did not exhibit surface changes, and the changes observed at 24 hours were similar to those at 96 hours. In fact Franchini *et al*. (2012) and Lusvardi *et al*. (2013) reported that HCA formation on Ga^{3+} doped BAG took as long as 30 days, due to the slow release of Ca^{2+} ions from the glass system.

Cell adhesion is an essential process involved in cell proliferation, cell migration and cell differentiation (Anselme *et al*., 1999). Due to the slow changes observed on the surfaces of both 45S5 Bioglass® and 3 mol% Ga doped BAG it is possible that MSCs and Saos-2 cells seeded onto the particles were unable to form a strong attachment. Gough *et al*. (2003) found

that a rough Bioglass® surface was conducive for osteoblast attachment and mineralised nodule formation, which they attributed to the rapid HCA formation. Furthermore, melt-derived powders of 45S5 Bioglass® exhibit very little porosity (Sepulveda *et al*., 2001). Porous scaffolds are necessary for bone formation because they allow migration and proliferation of osteoblasts and MSCs (Karageorgiou *et al*., 2005). Highly porous materials promote a higher degree of hydroxylation of the surface forming SiOH (silica-rich gel layer), which provides more sites for calcium phosphate layer nucleation (Sepulveda *et al*., 2001; Sepulveda *et al*., 2001).

These findings contradict those of Price *et al*. (2010) and Mayr-Wohlfart *et al*. (2001) who have demonstrated good proliferation rate of osteoblast-like cells when cultured on Bioglass®. These authors seeded osteoblast-like cells onto Bioglass® discs, which exhibit a slower dissolution rate due to the small surface area, whereas particles exhibit higher surface areas and therefore provide more exposed surface for dissolution (Sepulveda *et al*., 2001). A higher dissolution rate results in faster release of dissolution products Ca^{2+} and Na^{+} ions from the glass, which were present as network modifiers in both 45S5 Bioglass® and 3mol% Ga doped BAG, and thus leading to increased pH values. An increasing pH can affect cell growth, which could explain the reduced cell viability observed at higher glass concentrations. The pH increased (ranging from 8 to 9) as glass concentration increased because of the greater quantities of cations released from the glass systems.

It was found that 3 mol% Ga doped BAG was slightly more cytotoxic in its action, particularly against Saos-2 cells at 10 mg/ml (Figure 3.8). This could be attributed to the leaching of Ga^{3+} ions from the 3 mol% Ga doped BAG, which are known to possess antineoplastic and anti-proliferative properties (Chitamber, 2010). Gallium's antineoplastic activity has been attributed to its ability to bind to the iron-transport proteins transferrin (Tf), as well as lactoferrin and ferritin, enabling it to accumulate in proliferating tissue (including most tumours) where large amounts of Tf receptors (TfR) are expressed (Lessa *et al*., 2012; Daniels *et al*., 2006).

Internalisation of Ga-Tf complexes via TfR by cells leads to iron deprivation, which ultimately prevents cell division and may lead to apoptosis (Bernstein, 1998; Lessa *et al*., 2012). This could explain as to why reduced cell viability was observed for Saos-2 cells when cultured with 3 mol% Ga doped BAG at 10 mg/ml and at higher concentrations. Another factor could be the faster growth rate and confluence of Saos-2 cells during the culture.

Increasing evidence in the literature indicates that the stimulatory effects of BAGs are attributed to their dissolution products. Indirect contact experiments were conducted to elucidate whether the dissolution products released from 3 mol% Ga doped BAG and 45S5 Bioglass® exerted a cytotoxic effect on Saos-2 cells and MSCs. The results demonstrated that the cytotoxicity of dissolution products was concentration dependent. This effect was also observed for conditioned DMEM-Hams/F12 media generated under static and shaker incubation conditions, the degree of cytotoxicity varied. Viability was only observed for non-treated Saos-2 cells, whereas Saos-2 cells cultured with dissolution products of 45S5 Bioglass® and 3 mol% Ga doped BAG showed reduced viability. The magnitude of cytotoxicity varied between the two glasses, with 45S5 Bioglass® presenting a slightly greater cytotoxic effect. This outcome was noted for conditioned DMEM-Hams/F12 media generated under static and shaker incubation conditions. Saos-2 cell viability was significantly reduced when treated with conditioned media generated under shaker incubating conditions. Similar results were also observed for MSCs when treated with conditioned DMEM-Hams/F12 media with 45S5 Bioglass® and 3 mol% Ga doped BAG dissolution products generated under static and shaker incubating conditions. In addition, phase bright images of Saos-2 cells and MSCs treated with variable concentrations of 3 mol% Ga doped BAG and 45S5 Bioglass® dissolution products at variable concentrations, support the MTT assay results. The cells appeared to reduce in size and number as the concentration increased.

The cytotoxic effect of 45S5 Bioglass® could be attributed to the slow degradation rate of 3 mol% Ga doped BAG. Franchini *et al*., (2012) found that increasing the concentration of Ga^{3+}

ions in the 45S5 Bioglass® glass system reduced the amount of Ca^{2+} and Na^{+} ions leached into solution. The concentration of Ca^{2+} and Na^{+} ions leached from 45S5 Bioglass® was reported to be 3600 ppm and 245 ppm, whereas for 3.5% Ga doped BAG 3490 ppm and 101 ppm was reported, after 1 day of SBF soaking. Furthermore, the leaching of Ga^{3+} was found to be very slow due to the participation of gallium as a network former along with silicon and its high electric charge. Due to these two factors the release of Ga^{3+} ions from the glass system into the solution becomes a slow process (Franchini *et al*., 2012). Nevertheless, the concentration of Ga^{3+} ions following a 30 day soaking period in solution did not exceed its toxicity level of 14 ppm (Franchini *et al*., 2012; Bernstein, 1998).

It is important to know the extracellular concentration of dissolution products needed to mediate controlled cellular responses. Xynos *et al*. (2000) observed that the dissolution products of 45S5 Bioglass® activated several families of genes, including genes known to control and facilitate osteoblast proliferation, differentiation and extracellular matrix production. Based on Xynos *et al*. (2000) studies Hench stated that approximately 17 – 20 ppm of soluble Si^{4+} and 88 – 100 ppm of soluble Ca^{2+} ions are required for the up-regulation of several osteogenic genes (Hench et al., 2004). At present it is unknown which dissolution product is responsible for cell activation and the exact mechanisms of interaction between the ionic products and cells also remains unclear. However, the role of Ca^{2+} in bone metabolism is well established, and the ability of extracellular Ca^{2+} to regulate cell specific responses has only recently been demonstrated. Increased levels of extracellular Ca^{2+} enhance osteoblast proliferation and migration. Although the mechanism by which osteoblasts respond to Ca^{2+} is unclear, one possibility is that Ca^{2+} acts on the G-protein coupled extracellular calcium sensing receptor (CaSR) (Pierre, 2010). The CaSR plays a key role in maintaining extracellular Ca^{2+} ion concentration through its action on PTH secretion (Brown *et al*., 1998). Yamaguchi *et al*. (1998) identified that the osteoblast-like MC3T3 cells possess both CaSR protein and mRNA following exposure to Ca^{2+}. Additionally, Chattopadhyay *et al*. (2004) found that treatment of rat calvarial osteoblasts with Ca^{2+} enhanced CaSR mRNA expression, as well as up regulating

cyclin D genes, which are involved in cell proliferation. Previous work has demonstrated that Si^{4+} is associated with the formation and calcification of bone tissue (Carlisle *et al*., 1981; Hott *et al*., 1993). Keeting *et al*. (1992) found that Si^{4+} induced proliferation and differentiation of cells of the osteoblast lineage. They reported that Si^{4+} ions increased DNA synthesis and also ALP activity and OCN release. Similarly, Tousi *et al*. (2013) found enhanced OCN gene expression and biomineralisation in osteoblasts treated with Si^4. Although, Si^{4+} is known to be associated with the formation and calcification of bone tissue, a cellular receptor has not been identified (Xynos *et al*., 2000).

Valerio *et al*. (2004) found that viability of osteoblasts decreased as the concentration of Ca^{2+} ions in the media increased (> 300 mg/ml). Maeno *et al*., (2005) also demonstrated that extracellular Ca^{2+} concentrations greater than 10 mmol are cytotoxic. Moreover, high Ca^{2+} concentrations of 80 – 109 ppm have been shown to reduce Saos-2 cells proliferation when exposed to mesoporous BAG 85 (85 mol% SiO_2, 10 mol% CaO, 5 mol% P_2O_5) (Alcaide *et al*., 2010). Although these authors worked with different glass compositions, the size of the BAG particles were smaller to those of the 45S5 Bioglass® used in the studies of Xynos *et al*. (2000). Valerio *et al*. (2004) worked with 35µm and Alcaide *et al*., (2005) with 300-355µm, whereas the particle size of 45S5 Bioglass® in the Xynos *et al*. (2000) studies ranged between 300-710µm. Finer powders exhibit larger surface areas, and therefore they provide more exposed surface for dissolution (Sepulveda *et al*., 2001). This could explain as to why 45S5 Bioglass® and 3 mol% Ga doped BAG exhibited cytotoxicity against Saos-2 cells and MSCs, as the size of the particles was < 63µm. Furthermore, the highest concentration of 10 mg/ml reduced Sasos-2 and MSC cell viability, particularly for shaker conditioned media. Jones *et al*. (2001) found that the dissolution of the active products into solution increased as glass particle concentration in solution increased.

In this study the alkalinisation of conditioned DMEM-Hams/F12 media was neutralised to investigate whether cell viability was influenced by the dissolution products or pH. Saos-2 cell

viability following pH neutralisation of 3 mol% Ga doped BAG conditioned DMEM-Hams/F12 media generated under static and shaker incubating conditions was similar to Saos-2 cells cultured with alkaline conditioned DMEM-Hams/F12 media. However, dissolution products of 45S5 Bioglass® increased the metabolic activity of Saso-2 cells following pH neutralisation, particularly at 2.5 mg/ml. Viability of Saos-2 cells cultured with neutralised conditioned DMEM-Hams/F12 media generated under shaker incubation conditions decreased at 10 mg/ml, whereas when cultured with alkaline media a decrease was seen for 5 mg/ml too. Similar results were observed for MSCs however dissolution products of 45S5 Bioglass® present in static conditioned media significantly increased MSC viability compared to control group (0 mg/ml) and Saos-2 cells. These findings indicate that cytotoxicity of 45S5 Bioglass® and 3 mol% Ga doped BAG is dependent on both the pH and the presence of high levels of dissolution products. These results contradict the findings of Silver *et al*. (2001) who demonstrated that 45S5 Bioglass® enhanced osteoblast proliferation, due to the external alkalisation. In their study 45S5 Bioglass® did cause alkalisation as a pH reading of 7.71 was reported, however in the current study the pH values were greater than 7.71 for all concentrations tested. This difference could be attributed to the particle size, as Silver *et al*. (2001) used particles ranging from 90-150µm, whilst < 63µm were used in the current study.

BAGs increase pH when immersed into physiological solutions due to the reactions that take place at the surface. The release of Ca^{2+} and Na^{+} ions are responsible for the alkalinisation of the surrounding solution. The disappearance of protons (H^{+}) becomes inevitable following the release of Na^{+} and Ca^{2+} ions, as they are required for the formation of silanol bonds (Si – OH) on the glass surface. Formation of the silanol bonds is the first reaction step in the establishment of the HCA layer:

$$Si - O^{-}Na^{+} + H^{+} + OH^{-} \longrightarrow Si - OH^{+} + Na^{+}{}_{(aq)} + OH^{-}$$

The leaching of the dissolution products into the surrounding solution would also mean increased soluble ion content within the cell. Changes in intracellular Ca^{2+} are essential regulators of many physiological processes including proliferation, gene expression, oxidative stress and apoptosis (Bernardi and Rasola. 2007; Labbaf *et al*., 2011). Overload of the intracellular Ca^{2+} levels affects mitochondrial function, ultimately leading to cell death (Giorgi *et al*., 2008). Adams *et al*. (2000) demonstrated that in the presence of Ca^{2+} ions, primary human osteoblasts exhibited characteristics of apoptosis, including contraction of the cells, release of osteoblasts from the surface and loss of contact with neighbouring cells and a marked change in the mitochondrial membrane potential. Therefore, the decrease in cell viability observed for Saos-2 cells and MSCs cultured in shaker conditioned DMEM-Hams/F12 media for the higher concentrations could be attributed to the apoptotic inducing mechanisms of Ca^{2+} ions. Under shaker incubation conditions high levels of Ca^{2+} ions are expected because the particles are suspended in solution and therefore, are far more likely to come into contact with the solution resulting in increased dissolution.

3.6 CONCLUSION

The particles and dissolution products of 3 mol% Ga doped BAG did not promote proliferation when tested against MSCs and osteoblast-like Saos-2 cells. 45S5 Bioglass® dissolution products exerted greater cytotoxicity, however following pH neutralisation increased viability of both cell types was seen. It is possible that particle size as well as glass composition are important factors to consider when fabricating BAGs.

CHAPTER FOUR

FINAL DISCUSSION and FUTURE WORK

4.1 DISCUSSION AND FUTURE WORK

Implant failure due to interfacial instability and infection leads to reduced implant survivability and as a result revision surgery. It has been estimated that annually 1 million hip replacement surgeries are performed and more than 250,000 knee replacements, worldwide (Schierholz and Beuth, 2001). The implications associated with revision surgery include patient trauma, prolonged hospitalisation, as well as health and social costs. It has been reported that it costs the NHS £9,655 to replace a single knee arthroplasty and revision surgery due to infection costs £30,011 (Kallala *et al*., 2015). The number of replacements and costs are expected to increase in the future, in light of the ageing population as it has been forecasted that by 2050 nearly one in five people will be over the age of 60 (Hench *et al*., 2010). The limitations of current orthopaedic implants has pushed research to explore alternative avenues and one such potential avenue is the use of BAGs. Bioactive glasses such as the 45S5 Bioglass® have shown great clinical success, due to their ability to regenerate living tissue. Furthermore they have also been shown to exhibit antibacterial activity when used as therapeutic materials and therefore would be ideal implants (Munukka *et al*., 2007; Mortazavi *et* al., 2009).

The objectives of chapter 2 were to evaluate the antibacterial efficacy of 3% Ga doped BAG, as well as investigating and comparing the antibacterial activity of 45S5 Bioglass®. The results of the work can be summarised briefly as follows:

(1) Doping the silicate glass system with 3 mol% Ga^{3+} did not enhance antibacterial activity, as similar results were observed for both BAGs. This suggests that Ga^{3+} ions do not possess greater antibacterial efficacy as the other components found within the 45S5 Bioglass® system. However, Ga^{3+} may not have been released from the glass system, as it has been reported that Ga^{3+} ions increase connectivity of BAGs and thus act as a network former (Valappil *et al*., 2008; Franchini *et al*., 2012). Further studies could utilise inductively coupled plasma-mass

spectrometry (ICP-MS) to investigate the dissolution rate of Ga^{3+}ions in the silicate glass system.

(2) The antibacterial activity of both BAGs was concentration dependent. This was observed for the lower (2.5 mg/ml, 5 mg/ml and 10 mg/ml) and higher (25 mg/ml, 50 mg/ml and 100 mg/ml) concentrations tested. The antibacterial effect increased as glass concentration increased because of the greater quantities of cations released from the BAGs. The inconsistency in the literature regarding whether BAGs possess antibacterial activity could be attributed to the concentration levels used. Several authors have reported antibacterial efficacy as the concentrations they used ranged from 10 mg/ml – 100 mg/ml (Munukka *et al*., 2008; Hu *et al*., 2008; Allan *et al*., 2001; Mortzavi *et al*., 2009). However, Bellantone *et al*. (2002) demonstrated that BAGs are not antibacterial, which could be due to the low levels of concentrations tested (0.05 – 1 mg/ml).

(3) 3 mol% Ga doped BAG and 45S5 Bioglass® particles did not exhibit a broad-spectrum antibacterial effect, as growth reduction was only observed for *E.coli* and not *S. aureus*. The difference between *E. coli* and *S.* aureus could be due to their cell structures. As mentioned previously *S. aureus* lacks an outer membrane but its cell wall is mainly composed of a thick peptidoglycan layer. It can be assumed that the dissolution products, chiefly Ca^{2+} and Na^{+} ions released from the BAG particles bonded to the peptidoglycan layer which provides highly charged anionic clusters (Doyle *et al*., 1980; Hughes *et al*., 1973). As shown in the SEM images, this could be the reason as to why a higher number of *S. aureus* were attached onto the particles. Because SEM analysis does not indicate whether the attached *S. aureus* are viable or non-viable, this warrants further investigation.

However, the peptidoglycan layer of *E. coli* is encased within an outer membrane which consists of pore proteins through which the dissolution products can enter the cell, resulting in cell death.

(4) The antibacterial mechanism of both BAGs is dependent on pH and particle presence as the dissolution products in the absence of the particles were unable to reduce bacterial growth. Hu

et al. (2009) and Zhang *et* al. (2008) found that the local pH value on the surface of 45S5 Bioglass® particles was higher than that of the area far from the particles. An elevated pH disturbs the pH gradient and structure of the bacterial membrane, leading to increased toxicity and structural collapse.

(5) The incubation conditions influenced the results, as particles under shaker incubation conditions caused a significant antibacterial effect. The agitation rate influences the rate of glass powder dissolution as it exposes more surfaces, whereas under static conditions the saturated area at the particle surface is not carried away and thus reducing the rate of dissolution (Jones *et al*., 2001).

The objectives of chapter 3 were to evaluate the cytotoxic effect of 3 mol% Ga doped BAG on growth and viability of osteoblast-like cells (Saos-2) and bone marrow derived MSCs. Cytotoxic effect of 45S5 Bioglass® was also investigated for comparison purposes. The results of the current study can be summarised briefly as follows:

(1) The particles of 3 mol% Ga doped BAG failed to affect the viability of MSCs and Saos-2 cells. However, 3 mol% Ga doped BAG exhibited a similar concentration-dependent cytotoxic effect as 45S5 Bioglass®. This could be attributed to the surface characteristics of both BAGs, which were not conducive for cell attachment and thus preventing cell growth. Gough *et al*. (2003) have reported that a rough surface with a HCA layer is required for osteoblast attachment. In this study the surfaces of 45S5 Bioglass® and 3 mol% Ga doped BAG were smooth as shown in the SEM images.

Furthermore, it was found that 3 mol% Ga doped BAG exerted a greater cytotoxic effect at 10 mg/ml, particularly against Saos-2 cells. Since, Saos-2 cells are a tumour cell line they probably were susceptible to the antineoplastic action of Ga^{3+} ions, which interfere with cellular metabolism due to the chemical similarity shared with Fe^{3+} ions.

(2) Like the particles the dissolution products also exhibited a concentration-dependent cytotoxic effect. It has been established that when BAGs are immersed into solution they release Ca^{2+} and Na^{+} ions which increase the aqueous pH. High concentrations of Ca^{2+} ions (80 – 109 ppm) have been shown to reduce osteoblast cell proliferation (Valerio *et al*., 2004; Maeno *et al*., 2005; Alcaide *et al*., 2010). However, dissolution studies were not conducted to determine the rate at which the inorganic ions were released when immersed into an aqueous environment. Future experiments could therefore incorporate ICP-MS to quantify then dissolution ions present in DMEM/Ham's-f12 culture media.

(3) Following pH neutralisation an increase in viability was observed for both cell types at the lower concentrations (2.5 mg/ml and 5 mg/ml) of 45S5 Bioglass. According to the *in vitro* studies of Xynos *et al*. (2001 and 2000) dissolution products activate several families of genes, including genes known to control and mediate osteoblast proliferation, differentiation and extracellular matrix production. Therefore it is important to assess whether the lower concentrations of Ga^{3+} doped BAG dissolution products induce MSC differentiation towards osteogenesis, by measuring the expression of early and late osteogenic genes. Furthermore, the ability of Ga^{3+} doped BAG to stimulate pre-osteoblast maturation should also be determined.

(4) The incubation methods employed influenced the outcome, as conditioned media generated under shaker incubation conditions displayed a greater cytotoxic effect against both cell types. As mentioned earlier the agitation rate influences glass dissolution, therefore it can be assumed that a greater quantity of dissolution products were released under shaker incubation conditions from both glass systems.

The current work illustrates that incorporating 3 mol% Ga within the silicate glass system does not enhance the biological properties, possibly due to the network forming properties of Ga^{3+} ions. However, previous studies have reported that glass systems with lower concentrations of Ga^{3+} ions have improved rates of glass solubility, and as a result biological properties.

Therefore, it is important to improve and develop novel glass compositions for clinical applications.

REFERENCES

A

Abou Neel, E.A., Ahmed, I., Pratten, J., Nazhat, S.N., and Knowles, J.C. (2005). Characterisation of antibacterial copper releasing degradable phosphate glass fibres. *Journal of Biomaterials* **26**, 2247-2254.

Abou Neel, E.A., Ahmed, I., Ready, D., Wilson M., and Knowles, J.C. (2006). Antimicrobial effect of silver-doped phosphate-based glasses. *Journal of Biomedical Materials Research: Part A*. **79**, 618-626.

Adams, C.S., Mansfield, K., Perlot, R.L., and Shapiro, I.M. (2001). Matric Regulation of Skeletal Cell Apoptosis. *The Journal of Biological Chemistry*. **276**(23), 20316-203222.

Ahmed, I., Ready, D., Wilson M., and Knowles, J.C. (2006). Antimicrobial effect of silver-doped phosphate-based glasses. *Journal of Biomedical Materials Research: Part A*. **79**, 618-626.

Alcaide, M., Portolés, P., López-Noriega, A., Arcos, D., Vallet-Regí, M., and Portolés, M.T. (2010). Interaction of an ordered mesoporous bioactive glass with osteoblasts, fibroblasts and lymphocytes, demonstrating its biocompatibility as a potential bone graft material. *Acta Biomateriallia*. **6**, 892-899.

Allan, I., Newman, M., and Wilson, M. **(**2000). Antibacterial activity of particulate Bioglass® against supra- and subgingival bacteria. *Journal of Biomaterials*. **22**, 1683-1687.

Anderson, J.M. (2001). Biological Responses to Materials. *Annual Review of Materials Research*. **31**, 81-110.

Anderson, J.M., Rodriguez, A., Chang, D.T. (2008). Foreign body reaction biomaterials. *Seminars in Immunology*. **20**, 86-100.

Anselme, K., Bigerelle, M., Noel, B., Dufresne, E., Judas, D., Iost, A., and Hardoiun, P. (2000). Qualitative and quantitative study of human osteoblast adhesion on materials with various surface roughness. *Journal of Biomedical Materials Research*. **49**(2), 155-166.

Arciola, C.R., An, Y.H., Campoccia, D., Baldi, R., Donati, M.E., and Montananaro, L. (2005). Etiology of implant orthopaedic infections: A survey on 1207 clinical isolates. *Journal of Artificial Organs.* **28**(11), 1091-100.

Arnold, C.E., Bordin, A., Lawhon, S.D., Libal, M.C., Bernstein, L.R., and Cohen, N.D. (2012). Antimicrobial activity of gallium maltolate against *Staphylococcus aureus* and methicillin-resistant *S. aureus* and *Staphylococcus pseudintermedius*: An *in vitro* study. *Journal of Veterniary Microbiology*. **155**, 389-394.

B

Ballouche, M., Cornelis, P., and Baysse, C. (2009). Iron metabolism: A Promising Target for Antibacterial Strategies. *Journal of Recent Patents on Anti-Infective Drug Discovery*. **4**, 190-205.

Baldoni, D., Steinhuber, A., Zimmerli, W., and Trampuz. (2010). In Vitro Activity of Gallium Maltolate against Staphylococci in Logarithmic, Stationary, and Biofilm Growth Phases: Comparison og Conventional and Calorimetric Susceptibility Testing Methods. *Journal of Antimicrobial Agents and Chemotherapy*. **54**(1), 167-163.

Bellantone, M., Williams, H.D., and Hench, L.L. (2002). Broad-Spectrum Bactericidal Activity of A_g2O-Doped Bioactive Glass. *Journal of Antimicrobial Agents and Chemotherapy*. **46**, 1940-1945.

Bernstein, L.R. (1998). Mechanisms of Therapeutic Activity for Gallium. *Pharmacological Reviews*. **50**(4), 665-680.

Bernstein, L.R. (2013). Gallium, Therapeutic Effects. In Kretsinger, R.H., Uversky, V.N., Permyakov, E.A. (eds.). *Encyclopedia of Mettslloproteins*. 823-835. Springer (New York).

Bernardi, P., and Rasola, A. (2007). Calcium and Cell Death: The Mitochondrial Connection. In Carafoli, E., and Brini, M. (eds.). *Subcellular Biochemistry*. **45**, 481-506. Springer.

Beveridge, T.J., and Murray, R.G.E. (1976). Uptake and Retention of Metals by cell Walls of *Bacillus subtilis*. *Journal of Bacteriology*. **127**(3), 1502-1518.

Bockman, R.S., Adelman, R., Donelly, R., Brody, L., and Warrell, R. (1990). Gallium a Unique Anti-Resorptive Agent in Bone: Preclinical Studies on Its Mechanism of Action. Presented at

First International Symposium on Metal Ions in Biology. *The International Nuclear Information System*. **21**(17).

Bockman, R.S. (1993). Gallium Nitrate Increases Type I Collagen and Fibronectin mRNA and Collagen Protein Levels in Bone and Fibroblast Cells. *Journal of Cellular Biochemistry*. **52**(4), 396-403.

Bock, A. K., Ibarreta, D., and Rodriguez-Cerezo, E. (2003). Human Tissue Engineered Products - Today's Markets and Future Prospects. Synthesis Report. Report EUR 21 000 EN. Seville: Institute for Prospective Technological Studies.1-49

Bonchi, C., Imperi, F., Minandri, F., Visca, P., and Frangipani, E. (2014). Repurposing of gallium-based drugs for antibacterial therapy. *Journal of International Union of Biochemistry and Molecular Biology*. **40** (3), 303-312.

Bosetti, M., and Cannas, M. (2005), the effect of bioactive glasses on bone marrow stromal cell differentiation. *Journal of Biomaterials*. **26**, 3873-3879.

Brown, L.S., Darmoc, M.M., Havener, M.B., and Clineff, T.D. (2009). Antibacterial Effects of 45S5 Bioactive Glass against Four Clinically Relevant Bacterial Species. *Presented at the 55th Annual Meeting of the Orthopaedic Research Society.*

Brown, E.M., Polak, M., Herbert, S.C. (1998). The extracellular calcium-sensing receptor: its role in health and disease. *Annual Review of Medicine*. **49**, 15-29.

C

Cao, W., and Hench, L.L. (1996). Bioactive Materials. *Journal of Ceramics International*. **22**, 493-507.

Carlisle, E.M. (1981). Silicon: A requirement in bone formation independent of vitamin D1. *Journal of Calcified Tissue International*. **33**(1), 27-34.

Clarke, B. (2008). Normal Bone Anatomy and Physiology. *Clinical Journal of the American Society of Nephrology*. **3**, 131-136.

Clark, R. (2005). Anatomy and Physiology: Understanding the Human Body. *Jones and Bartlett Publishers* (USA).

Campoccia, D., Montanaro, L., and Arciola, C.R. (2006). The significance of infection related to orthopaedic devices and issues of antibiotic resistance. *Journal of Biomaterials*. **27**, 2331-2339.

Chattopadhyay, N., Yano, S, Tfelt-Hansen, J., Rooney, P., Kanuparthi, D., Kanuparthi, D., Bandyopadhyay, S., Ren, X., Terwilliger, E., Brown, E.M. (2004). Mitogenic Action of Calcium-Sensing Receptor on Rat Calvarial Osteoblasts. *Endocrinology*. **145**, 3451-3462.

Chitamber, C.R. (2010). Medical Applications and Toxicities of Gallium compounds. *Internal Journal of Environmental Research and Public Health*. **7**, 2337-2361.

Christodoulou, I., Buttery, L.D.K., Saravanapavan, P., Tain, G., Hench, L.L., and Polak, J. (2005). Dose- and Time-Dependent Effect of Bioactive Gel-glass-Ionic-Dissolution Products on Human Fetal Osteoblast-Specific Gene Expression. *Journal of Biomedical Materials Research: Part B, Applied Biomaterials*. **74**(1), 529-537.

Coleman, N.J., and Nicholson, J.W. (2006). Glass bones. *Education in Chemistry*: *Bioceramics*. **43**(6).

Collery, P., Keppler, B., Madoulet, C., and Desoize, B. (2002). *Critical Reviews in Oncology/Hematology*. **42**, 283-296.

Cordero, J., Munuera, L., Folgueira, M.D. (1996). Influence of Bacterial Strains ion Bone Infection. *Journal of Orthopaedic Research*. **14**, 663-667.

Cutinelli, C., and Galdiero, F**.** (1967.) Ion-binding Properties of the Cell Wall of *Staphylococcus aureus*. *Journal of Bacteriology*. **6**, 2022-2023.

Czekanska, E.M., Stoddart, M.M., Richards, R.G., and Hayes, J.S. (2012). In Search of an Osteoblast Model for *In Vitro* Research. *European Cells and Materials*. **24**, 1-17.

D

Daniels, T.R., Delgado, T., Rodriguez, J.A., Helguera, G., and Penichet, M.L. (2006). The transferrin receptor part I: Biology and targeting with cytotoxic antibodies for the treatment of cancer. *Journal of Clinical Immunology*. **121**, 144-158.

DeLeon, K., Balldin, F., Watters, C., Hamood, A., Griswold, J., Sreedharan, S., and Rumbaugh, K.P. (2009). Gallium Maltolate Treatment Eradicates *Pseudomonas aeruginosa* Infection in

Thermally Injured Mice. *Journal of Antimicrobial Agents and Chemotherapy*. **55**(4), 1331-1337.

Dominici, M., Le Blanc, K., Mueller, I., Slaper-Cortenbach, I., Marini, F., Krause, D., Deans, R., Keating, A., Prockop, D and Horwitz., E. 2006. Minimal criteria for defining multipotent mesenchymal stromal cells. The international Society for Cellular Theray position statement. Cytotherapy. 8(**4**) 315-317.

Doostmohammadi, A., Monshi, A., Salehi, R., Fathi, M.H., Seyedjafari, E., SHafiee, A., and Soleimani, M. (2001). Cytotoxicity Evaluation of 63S Bioactive Glass and Bone-Derived Hydroxyapatite Particles Using Human Bone-Marrow Stem Cells. *Biomedical Papers of the Medical Faculty of the University of Palacký, Olomouc, Czechoslovakia*. **155**(4) 323-326.

Doyle, R.J., Matthews, T.H., and Streips U.N. (1980). Chemical basis for selectivity of metal ions by the *Bacillus subtilis* cell wall. *Journal of Bacteriology*. **143**, 471-480.

E

El-Ghannam, A., Ducheyne, P., and Shapiro, I.M. (1995). Bioactive material template for *in vitro* synthesis of bone. *Journal of Biomedical Materials Research*. **29**, 359-370.

F

Fowle, D.A, and Fein, J.B. **(**1999). Competitive adsorption of metal cations onto two gram positive bacteria: Testing the chemical equilibrium model. *Geochimica et Cosmochimica Acta*. **19**, 3059-3067.

Franchini,M., Lusvardi, G., Malavasi, G., Menabue, L. (2012).Gallium-containing phosphor-silicate glasses: Synthesis and in vitro bioactivity. *Journal of Material Science and Engineering*. **32**, 1401-1406.

G

Gao, T., Aro, H.T., Ylänen, H., and Vuorio, E. (2001). Silica-based bioactive glasses modulate expression of bone morphogenetic protein-2 mRNA in Saos-2 osteoblasts in vitro. *Journal of Biomaterials*. **22**, 1475-1483.

Gentleman, E., Fredholm, Y.C., Jell, G., and Lotfibkhshaiesh, N. (2010). The effects of strontium-substituted bioactive glasses on osteoblasts and osteoclasts *in vitro*. *Journal of Biomaterials*. **31**, 3949-3956.

Geris, L., Vander Sloten, J., and Van Oosterwyck, H. (2009). In silico biology of bone modelling and remodelling: regeneration. *Philosophical Transactions: Series A, Mathematical, Physical, and Engineering Sciences*. **367**(1895), 2031-2053.

Gerhardt, L.C., and Boccaccini, A.R. (2010). Bioactive Glass and Glass-Ceramic Scaffolds fo Bone Tissue Engineering. *Journal of Materials.* **3**, 3867-3910.

Gentleman, E., Fredholm, Y.C., Jell, G., and Lotfibkhshaiesh, N. (2010). The effects of strontium-substituted bioactive glasses on osteoblasts and osteoclasts *in vitro*. *Journal of Biomaterials*. **31**, 3949-3956.

Giannoudis, P.V., Dinopoulos, H., and Tsiridis, E. (2005). Bone substitutes: An update. *International Journal of the Care of the Injured*. **36**, 20-27.

Giorgi, C., Romagnoli, A., Pinton, P., and Rizzuto, R. (2008). Ca^{2+} Signalling, Mitochondria and Cell Death. *Journal of Current Molecular Medicine*. **8**, 119-130.

Gorriti, M.F., López, J.M.P., Boccaccini, A.R., Audisio, C., and Gorustovich, A.A. (2009). In vitro Study of the Antibacterial Activity of Bioactive Glass-ceramic Scaffolds. *Journal of Advanced Engineering Materials*. **11**(7), 67-70.

Gough, J.E., Notingher, I., Hench, L.L. (2004). Osteoblast attachment and mineralised nodule formation on rough and smooth 45S5 bioactive glass monoliths. *Journal of Biomedical Materials Research: Part A.* **68**, 640-650.

Gristina, A.G. (1989). Biomaterial-Centered Infection: Microbial Adhesion versus Tissue Integration. *Science (New York).* **237**(4822), 1588-1595.

Guidon, P.T., and Bockman, R, S. (1990). Iron, zinc and gallium regulate transcription of the osteocalcin gene in an osteoblastic cell line. *Journal of Clinical Research*. **38**, 328A.

H

Hadjidakis, D.J., and Androulakis, I.I. (2006). Bone Remodelling. *Annals of the New York Academy of Sciences*. **1092**, 385-396.

Hamadouche, M., Meunier, A., Greenspan, D.C., Blanchant, C., Zhong, J.P., La Torre, G.P., and Sedel, L. long-term *in vivo* bioactivity and degradability of bulk sol-gel bioactive glasses. *Journal of Biomedical Materials Research*. **54**, 560-566.

Heikkilae, J.T., Aho, H.J., and Yli-Urpo, A. (1995). Bone formation in rabbit cancellous bone defects filled with bioactive glass granules. *Acta Orthopaedica Scandinavica*. **66**(5), 463-467.

Hench, L.L, Splinter, R.J., Allen, W.C., and Greenlee, T.K. (1971). Bonding Mechanisms at the Interface of Ceramic Prosthetic Materials. *Journal of Biomedical Materials Research*. **2** (Part 1), 117-141.

Hench, L.L., Polak, J.M., Xynos, I.D., and Buttery, L.D.K. (2000). Bioactive materials to control cell cycle. *Journal of Materials Research Innovations*. **3**, 313-323.

Hench, L.L, Xynos, I.D., and Polak, J.M. (2004). Bioactive glasses for *in situ* tissue regeneration. *Journal of Biomaterials Science Polymer Edition*. **15**(4), 543-562.

Hench, L.L. (2006). The Story of Bioglass®. *Journal of Material Science: Materials in Medicine*. **17**, 967-978.

Hench, L.L., Day, D.E., Hölland, W.H., and Rheinberger, V.M. (2010). Glass and Medicine. *International Journal of Applied Glass Science*. **1**, 104-117.

Hoppe, A., Gűldal, N.S., and Boccaccini, A.R. (2011). A review of the biological response to ionic dissolution products from bioactive glasses and glass-ceramics. *Journal of Biomaterials*. **32**, 2757-2774.

Hott, M., De Polak, C, Modrowski, D., Marie, P. (1993). Short-term effects of organic silicon on trabecular bone in mature overiectomized rate. *Journal of Calcified Tissue International*. **53**(3), 174-179.

Hughes, A.H., Hancock, I.C., and Baddiley, J. (1972). The Function of Teichoic acids in Cation Control in Bacterial Membranes. *Journal of Biochemistry*. **132**, 83-93.

Hu, S., Chang, J., Liu, M., and Ning, C. (2009). Study on antibacterial effect of 45S5 Bioglass®. *Journal of Materials Science: Materials Medicine* **20**, 281-286.

Hudson, M.C., Ramp, W.K., and Frankenburg, K.P. (1999). *Staphylococcus aureus* adhesion to bone matrix and bone-associated biomaterials. *FEMS Microbiology Letters*. **173**, 279-288.

Jenis, L.G. (1993). Effect of Gallium Nitrate In Vitro and in Normal Rats. *Journal of Cellular Biochemistry*. **52**(3), 330-336.

J

Jenis, L.G. (1993). Effect of Gallium Nitrate In Vitro and in Normal Rats. *Journal of Cellular Biochemistry*. **52**(3), 330-336.

Jones, J.J. (2013). Review of bioactive glass: From Hench to hybrids. *Acta Biomaterialia*. **9**, 4457-4486.

Jones, J.K., and Clare, A.G. (2012). Bio-glasses. An Introduction. *John Wiley and Sons Ltd. Publications* (UK).

Jones, J.R., Sepulveda, P., and Hench, L.L. (2001). Dose-Dependent Behaviour of Bioactive Glass Distribution. *Journal of Biomedical Materials Research: Applied Biomaterials*. **58**, 720-726.

K

Kapinas, K., and Delany, A.M. (2011). MicroRNA biogenesis and regulation of bone remodelling. *Journal of Arthritis Research and Therapy*. **13**(220), 1-11.

Kallala, R.F., Vanhegan, I.S., Ibrahim, M.S., Sarmah, S., and Haddad, F.S. (2015). *The Bone and Joint Journal*. Financial analysis of knee revision surgery based on NHS tariffs and hospital costs: does it pay to provide a revision surgery? **97**, 197-201.

Kaneko, Y., Theondel, M., Olakanmi, O., Britigan, B.E., and Singh, P.K. (2007). The transition metal gallium disrupts *Pseudomonas aeruginosa* iron metabolism and has antimicrobial and antibiofilm activity. *Journal of Clinical Investigation*. **117**(4), 877-888.

Karageorgiou, V., and Kaplan, D. (2005). Porosity of 3D biomaterial scaffolds and osteogenesis. *Journal of Biomaterials*. **26**, 5474-5491.

Keeting, P., Oursler, M., Wiegand, K., Bonde, S., Spelsberg, T., Riggs, B. (1992). Zeolite A increases proliferation, differentiation, and transforming growth factor beta production in normal adult human osteoblast-like cells *in vitro*. *Journal of Bone Mineral Research*. **7**(11), 1281-1289.

Kelson, A.B., Carnevali, M., and Truong-Le, V. (2013). Gallium-based anti-infectives: targeting microbial iron-uptake mechanisms. *Current Opinion in Pharacology*. **13**, 707-716.

Kini, U., and Nandesshe, B.N. (2012). Physiology of Bone Formation, Remodeling, and Metabolism. Fogleman, I., Gnanasegaran, G., Wall, H.V.D. (eds.). *Radionuclide and Bone Imaging*. 29-57. Springer.

Kloss, F.R., and Gassner, R. (2006). Bone and aging: Effects on the maxillofacial skeleton. *Journal of Experimental Gerontology*. **41,** 123-129**.**

L

Labbaf, S., Tsigkou, O., Müller, K.H., Stevens, M.M., and Porter, A.E. (2011). Spherical bioactive glass particles and their interaction with human mesenchymal stem cells *in vitro*. *Journal of Biomaterials*. **32**, 1010-1018.

Lane, N.E. (2006). Epidemiology, etiology, and diagnosis of osteoporosis. *American Journal of Obstetrics and Gynecology*. **194**, 3-11.

Lasch, P., and Kneipp, J. (2008). Biomedical Vibrational Spectroscopy. *John Wiley and Sons (Publishers)*.

Lentino, J.R. (2003). Prosthetic Joint Infections: Bane of Orthopedists, Challenge for Infectious Disease Specialists. *Journal of Clinical Infectious Diseases*. **36**(9), 1157-1161.

Leppäranta, O., Vaahtio, M., Peltola, T., Zhang, D., Hupa, L., Hupa, M., Ylänen, H., Salonen, J.I., Viljanen, M.K., Eerola, E. (2008). *Journal of Material Science: Material Medicine*. **19**, 547-551.

Lessa, J.A., Parrilha, G.L., and Beraldo, H. (2012). Gallium complexes as new promising metallodrug candidates. *Inorganica Chimica Acta*. **393**, 53-63.

Livingston, T., Ducheyne, P., and Garino, J. (2002). *In vivo* evaluation of a bioactive scaffold for bone tissue engineering. *Journal of Biomedical Materials Research*. **62**, 1-13.

Long, P.H. (2008). Medical Devices in Orthopedic Applications. *Toxicological Pathology*. **36**, 85-91.

Lusvardi, G., Malavasi, G., Menabue, L., and Shruti, S. (2013). Gallium-containing phosphosilicate glasses: Functionalization and in-vitro bioactivity. *Journal of Material Science and Engineering C*. **33**, 3190-3196.

M

Mami, M., Oudadesse, H., Dorbez-Sridi, R., Capiaux, H., Pellen-Mussi, P., Chauvel-Lebret, D., Chaair, H., and Cathelineaue, G. (2008). Synthesis and *In Vitro* Characterisation of Melt Derived 47S CaO-P_2O_5-SiO_2-NaO Bioactive Glass. *Journal of Ceramic-Silikáty*. **52**(3), 121-129.

Manolagas, S.T., and Jilka, R.L. (1995). Bone Marrow, Cytokines, and Bone Remodeling. Emerging Insights into the Pathophysiology of Osteoporosis. Epstein, F.H (ed.). *Mechanisms of Disease*. **332**(5), 305-311.

Maeno, S., Niki, Y., Matsumoto, H., Morioka, H., Yatabe, T., Funayama, A., Toyama, Y., Taguchi, T., and Tanaka, J. (2005). *Journal of Biomaterials*. **26**, 4847-4855.

Matsuura, T., Hosokawa, R., Okamoto, K., Kimoto, T., and Akagawa, Y. (2000). Diverse mechanisms of osteoblast spreading on hydroxyapatite and titanium. *Journal of Biomaterials*. **21**, 1121-1127.

Mayr-Wohlfart, U., Fiedler, J., Günther, K.P., Puhl, W., and Kessler, S. (2001). Proliferation and differentiation rates of a human osteoblast-like cell line (Saos-2) in contact with different bone substitute materials. *Journal of Biomedical Materials Research*. **57**, 132-139.

Martin, R.A., Yue, S., Hanna, J.V., Lee, P.D., Newport, R.J., Smith, M.E., and Jones, J.R. (2012). Characterizing the hierarchical structures of bioactive sol–gel silicate glass and hybrid scaffolds for bone regeneration. *Philosophical Transactions of the Royal Society*: Part A.**370**, 1422-1433.

McGarry, S.A., Engemann, J.J., Schmader, K., Sexton, D.J., and Kaye, K.S. (2004). Surgical-Site Infection due to Staphylococcus Aureus among Elderly Patients: Mortality, Duration of Hospitalization, and Cost. *Journal of Infection Control and Hospital Epidemiology*. **25**(6), 461-467.

Minandri, F., Bonchi, C., Frangipani, E., Imperi, F., and Vica, P. (2014). Promises and failures of gallium as an antibacterial agent. *Journal of Future Microbiology*. **9**(3), 379-397.

Mills, B.G., Masuoka, L.S., Graham, C.C., Singer, F.R., and Waxman, A.D. (1988). Gallium-67 citrate localisation in osteoclast nuclei of Paget's disease of bone. *Journal of Nuclear Medicine*. **29**, 1083-1087.

Mitchell, P., Dolan, L., Sahota, O., Cooper, A., Elliot, M., McQuillian, C., Stone, M., Hosking, D., Sandhu, B., Shervington, P., Moger, S., Mullan, K. (2010). Osteoporosis in the UK at breaking point. The British Menopause Society. 1-16.

Downloaded from: http://www.thebms.org.uk/publicdownloads/Osteo_Report2010.PDF.

Moore, W., Graves, S.R., and Bain, G.I. (2001). Synthetic Bone Graft Substitutes. *ANZ Journal of Surgery*. **71**, 354-361.

Munukka, E., Leppäranta, O., Korkeamäki, M., Vaahtio, M., Peltola, T., Zhang, D., Hupa, L., Ylänen, H., Salonen, J.I., Viljanen M.K., and Eerola, E. (2007). Bactericidal effects of bioactive glasses on clinically important aerobic bacteria. *Journal of Materials Science: Materials in Medicine*. **19**, 27-32.

Mortazavi, V., Nahrkhalaji, M.M., Faith, M.H., Mousavi, S.B., and Esfahani, B.N. (2009). Antibacterial effects of sol-gel-derived bioactive glass nanoparticle on aerobic bacteria. *Journal of Biomedical Materials Research: Part A*. **94**, 160-168.

Moseke, C., Gbureck, U., Elter, P. Drechsler, P., Zoll A., Thull, R., and Ewald, A. (2011). Hard implant coatings with antimicrobial properties. *Journal of Material Science: Materials in Medicine*. **22**, 2711-2720.

Mulligan, A.M., Wilson, M., and Knowles, J.C. (2002). The effect of increasing copper content in phosphate-based glasses on biofilms of *Streptococcus sanguis*. *Journal of Biomaterials* **24**, 1797-1807.

Munukka, E., Leppäranta, O., Korkeamäki, M., Vaahtio, M., Peltola, T., Zhang, D., Hupa, L., Ylänen, H., Salonen, J.I., Viljanen M.K., and Eerola, E. (2007). Bactericidal effects of bioactive glasses on clinically important aerobic bacteria. *Journal of Materials Science: Materials in Medicine*. **19**, 27-32.

N

Nandi, S.K., Roy, S., Mukherjee, P., Kundu, B., De, D.K., and Basu, D. (2010). *Indian Journal of Medical Research*. **132**, 15-30.

Nikaido, H. (2003). Molecular Basis of Bacterial Outer Membrane Permeability Revisited. *Microbiology and Molecular Biology Reviews*. **67**(4), 593-656.

Nouri, A., Hodgson, P.D., Cui'e, W. (2010). Biomimetic porous titanium scaffolds for orthopaedic and dental applications. *In Biomimetics Learning from Nature*: *Advances in Bioengineering.* 415-450.

Nuss, K.M.R., and Rechenberg, B.V. (2008). Biocompatibility Issues with Modern Implants in Bone – A Review for Clinical Orthopedics. *The Open Orthopedics Journal*. **2**, 66-78.

O

O'Donnell, MD., Watts, S.J., Hill, R.G., and Law, R.V. (2009). The Effect of Phosphate Content on the Bioactivity of Soda-Lime-Phosphosilicate Glasses. *Journal of Material Science: Materials in Medicine*. **20** (8), 1611-1618.

Olakanmi, O., Kesavalu, B., Pasula, R., Abdalla, M.Y., Schlesinger, L.S., and Britigan, B.E. (2013). Gallium Nitrate Is Efficacious in Murine Models of Tuberculosis and Inhibits Key Bacterial Fe-Dependent Enzymes. *Journal of Antimicrobial Agents and Chemotherapy*. **57**(12), 6074-6080.

Olaknmi, O., Gunn, J.S., Su, S., Soni, S., Hassett, D., and Britigan, B.E. (2010). Gallium Disrupts Iron Uptake by Intracellular and Extracellular *Francisella* Strains and Exhibits Therapeutic Efficacy in a Murine Pulmonary Infection Model. *Journal of Antimicrobial Agents and Chemotherapy*. **54**(1), 244-253.

P

Pierre, J.M. (2010). The calcium-sensing receptor in bone cells: A potential therapeutic target in osteoporosis. *Bone*. **46**(3), 571-576.

Pratten, J., Nazhat, S.N., Blaker, J.J. and Boccaccini, R. (2004). *In Vitro* Attachment of *Staphylococcus epidermidis* to Surgical Sutures with and without Ag-containing Bioactive Glass Coating. *Journal of Biomaterials Applications*. **19**, 47-57.

R

Radin, S., Reilly, G.C., Bhargave, P.S., and Ducheyne, L.P. (2005). Osteogenic effects of bioactive glass on bone marrow stromal cells. *Journal of Biomedical Material Research: Part A*. **73**, 21-29.

Raisz, L.G. (1999). Physiology and Pathophysiology of Bone Remodelling. *Journal of Clinical Chemistry*. **45**(8), 1353-1358.

Raggatt, L.J., and Partridge, N.C. (2010). Cellular and Molecular Mechanisms of Bone Remodelling. *Journal of Biological Chemistry*.

Reilly, G.C., Radin, S., Chen, A.T., and Ducheyne, P. (2007). Differential alkaline phosphatase responses of rat and human bone marrow derived mesenchymal stem cells to 45S5 bioactive glass. *Journal of Bimaterials*. **28**, 4091-4097.

Repo, M.A., Bockman, R.S., Betts, F., Boskey, A.L., Alcock, N.W., and Warrell, R.P (1988). Effects of gallium on mineral properties. *Journal of Calcified Tissue International*. **43**, 300-306.

Rose, F.R.A.J., and Oreffo, R.O.C. (2002). Bone Tissue Engineering: Hope vs Hype. *Journal of Biochemical and Biophysical Research Communications*. **292**(1), 1-7.

Scanlon, V.C., and Sanders, T. (2007). Essentials of Anatomy and Physiology Fifth Edition. *F.A. Davis Publishers.*

S

Schierholz, J.M., and Beuth, J. (2001). Implant infections: a haven for opportunistic bacteria. *Journal of Hospital Infection*. **49**, 87-93.

Sepulveda, P., Jones, J.J., and Hench, L.L. (2001). Characterisation of Melt-Derived 45S5 and sol-gel-derived 58S Bioactive Glasses. *Journal of Biomedical Materials Research: Applied Biomaterials*. **58**, 734-740.

Sepulveda, P., Jones, J.J., and Hench, L.L. (2002). *In vitro* dissolution of melt-derived 45S5 and sol-gel-derived 58S bioactive glasses. *Journal of Biomedical Materials Research: Applied Biomaterials*. **61**, 301-311.

Sevastianov, V. (1988). Role of protein adsorption in blood compatibility of polymers. *Critical Review Biocompatibility*. **44**, 109-154.

Silver, I.A., Deas, J., and Erecińska, M. (2001). Interactions of bioactive glasses with osteoblasts in vitro: effects of 45S5 Bioglass®, and 58S and 77S bioactive glasses on metabolism, intracellular ion concentrations and cell viability. *Journal of Biomaterials*. **22**, 175-185.

Steele, G., and Bramblett, C.A. (2007). The Anatomy and Biology of the Human Skeleton. *Texas A&M University Press* (USA).

Stoor, P., Kirstila, V., Soderling, E., Kangasniemi, I., Herbst, K., and Yli-Upro, A. (1996). Interactions between bioactive glass and periodontal pathogens. Journal of *Microbial Ecology in Health and Disease*. **9**, 109-114.

Stoor, P., Söderling, E., and Salonen, J.I. (1998). Antibacterial effects of a bioactive glass paste on oral microorganisms. *Acta Odontologica*. **56**, 161-165.

T

Tilocca, A. (2010). Models of structure, dynamics and reactivity of bioglass: a review. *Journal of Materials Chemistry*. **20**, 6848-6858.

Thompson, G.S. (2013). Understanding Anatomy and Physiology. *F.A. Davis Company* (Philadelphia).

Tousi, N.S., Velten, M.F., Bishop, T.J., Leong, T.J., Barkhordar, N.S., Marshall, G.W., Loomer, P.M., Aswath, P.B., and Varanasi, V.G. (2013). Combinatorial effect of Si^{4+}, Ca^{2+}, and Mg^{2+} released from bioactive glasses on osteoblast osteocalcin expression and biomineralisation. *Journal of Materials Science and Engineering: Part C, Materials for Biological Application*. **33**(5), 2757-2765.

Turner, C.H. (2002). Biomechanics of bone: determinants of skeletal fragility and bone quality. *Osteoporosis International*. **13**(2), 97-104.

V

Valappil, S.P., Pickup, D.M., Carroll, D.L., Hope, C.K., Pratten, J., Newport, R.J., Smith, M.E., Wilson, M., and Knowles, J.C. (2007). Effect of Silver Content on the Structure and

Antibacterial Activity of Silver-Doped Phosphate-Based Glasses. *Journal of Antimicrobial Agents and Chemotherapy*. **51**, 4453-4461.

Valappil, S.P., Readt, D., Abou Neel, E.A., Pickup, D.M., Chrzanowski, W., O'Dell, L.A., Newport, R.J., Smith, M.E., Wilson, M., and Knowles, J.C. (2008). Antimicrobial Gallium-Doped Phosphate-Based Glasses. *Journal of Advanced Functional Materials*. **18**, 732-741.

Valerio, P., Pereira, M.M., Goes, A.M., and Fatima Leite, M. (2004). The effect of ionic products from bioactive glass dissolution on osteoblast proliferation and collagen production. *Journal of Biomaterials*. **25**, 2941-2948.

Verron, E., Masson, M., Khosniat, S., Duplomb, L., Wittrant, Y., Baud'huin, M., Badran, Z., Bujoli, B., Janvier, P., Scimeca, J.C., Bouler, J.M., and Guicheux, J. (2010). Gallium modulates osteoclastic bone resorption *in vitro* without affecting osteoblasts. *British Journal of Pharmacology*. **159**, 1681-1692.

Vogel, M., Voight, C., Gross, U.M., Muller-Mai, C.M. (2001). *In vivo* comparison of bioactive glass particles in rabbits. *Journal of Biomaterials*. **22**, 357-362.

W

Warrell, R.P., Bockman, R.S., Coonley, C.J., Isaacs, M., and Staszewski, H. (1984). Gallium Nitrate Inhibits Calcium Resoprtion from Bone and Is Effective Treatment for Cancer-related Hypercalcemia. *Jounal of Clinical Investigations*. **73**, 1487-1490.

Warrell, R.P. (1997). Gallium Nitrate for the Treatment of Bone Metastases. *Journal of American Cancer Society*. **80**(8), 1680-1685.

Wiegand, C., Abel, M., Ruth, P., Elsner, P., and Hipler, U.C. (2014). In vitro assessment of the antimicrobial activity of wound dressings: influence of the test method selected and impact of the pH. *Journal of Materials Science: Materials in Medicine*. **26**, 3-13.

X

Xie, Z.P., Zhang, C.Q., Yi, C.Q., Qiu, J.J., Wang, J.Q. and Zhou, J. (2008). *In vivo* Study Effect of Particulate Bioglass® in the Prevention of Infection in Open Fracture Fixation. *Journal of Biomedical Materials Research: Applied Biomaterials*. **90**,195-201.

Xynos, I.D., Hukkanen, M.V.J., Batten, J.J., Buttery, L.D., Hench, L.L., and Polak, J.M. (2000). Bioglass 45S5® Stimulates Osteoblast Turnover and Enhances Bone Formation *In Vitro*: Implications and Applications for Bone Tissue Engineering. *Journal of Calcified Tissue International*. **67**, 321-329.

Xynos, I.D., Edgar, A.J., Buttery, L.D., Hench, L.L., and Polak, J.M. (2001). Gene-expression profiling of human osteoblasts following treatment with the ionic products of Bioglass® 45S5 dissolution. *Journal of Biomedical Materials Research*. **55**(2), 151-157.

Xynos, I.D., Hukkanen, M.V.J., Batten, J.J., Buttery, L.D., Hench, L.L., and Polak, J.M. (2000). Bioglass ®45S5 Stimulates Osteoblast Turnover and Enhances Bone Formation *In Vitro*: Implications and Applications for Bone Tissue Engineering. *Journal of Calcified Tissue International*. **67**, 321-329.

Y

Yamaguchi, T., Chattopadhyay, N., Kifor, O., Butters, Jr, R.R., Sugimoto, T., and Brown, E.M. (1998). Mouse Osteoblastic Cell Line (MC3T3-E1) Expresses Extracellular Calcium (Ca^{2+}_o)-Sensing Receptor and Its Agonists Stimulate Chemotaxis and Proliferation of MC3T3-E1 Cells. *Journal of Bone and Mineral Research*. **13**(10), 1530-1538.

Z

Zimmerli, W., and Ochsner, P.E. (2003). Management of Infection Associated with Prosthetic Joints. *Journal of Infection*. **2**, 99-108.

Zhang, D., Leppäranta, O., Munukka, E., Ylänen, H., Viljanen, M.K., Eerola, E., Hupa, M., and Hupa, L. (2010). Antibacterial effects and dissolution behaviour of six bioactive glasses. *Journal of Biomedical Material Research: Part A*. **93**,475-483.

Zhu, Y., Ouyang, Y., Chang, Y., Luo, C.., Xu, J., Zhnag, C., and Huang, W. (2013). Evaluation of the proliferation and differentiation behaviours of mesenchymal stem cells with partially

converted borate glass containing different amounts of strontium *in vitro*. *Molecular Medicine Reports*. **7**, 1129-1136.

Zimmermann, G., and Moghaddam, A. (2011). Allograft bone matrix versus synthetic bone graft substitutes. *Injury*. *International Journal of the Care of the Injured*. **42**(2), 16-21.

APPENDIX

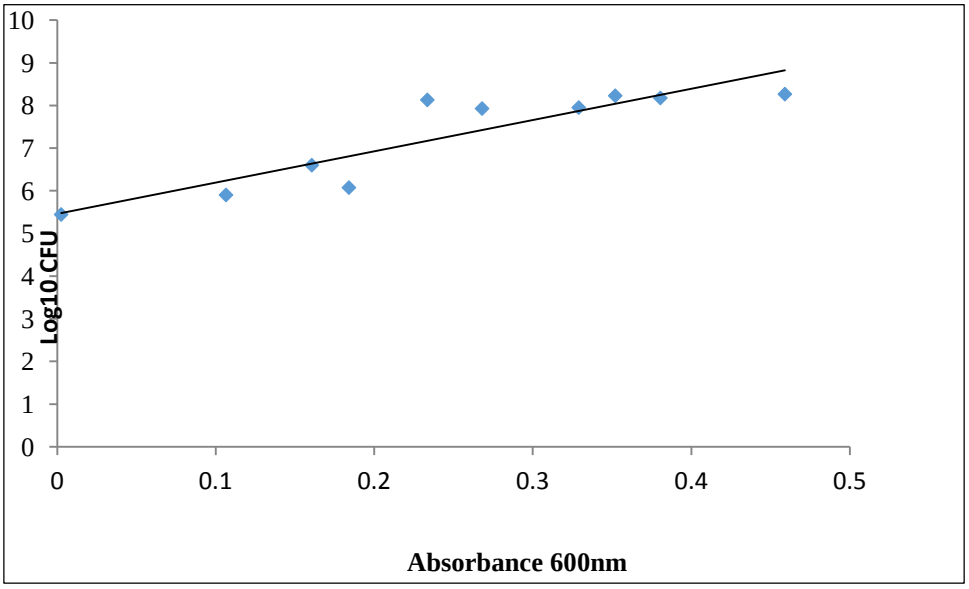

Figure A.1. Mean (n=2) colony forming units (CFU) of *S. aureus* cell suspension correlated to turbidity measured at an absorbance of 600 nm.

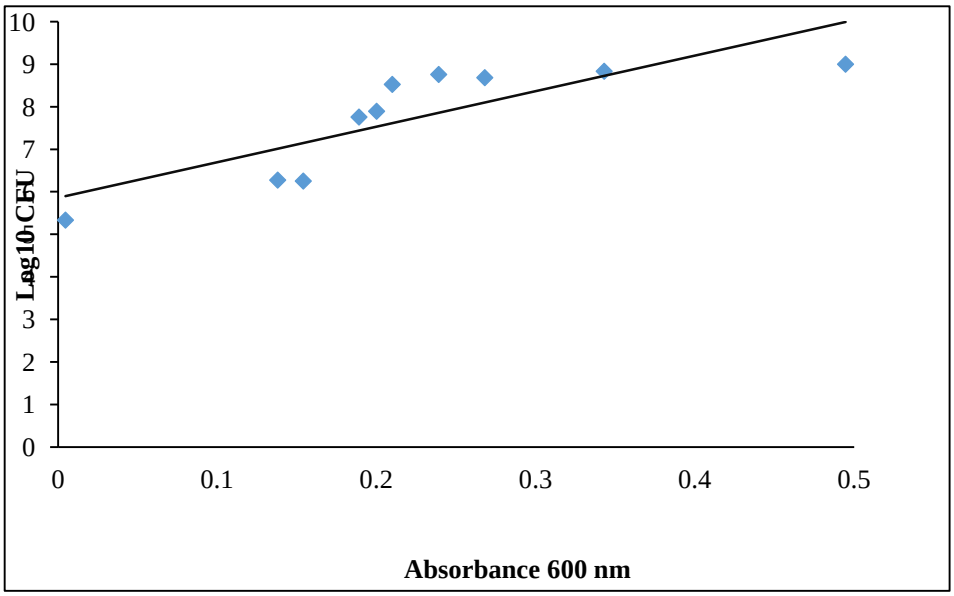

Figure A.2 Mean (n=2) colony forming units (CFU) of *E. coli* cell suspension correlated to turbidity measured at an absorbance of 600 nm.

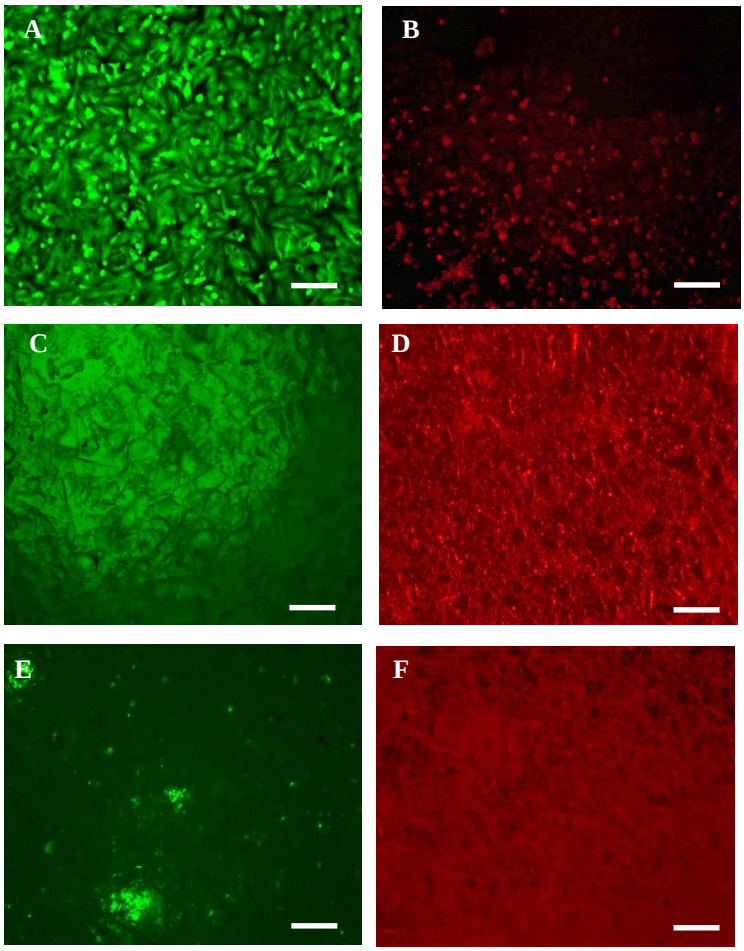

Figure A.3 Fluorescent microscopy images at x10 objective are shown for LIVE/DEAD staining of Saos-2 cells cultured with and without 3 mol% Ga doped BAG and 45S5 Bioglass® particles at 100 mg/ml for 96 hours. (**A**) Live (green) Saos-2 cells cultured without 3 mol% Ga doped BAG and 45S5 Bioglass® particles, (**B**) dead (red) Saos-2 cells cultured without 3 mol% Ga doped BAG and 45S5 Bioglass®, (**C**) 45S5 Bioglass® particles stained with Calcein-AM without the presence of live Saos-2 cells, (**D**) 45S5 Bioglass® particles stained with Propodium iodide without the presence of dead Saos-2 cells, (E) 3 mol% Ga doped BAG stained with Calcein-AM without the presence of live Saos-2 cells, and (**F**) 3 mol% Ga doped BAG stained with Propodium iodide without the presence of dead Saos-2 cells. Bar indicates 100 µm.